Species discrimination from a hyperspectral perspective

Md. Istiak Sobhan

Promoters:

Prof. Dr. Andrew K. Skidmore
Professor of Vegetation and Agricultural Land Use Survey
International Institute for Geoinformation Science and Earth Observation (ITC)
Enschede and Wageningen University,
The Netherlands

Prof. Dr. Herbert H.T. Prins
Professor of Resource Ecology
Wageningen University, the Netherlands

Examination committee:

Prof. Dr. Ir. P.C. Struik
Wageningen University, Wageningen, The Netherlands

Prof. Dr. F. D. van der Meer
International Institute for Geoinformation Science and Earth Observation (ITC) Enschede
and
University Utrecht, Utrecht, The Netherlands

Prof. Dr. A.M. Cleef
University of Amsterdam, Amsterdam, The Netherlands

Dr. Khaled Hasan
University of Dhaka, Dhaka, Bangladesh

This research is carried out within the C.T de Wit Graduate School for Production Ecology and Resource Conservation (PE&RC) in Wageningen University, the Netherlands

Species discrimination from a hyperspectral perspective

Md. Istiak Sobhan

THESIS

To fulfil the requirements for the degree of doctor on the authority of the Rector Magnificus of Wageningen University, Prof. Dr. M.J. Kropff
To be publicly defended on 7 December 2007 at 15:00 hrs in the auditorium of ITC, Enschede

Species discrimination from hyperspectral perspective

ISBN: 978-90-8504-809-1
International Institute for Geo-information Science & Earth Observation,
Enschede, the Netherlands (ITC)
ITC Dissertation Number: 150

Table of Content

Table of Content ..... **i**
Abstract ..... **v**
Samenvatting ..... **vi**
Acknowledgements ..... **vii**

Chapter 1 ..... **1**
General Introduction **1**
1.1 Imaging spectroscopy or hyperspectral remote sensing **3**
1.2 Vegetation spectroscopy **3**
1.2.1 Vegetation quantity and hyperspectral data 4
1.2.2 Vegetation quality and hyperspectral data 4
1.3 Species discrimination with hyperspectral data **5**
1.3.1 Why we need to discriminate plant species 5
1.3.2 Use of hyperspectral remote sensing in species discrimination 5
1.4 Study objectives **7**
1.5 General Method **8**
1.5.1 Study area 8
1.6 Thesis outline **9**

Chapter 2 ..... **13**
Changes in spectral properties following leaf clipping and its implications on spectral indices **13**
2.1 Introduction **15**
2.2 Materials and method **16**
2.2.1 Collection and preservation of leaf specimens 16
2.2.2 Collection of leaf spectra 17
2.2.3 Data analysis 18
2.2.3.1 Use of indices 18
2.2.4 Statistical analysis 22
2.2.5 Histology 22
2.3 Results **23**
2.3.1 Post-harvest changes in leaf spectra 23
2.3.2 Post-harvest changes in vegetation indices 23
2.3.3. Influence of species on spectral change 25
2.3.4 Histology 29
2.4 Discussion **31**
2.5 Conclusion **33**

Chapter 3 ..... **37**
Spectral regions for maximizing species discrimination **37**
3.1 Introduction **39**

3.2 Materials and method **40**
3.2.1 Collection of leaf samples 40
3.2.2 Collection of Spectra 40
3.2.3 Discrimination procedure 42
3.2.3.1 U-test 42
3.2.3.2 Principal Component Analysis (PCA) 43
3.2.3.3 Stepwise Discriminant Analysis 43
3.2.3.4 Wrapper feature selection approach 44
3.2.4 Finding the important regions 45
3.2.5 Testing Procedure 45
3.3 Results **46**
3.3.1 U-Test 46
3.3.2 Principal component analysis 47
3.3.3 Stepwise discriminant analysis 49
3.3.4 Wrapper feature selection 50
3.3.5 Finding the important regions 51
3.3.6 Testing Procedure 51
3.4 Discussion **52**
3.5 Conclusion **57**

Chapter 4 ..... **61**
Spectral similarity measures for plant species discrimination **61**
4.1 Introduction **63**
4.2 Materials and method **64**
4.2.1 Collection of leaf samples 64
4.2.2 Collection of spectra 65
4.2.4 Spectra similarity measures 67
4.2.4.1 Spectral correlation measure (SCM) 67
4.2.4.2 Spectral angle mapper (SAM) 68
4.2.4.3 Spectral information divergence (SID) 68
4.2.4.4 SID-SAM mixed measure 69
4.2.5 Measurements for discriminability 69
4.2.5.1 Relative spectral discriminatory probability (RSDPB) 71
4.2.5.2 Relative spectral discriminatory power (RSDPW) 71
4.2.6 Use of similarity measure as classifier 71
4.3 Results **72**
4.3.1 Similarity of spectra within and between species 72
4.3.2 Spectral similarity 74
4.3.2.1 Laboratory spectra 74
4.3.2.2 Spectra from image 76
4.3.3 Similarity measures as classifier 76
4.4 Discussion **79**

4.5 Conclusion **80**

Chapter 5 ..... **85**
Use of phenological events to increase species discrimination **85**
5.1 Introduction **87**
5.2 Materials and method **88**
5.2.1 Collection of samples 88
5.2.2 Collection of spectra 89
5.2.3 Data Analysis 90
5.2.3.1 Discrimination through similarity measures 90
5.2.3.2 Continuum removed band depth analysis 91
5.2.4 Effect of phenological differences on classification accuracy 92
5.3 Results **93**
5.3.1 Visual differences in spectra 93
5.3.2 Comparison of discriminations 94
5.3.3 Continuum removed band depth analysis 96
5.3.4 Classification accuracy 96
5.4 Discussion **99**
5.5 Conclusion **100**

Chapter 6 ..... **103**
Mapping shrub and tree species richness from hyperspectral imagery using a matched filtering unmixing technique **103**
6.1 Introduction **105**
6.2 Materials and method **107**
6.2.1 The study area 107
6.2.2 Field data collection 107
6.2.3 Image acquisition and pre-processing 108
6.2.3.1 Geometric and atmospheric correction 108
6.2.4 Collection of endmember spectra from image 109
6.2.5 Per pixel assessment of shrubs and tree species 110
6.2.5.1 Resampling 110
6.2.5.2 Spectral unmixing process 110
6.2.5.2 Preparation of species composition map 112
6.2.6 Validation 113
6.3 Results **113**
6.3.1 Endmembers 113
6.3.2 Spatial distribution of individual species and mapping species richness per pixel 113
6.3.2 Comparison of unmixing results with field measurements 116
6.4 Discussion and conclusion **118**

Chapter 7 ..... **125**
Plant species discrimination using hyperspectral remote sensing **125**
The synthesis **125**
7.1 Plant species discrimination **126**
7.2 Reliability of laboratory measurement **126**
7.3 Dimensionality: Are all bands necessary? **127**
7.4 Which part of the spectrum is most important? **128**
7.5 What is essential to optimize a sensor for species discrimination? .. **129**
7.6 When to measure? **130**
7.7 Discriminating species at a landscape scale **132**
7.8 Conclusion: Species discrimination – is it possible? **134**

Bibliography **137**
Author's Biography **153**
ITC Dissertation list **155**

Abstract

Sustainable management of natural ecosystems requires comprehensive information on species distribution and composition. Traditional description of species composition for floristic mapping involves exhaustive and time-consuming field work. Remote sensing has the potential to improve the collection of information on species composition. Compared to other vegetation attributes plant species so far remained a difficult attribute to detect with remote sensing. Broad band remote sensing sensors, which have been used extensively for mapping of plant communities, are however not sufficiently sensitive to allow discrimination of individual plant species. The advent of hyperspectral and high spatial resolution sensors offers new opportunities in this respect.

This study aims to investigate a number of methods to discriminate plant species using hyperspectral remote sensing. Extensive use was made of measurements of leaf and canopy reflectance spectra derived from laboratory spectrometry and airborne hyperspectral imagery.

Studies on the spectral reflectance of plant species are frequently carried out under laboratory conditions. We investigated whether the time lag between leaf detachment and measurement in the laboratory influenced the spectral response. Six hours appeared to be the time lag within which the laboratory measurements remained similar to the in situ response.

We next investigated which regions of the spectrum provided the richest information for species discrimination. Four different band selection procedures selected sets of ten bands. Although the bands selected by the various procedures differed, they were localized broadly in the same spectral regions. The procedure thus enabled to localize optimal regions for species discrimination.

The possibility to discriminate species depends on their distance in hyperspectral feature space. In a next study we explored the possibility to discriminate six species using four spectral matching algorithms on full spectral configuration. The results reveal the dissimilarities between spectra of different plant species, which was used to find out relative separability between them

The possibility to discriminate species might change during the life cycle of plants. In a fourth paper we investigated the change in spectral response over the life cycle. It was demonstrated that 13 out of 15 species pairs were easier discriminated in their flowering than non flowering stage. The results demonstrate that selection of the optimum phenological stage may enhance the spectral separability of species.

Another problem arises when various species occur within one pixel. We investigated whether sub-pixel unmixing techniques allowed discriminating species occurring within a pixel. The sub-pixel unmixing technique allowed to estimate the per pixel contribution of individual plant species. Sub pixel unmixing thus offers the possibility to provide more detailed taxonomic information.

This thesis concludes by confirming the main hypothesis that discrimination of plant species can be enhance while using hyperspectral and high spatial resolution imagery.

Samenvatting

Informatie over samenstelling en verspreiding van soorten is noodzakelijk voor duurzaam beheer van natuurlijke ecosystemen. Uitgebreid en tijdrovend veldwerk is onderdeel van traditionele beschrijving van soortsamenstelling. Aardobservatie heeft potentie om inwinnen van informatie over soortsamenstelling te verbeteren. Plantensoorten zijn echter, vergeleken met andere vegetatie eigenschappen, moeilijk te detecteren met aardobservatie. De tot op heden voor vegetatiekartering gebruikte breed band aardobservatie sensoren zijn niet voldoende gevoelig om plantensoorten te onderscheiden. De komst van hyperspectrale aardobservatie biedt in dit opzicht nieuwe mogelijkheden.

Deze studie had tot doel methodes te bestuderen om plantensoorten te onderscheiden met behulp van hyperspectrale aardobservatie. Er is gebruik gemaakt van reflectie spectra van blad en bladerkroon verkregen door middel van laboratorium spectrometrie en airborne hyperspectrale beelden.

Spectra van planten worden vaak in het laboratorium bestudeerd. Wij bestudeerden of het tijdsverschil tussen verzamelen van blad en meting in het laboratorium de spectrale respons beïnvloedt. Laboratorium meting week tot zes uur na verzamelen niet af van de in situ response.

Vervolgens onderzochten wij welke spectrale regio's de rijkste informatie leverden over soortsamenstelling. Vier verschillende band selectie procedures selecteerden sets van tien banden. De geselecteerde banden die verschilden tussen de procedures, waren over het algemeen gelokaliseerd in dezelfde spectrale regios. De procedure maakte het dus mogelijk om optimale spectrale regio's aan te wijzen voor het onderscheiden van soorten.

De mogelijkheid om soorten te onderscheiden hangt af van de onderlinge afstand in de hyperspectrale ruimte. In een vervolgstudie exploreerden we de mogelijkheid soorten te onderscheiden met behulp van vier spectrale matching algoritmes en het volledige hyperspectrale spectrum. De resultaten toonden spectraal onderscheid tussen de verschillende plantensoorten, dat werd gebruikt om hun relatieve onderscheidbaarheid te

De onderscheidbaarheid van soorten kan gedurende hun levenscyclus veranderen. In een vierde artikel onderzochten we de verandering in spectrale respons gedurende de levenscyclus. Dertien uit 15 paren plantensoorten waren bloeiend gemakkelijker te onderscheiden dan vegetatief. Deze resultaten tonen aan dat selectie van de optimale fenologische fase de onderscheidbaarheid van soorten bevordert.

Een ander probleem ontstaat als meerdere soorten in een pixel voorkomen. We bestudeerden of subpixel-ontmixing soorten binnen een pixel kan onderscheiden. Sub pixel ontmixing maakte het mogelijk de bijdrage van individuele soorten per pixel te schatten. Sub pixel ontmixing maakt het dus mogelijk om meer gedetailleerde taxonomische informatie te leveren.

De thesis besluit met bevestiging van de hypothese dat onderscheid van plantensoorten verbeterd kan worden door gebruik te maken van hyperspectrale en hoge resolutie beelden.

Acknowledgements

In science the credit goes to the man who convinces the world,
not the man to whom the idea first occurs.
- Sir Francis Darwin, (1848-1925)

The many people who have helped in some way or the other to complete this work cannot all be mentioned. But yet, I take this opportunity to thank some of them.

First of all I am grateful to my promoters Prof. Andrew K. Skidmore of ITC and Prof. Herbert T. Prins of Wageningen University for their contribution, invaluable guidance and encouragement throughout this work. After finishing my MSc (ITC, 1999), Andrew was instrumental to motivate me to pursue for a PhD, he pushed me hard to write a proposal which could earn a PhD scholarship. Without his continuous encouragement and impulse it could not have been possible. Meanwhile, Herbert keeps providing stimulants for thought processes in our long and endless discussions during my entire PhD work. Discussion with him was always exciting but scientifically demanding as his knowledge is so profound in so many disciplines. All of our discussions with Andrew and Herbert were starting with thesis-related matters but end up either with Cricket (as Andrew is from down under) or some social issues.

To Nuffic and ITC (International Institute for Geo-information Science and Earth Observation), I am deeply indebted for providing me a fully funded PhD position to work on this thesis. Moreover, ITC also provided the fund for hyperspectral imaging mission in Majella National Park.

I also like to thank all the faculty members of our Natural Resource Study department of ITC. Special thank goes to Dr. Jan de Leeuw, Dr. Kees de Bie, Dr. Yousif Hussin, Dr. Patrick van Laake, Dr. Mike McCall, Dr H. van Giles and Prof. Eric Smaling for their critical advises during the course of my work. My sincere gratitude also extended to Dr. Fabio Corsi and Dr. Clement Atzberger for their great contribution during the field work and beyond. Fabio's understanding about both the Mediterranean ecosystem as well as the Italian bureaucracy was absolute necessary during the field work phase. I am also happy to express thanks to the colleagues of my research school (Production Ecology and Resource Conservation) at Wageningen University. Gratitude to Dr. Sip van Wieren and Dr. Claudius van de Vijver for their wonderful scientific guidance and insight.

My deepest appreciation extended to all the members of Majella National Park authority both in St' Eufemia a Majella where we stayed during the field work as well as Campo di Giove, the administrative headquarter. The accommodation they provided us in St' Eufemia was truly fantastic where every morning we refreshed just by looking at the sunny peak of Monte Morrone. It was really a pleasant experience to work with them in the woods. Special thanks to Dr. Theodoro Andrisano and Elena for their kind cooperation.

I would like to express my profound gratitude to Prof. Martin Hale and Ms. Loes Colenbrander, who ensured that I had excellent research administration. My stay in ITC was also facilitated by the dynamic support of Education Affairs department, with special thanks to Marie Chantal Metz, Theresa van den Boogaard and Bettine Geerdink. Particular thanks to Carla Gerritsen, Marga Koelen and Petry Maas–Prijs of ITC library for their unparallel help of finding difficult articles. I thank Marjolein Woerlee and Saskia Groenendijk for always providing me with a nice accommodation during my stay in Enschede which became the home for my family and me. I also owe a great deal to Esther Hondebrink for her relentless secretarial supports. Also thanks to Marco van Druten, Frans Gollenbeek, Marion Pierik and Kim Velthuis for their kind help in all

financial difficulties. Special thanks to Thea de Kluijver for her persistent help to keep us healthy.

My heartfelt gratitude to the geo technical support team at ITC, without their appropriate and speedy support I could not have written this thesis, thanks to Wan Bakx, Chris Hecker, Jelger Kooistra and Boudewijn van Leeuwen. Whenever I got stuck particularly with spectrometers, there was always this support team to solve the technical problems. Thanks to Henk van Oosten, Willem Nieuwenhuis, Bas Retsios and Harald van der Werff for extending their help in software support, especially with IDL scripting throughout the study period. My acknowledgement goes to Ard Kosters, Gerard Leppink for their IT support and Benno Masselink and Job Duim for all other logistical help.

My sincerest thanks go to my generation of PhD candidates: you have been the best. It was great to be a part of such a splendid group. Due to the long tenure of a PhD candidateship it is difficult to mention all the friends and colleagues. But among them: Dr. Karin Schmidt, Dr. Onisimo Mutanga, Dr. Amon Murwira, Dr. Jella Ferwerda, Dr. Alfred Duker, Dr. Martin Yemefack, Dr. Chaichoke Vaiphasa, Dr. Pravesh Debba, Dr. Peter Minang, Dr. Marleen Nooman, Dr. Jamshid Farifteh, Dr. Masoud Kheirkhah, Dr. Grace Nangendo, Dr. Moses Cho, Dr. Arta Dilo, Dr. Uday Bhaskar Nidumolu, Dr. Chudamani Joshi, Richard Onchaga, Dr. Daniel van de Vlag, Dr. Ulanbek Turdukulov, Diana Chavarro, Graciela Peters, Prasun Gangopadhyay, Gabrielle Iglesias, Bobba Bharath, Peter Beck, Jane Bemigisha, Roshanak Darvishzadeh, Enrique Castellanos, Carolina Sigaran, Emmanuel Owusu, Si Yali, Yanqiu Xing, Guofeng Wu, Sitwala Wamunyima, Wang Tiejun, Claudia Pittiglio, Shadrack Ngene, Ha Nguyen, Nicky Knox, Mobushir Riaz Khan, Filiz Bektas, Tyas Mutiara Basuki, Mhosisi Masocha, Ajay Kumar Katuri, Anthony Arko Adjei, Lal Muthuwatta, Kitsiri Weligepolage, Rogier van der Velde, Saibal Ghosh, Sekhar Lukose Kuriakose, Tapas Martha, Wiebke Tegtmeier, Pankaj Jaiswal, Iswar Das and Rishiraj Dutta are worth mention.

Special thank goes Moses A. Cho not only because he was my office mate and field work partner but also for his relentless push at the time of confronting hills and fatigue during our field work. His brotherly support during the entire course of my work was unexplainable and his mathematical knowledge and support was of great help. He and his wife Matilda always managed to form a homely environment around them, which was really pleasing.

I am grateful to all Bangladeshi students supporting me during my stay at Enschede. All of you were really supportive and your encouragement kept me moving during the most difficult phases of this journey. Special appreciation goes to Ashiqur Rahman, Ahsanul Kabir, Nazmul Sohel and Shams Sikdar. I also thank all of my friends way back in Dhaka for their moral support.

My deepest support goes to my family as they always kept sending me good wishes and encouragement from so far. And last but not least my dearest wife who has been the source of all my aspiration. Without your support none of this was possible.

Chapter 1

General Introduction

1.1 Imaging spectroscopy or hyperspectral remote sensing

Spectroscopy is the study of the interaction between radiation and matter. It studies light as a function of wavelength that has been absorbed, reflected or scattered from a solid, liquid or gas. As photons enter matter, some are reflected from the surfaces, some pass through, and some are absorbed. Photons reflected from the surface or refracted by molecules inside the matter are said to be scattered, and can be detected and measured. Above absolute zero, all natural surfaces discharge photons (Clark et al., 1990). At a molecular level, scattering or absorption of sunlight depends on the atomic bonds or molecular structure of the intercepting molecule, and these absorptions or scatterings are very specific to the atomic bonds or molecular structure of the target. The properties that specify the response of the material at every wavelength are called spectral properties (Suits, 1983). In the 1970s, a group of scientists (Knipling, 1970; Hunt, 1977; Swain and Davis, 1978) studied the reflectance spectra of rocks, minerals and vegetation, and developed the concept of understanding the spectral properties in terms of the underlying quantum mechanical process in relation to the chemistry of the reflecting object.

This directed scientists to the suggestion that, by measuring the amount of light that reflects from a surface, one can possibly distinguish the composition of chemical elements of that surface. When an image is constructed from imaging spectrometer data that measure spectra from contiguous image pixels, the term changes to “imaging spectroscopy”. In the remote sensing community, the term “imaging spectroscopy” has many synonyms, such as imaging spectrometry and hyperspectral or ultraspectral imaging (Clark, 1999). The prefix “hyper” in the word “hyperspectral” refers to spectra consisting of large numbers of contiguous and narrow light sensors. The data from a hyperspectral sensor often consist of over 100 contiguous bands of 10 nm or less bandwidth. These contiguous bands and narrow ranges lead to the possibility of detecting surface chemistry and better understanding the underlying biophysical processes in vegetation. In the thesis research, two different hyperspectral sensors were used. Measurements were made at field and laboratory levels using the GER 3700 spectrometer with 647 spectral bands from 350 to 2500 nm, and at the airborne platform level using the HyMap sensor with 126 spectral bands from 400 to 2500 nm.

1.2 Vegetation spectroscopy

With the introduction of imaging spectroscopy and/or hyperspectral sensors, both quantitative and qualitative remote sensing of vegetation improved significantly on that produced using the older broadband multispectral sensors. As ecological studies require the quantification of biochemical and biophysical attributes (Asner, 1998), the high spectral resolution of hyperspectral data is vital for yielding quality information

about vegetation health, biomass and other physico-chemical properties (Curran, 1989; Curran et al., 1992; Peñuelas et al., 1997; Todd et al., 1998; Green et al., 1998; Kokaly and Clark, 1999; Asner et al., 2000; Soukupová, Rock and Albrechtova, 2002; Mutanga et al., 2003; Zarco-Tejada et al., 2003; Mutanga and Skidmore, 2004; Mutanga et al., 2004; Zarco-Tejada et al., 2005). Moreover, hyperspectral data have made it possible to measure more accurately both the quantity and particularly the quality of the vegetation.

1.2.1 Vegetation quantity and hyperspectral data

Measuring vegetation quantity (or biomass) at field level is a difficult and destructive process (Gower, Kucharik and Norman, 1999). In addition, it is expensive and can rarely be extended to cover large areas (Scurlock and Prince, 1993). However, with the arrival of remote sensing, quantifying biomass became a reality (Tucker, 1979; Elvidge, 1990; Daughtry et al., 1992). Various vegetation indices (i.e., NDVI, SR, TVI, SAVI) had been developed and successfully used to measure vegetation quantity and leaf area index (LAI). In spite of these successes, vegetation indices calculated from broadband sensors can be unstable, owing to the underlying soil colour, canopy and leaf properties, and atmospheric conditions (Huete and Jackson, 1988; Todd, Hoffer and Milchunas, 1998). Furthermore, NDVI measured by broadband sensors asymptotically saturate after a certain biomass density, and measurement accuracy drops considerably (Todd, Hoffer and Milchunas, 1998; Gao et al., 2000; Thenkabail, Smith and De Pauw, 2000). However, most of these problems have been tackled or at least reduced since the appearance of hyperspectral sensors. New narrow-band NDVI (Mutanga and Skidmore, 2004; Mutanga and Skidmore, 2004) that reduce the problem of saturation have been developed, while new indices such as red-edge position (REP) are able to measure biomass much more accurately than NDVI (Curran, Windham and Gholz, 1995; Cho and Skidmore, 2006).

1.2.2 Vegetation quality and hyperspectral data

Measuring the biochemical parameters necessary for uncovering vegetation quality is more difficult than remote sensing of biomass or LAI because specific absorption regions of these biochemicals are masked by broadband sensors (Curran, 1989; Johnson, Hlavka and Peterson, 1994). In plant tissue, the absorption of energy from radiation has been attributed to the energy transition of the molecular vibration in C-H, N-H, O-H, C-N and C-C bonds, which are the building blocks of all organic compounds (Elvidge, 1990). Hence, any reflection from a plant at a specific wavelength is a function of the chemical composition of that plant (Foley et al., 1998). However, after the introduction of spectrometry, a whole new branch of science started to develop. Scientists began to measure in plant materials the contents of various chemicals, including nitrogen and phosphorus, that are directly related to such plant qualities as pigment concentration, plant health, stress and damage (Curran et al.,

1992; Peñuelas, Baret and Filella, 1995; Kraft et al., 1996; Gamon and Surfus, 1999; Mutanga, Skidmore and Prins, 2004; Ferwerda, Skidmore and Mutanga, 2005; Ferwerda, Skidmore and Stein, 2006).

1.3 Species discrimination with hyperspectral data

1.3.1 Why we need to discriminate plant species

Plant species is the main building block of almost all ecosystems, and sustainable management of any ecosystem requires a comprehensive understanding of species composition and distribution (Nagendra, 2002). To achieve the goal of accurately revealing species composition and distribution by using remotely sensed data, species-level discrimination of plants is essential. Moreover, monitoring the changes of species richness through remote sensing, and particularly examining the composition of certain species in a specific area, can be achieved only if species-level identification and discrimination is possible, which in turn can make it viable to recognize the succession process of the ecosystem. Much research into discriminating invasive species from the native vegetation has been undertaken in order to develop a sustainable protection strategy (Everitt et al., 1995; Lass et al., 2002; Hunt et al., 2003; Hunt et al., 2004; Parker-Williams and Hunt, 2004).

1.3.2 Use of hyperspectral remote sensing in species discrimination

Traditionally, species discrimination for floristic mapping involved exhaustive and time-consuming fieldwork, including taxonomical information and the visual estimation of percentage cover for each species (Kent and Coker, 1992). After the introduction of aerial photography, the extrapolation of such point-based information became possible (Zonneveld, 1974). Even after the arrival of broadband sensors, vegetation cover mapping failed to make any headway beyond accurate mapping at Anderson level II (Anderson et al., 1976). This failure was caused mainly by the lack of spectral and spatial resolution necessary to differentiate species in the landscape.

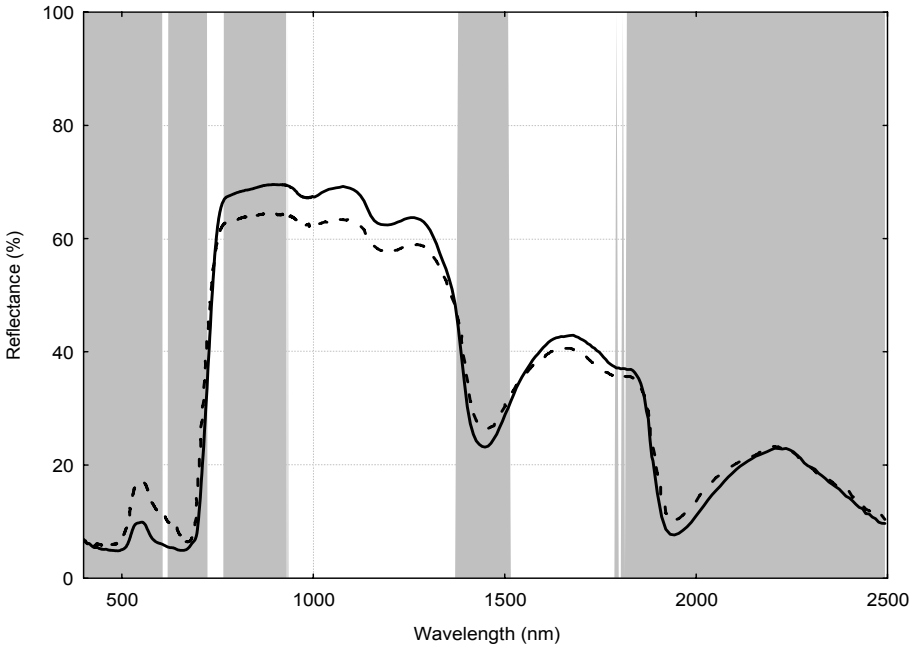

Figure 1.1 Leaf spectrum of two different species, *Acer campestre* (smooth line) and *Carpinus orientalis* (dashed line). Wavelengths at which these two spectra are significantly difference are shaded grey.

Technological advancement and the advent of hyperspectral sensors with both high spectral and spatial resolutions have raised new expectations about the possibilities for spectrally discriminating species (Figure 1.1) (Cochrane, 2000; Schmidt and Skidmore, 2003; Clark Roberts and Clark, 2005) and thus improving the discrimination and mapping of vegetation communities or species. Researchers have been able to discriminate and classify species based on their fresh leaf reflectance (Gausman and Allen, 1973; Goward, Huemmrich and Waring, 1994; Gong, Pu and Yu, 1997; Knapp and Carter, 1998; Kumar and Skidmore, 1998; Cochrane, 2000; Schmidt and Skidmore, 2001; Vaiphasa et al., 2005), field reflectance at canopy (Satterwhite and Ponder Henley, 1987; Petzold and Goward, 1988; Peñuelas et al., 1993; Schmidt and Skidmore, 2003; Yamano et al., 2003), or remotely sensed hyperspectral imagery (Bajjouk et al., 1996; Silvestri et al., 2003; Thenkabail et al., 2004; Clark et al., 2005). Availability of this high spectral resolution has not only improved the accuracy of conventional classifiers but also introduced the possibility of using sub-pixel-level spectral unmixing techniques that determine the relative abundance of endmembers present in a pixel (Adams et al., 1995). Different types of unmixing algorithms are available and have been used for mapping individual plant species or associations with mixed success (Roberts et al., 1998; McGwire, Minor and Fenstermaker, 2000; Parker Williams and Hunt, 2002; Robichaud et al., 2007).

However, even after all these successful applications of reflectance spectra for discriminating between species, some researchers claim that the leaf reflectances of different species are highly correlated because of their similar chemical composition (Portigal et al., 1997). Furthermore, Price (1994) suggests that several species may actually have quantitatively similar spectra owing to the variation in spectral signature present within a species. He argues that a spectrum is a mixture of physical and chemical properties that can change because of various environmental factors, and therefore their uniqueness is questionable (Price, 1994). Moreover, spectral variations can also occur within a species because of age differences, micro-climate, soil characteristics, precipitation, topography, phenology, and a host of other environmental factors, including stresses (Gausman, 1985; Westman and Price, 1987; Carter, 1993; Carter, 1994; Portigal et al., 1997; Roberts et al., 1998; Gracia and Ustin, 2001; Smith et al., 2004).

The high spectral resolution of hyperspectral data, which is the key feature and is essential for capturing and discriminating subtle differences in the targets, also contains redundant information at band level (Bajwa et al., 2004). This high data dimensionality makes computation difficult for classification and discrimination, and with traditional classifiers high dimensionality undermines the precision of the estimates of class distribution. To reduce redundancy or dimensionality, various univariate and multivariate band reduction techniques have been developed, such as multiple stepwise and partial least square regressions, discriminant analysis, principal component analysis and artificial neural network. However, many have argued against the band reduction techniques, indicating the loss of information (Roberts et al., 1998). It is therefore important to understand the advantages and disadvantages of both states and select accordingly. Moreover, using hyperspectral remote sensing for the species-level discrimination or mapping of plants is a complex process, and it is therefore important to understand all the different aspects before coming to a conclusion.

1.4 Study objectives

The main objective of this study was to investigate the various features of the potential of hyperspectral remote sensing for plant species discrimination. To realize this main objective, we subdivided it into sub-objectives: (1) to identify the potential spectral regions containing information regarding species discrimination, (2) to investigate the usefulness of spectral matching algorithms for discriminating spectra of different plant species, (3) to examine whether phenological events can be used to enhance the separability between species, and (4) to examine whether sub-pixel unmixing techniques can be used to map the species distribution and richness in a landscape.

This thesis work was performed in parallel with the study of Cho (2007), who worked on estimating biochemical and biophysical parameters from

plant reflectance and used the red-edge double-peak feature to do so. The combination of these two studies provides an overview of the biomass and species distribution in Majella National Park, Italy.

1.5 General Method

The major part of this study was based on laboratory measurements of leaf and canopy spectra, and different sensor devices, including field and laboratory spectrometers and an airborne hyperspectral sensor (i.e., HyMap), were adopted. Both univariate and multivariate statistical methods are featured in different chapters. The field-level data and plant materials were collected in Majella National Park, Italy (Figure 1.2).

1.5.1 Study area

The study site is located in Majella National Park, Italy (42°14' to 42°50'N and 13°50' to 14°14'E), which covers an area of 74,000 ha. The park extends into the southern part of Abruzzo, at a distance of 40 km from the Adriatic Sea. This region is situated in the massifs of the Apennine mountain range. The park is characterized by several mountain peaks,

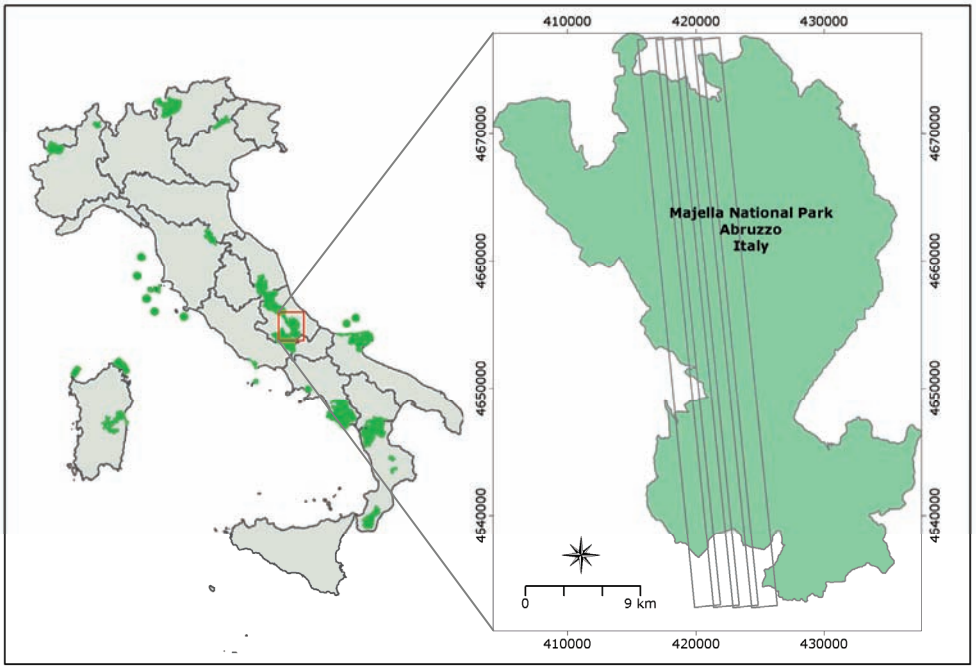

Figure 1.2 Location of Majella national park in Italy with airborne HyMap flight lines.

the highest being Mount Amaro (2794 m). More specifically, the study area (42°49' to 42°14'N and 13°57' to 14°06'E) is situated between Mount Majella and Mount Morrone to the east and west, respectively. It

covers an area of approximately 40 km x 6 km, as shown in Figure 1.2 (as flight lines). The flora of Majella National Park exhibit a wide range of species: more than 2100 species (covering 65% of Abruzzi flora and 37% of Italian flora) and various endemisms that amount to 142 species (covering 12% of endemic Italian flora) (Conti, 1998). The average yearly precipitation is approximately 800 mm.

1.6 Thesis outline

To achieve the main goal of discriminating plant species by using hyperspectral remote sensing, various aspects and alternatives have been explored. The chapters of this thesis, apart from the introduction and synthesis, have been written as stand-alone articles for peer-reviewed journals and can be read separately from the rest of the thesis. As a result, in a number of chapters overlap occurs in the sections "Introduction" and "Method".

Chapter 2 investigates the nature of post-harvest spectral changes in green leaves and their implications for widely used vegetation spectral indices, in order to determine a "safe" period of time within which spectral properties remain significantly unchanged. This was important because in most of the subsequent chapters leaves have been collected in the field and transported to the laboratory for spectral measurement since *in situ* spectroscopic measurements are often impractical because of poor or highly variable lighting conditions and inaccessibility for portable spectral equipment.

In Chapter 3, we compare the performance of different discrimination procedures and propose specific regions of the spectrum with the highest discriminating property.

The aim of Chapter 4 is to discriminate plant species by measuring spectral dissimilarities among different species, using four spectral similarity measures. In addition, we investigate the relative performance of these similarity measures in the context of discriminating plant species.

Chapter 5 examines the nature and magnitude of changes in spectral properties offered by a phenological event (i.e., flowering), with regard to maximizing species discrimination.

Chapter 6 investigates the utility of spectral unmixing techniques with airborne hyperspectral imagery (HyMap) for identifying shrub and tree species composition at pixel level (i.e., the type and number of species per pixel) in a semi-natural Mediterranean landscape, which would provide spatial information on the species distribution at landscape level.

Finally, Chapter 7 summarises all the findings in the context of the possibilities offered by hyperspectral remote sensing for plant species discrimination.

A number of investigations (chapter 3, 4 and 5) involved laboratory based spectroscopy of plant materials, with the assumption that detached leaves would retain spectral characteristics similar to that of in situ measurements. However, as the leaves dehydrate after detachment from the plant, it was important to know the "safe" time period within which the measurements remain similar to an in situ condition.

The aim of this chapter was to establish the "safe" time period for different species types and for different vegetation indices. Results from this investigation were essential for the subsequent chapters which assume that the laboratory measurements were representing an in situ state.

Chapter 2

Changes in spectral properties following leaf clipping and its implications on spectral indices

This chapter based on
Md. Istiak Sobhan, Moses A. Cho, Andrew K. Skidmore, Jan de Leeuw
(In review)
Changes in spectral properties following leaf clipping and its implications on spectral indices. Remote Sensing of Environment

Abstract

The objective of this study was to investigate the spectra of green leaves change after harvesting, and the implications for some widely used vegetation indices in order to elucidate the period of time within which spectral properties remain significantly unchanged. Leaf specimens of eleven species were harvested and spectral measurements were made at different time intervals. Readings were repeated at time 0, 1, 2, 3, 4, 6, 8, 12, 24, 36 and 48 hours from leaf collection and vegetation indices were calculated from these measurements. In order to observe at what point in time indices start to vary significantly from first reading (t_0) in leaf reflectance, two sample *t-test* with Bonferroni correction were conducted between the (t_0) and subsequent readings. The results reveal that the spectral properties of fresh leaves change significantly over time after detachment from the plant. A safe period during which spectral measurements under laboratory condition can be made (irrespective of variations caused by species) was found to be around six hours. However, the rate of change differs greatly due to the leaf structure of different species. Although leaf dehydration influences reflectance across the whole spectrum following detachment, the effects are more pronounce for NIR and SWIR compared with the visible part of the electro-magnetic spectrum. In the initial phase of the dehydration the indices which use NIR and SWIR wavebands started to change due to the rapid water loss. The changes were particularly pronounced for water indices such as NDWI and MSI, and for all species NDWI and MSI may be used to conservatively estimate the safe period for measurements. As the reflectance in NIR wavebands increase, indices such as REP and NDVI were also affected. Very little change was observed for the pigment based indices during the first 8 hours of the measurement, but these indices subsequently declined probably due to the deterioration of chlorophyll.

Keywords: Spectroscopy; leaf clipping; leaf dehydration; spectral indices

2.1 Introduction

Plant canopies play an important role in the exchange of water, energy and greenhouse gases between vegetation and the atmosphere (Blackburn, 1998a). These processes are controlled by foliar biochemical content e.g. chlorophyll, nitrogen concentrations (Asner, 1998) and the leaf hydration state. Hence information of leaf biochemistry could help to predict these processes. However, estimates of canopy chemistry by traditional field sampling methods are time consuming and difficult to undertake for large areas (Curran et al., 1991; Kokaly and Clark, 1999). Remote sensing provides a means of estimating canopy biochemistry over such large extent. Many studies have sought to understand the spectral properties of leaves, one of the primary controls of canopy reflectance (Gates et al., 1965; Boochs et al., 1990; Yoder and Pettigrew-Crosby, 1995; Blackburn, 1998b).

As detailed in Table 2.1, leaves are often collected in the field and transported to the laboratory for spectral measurement, because *in situ* spectroscopic measurements are often impractical due to poor or highly variable lighting conditions and inaccessibility for portable spectral equipments (Foley et al., 2006). However, a limitation with this approach is that leaf physiology changes over time. Harvested leaves are subjected to considerable stress due to the sudden disruption in energy, nutrient and hormone supplies (Page et al., 2001). The stress is manifested by changes in leaf biochemical constituents such as water content and pigment concentration (Böttcher et al., 2001; Able et al., 2005). As such changes in leaf physiology affect its spectral properties (Horler et al., 1983; Hunt and Rock 1989; Carter, 1993, 1994; Peñuelas et al., 1994; Carter and Knapp, 2001), results based on laboratory measurements may not truly reflect *in situ* spectra. A study of the literature (Table 2.1) shows varying time lapses between leaf specimen collection and spectral measurement.

Several specimen handling techniques have been proposed to maintain the physiological status of leaves after harvest in the field. For example, leaves have been stored in air tight plastic bags with a moist paper towel or a small quantity of water in order to construct a humid environment which reduces the vapour pressure gradient between the leaf and air (Horler et al., 1983; Skidmore and Knowles 1996; Datt, 1999; Foley et al., 2006). In other experiments, leaf petioles were cut and dipped into water to protect them from dehydration (Peñuelas et al., 1994; Foley et al., 2006). Artificial cooling or keeping the specimen in dark cold room has also been used to reduce transpiration (Lacaze and Joffre, 1994; Cao, 2000; Sims and Gamon, 2002). Covered metal containers were also used for similar purpose (Keegan et al., 1955).

A number of recent studies have developed indices which are sensitive to water e.g. normalized different water index (NDWI), moisture stress index (MSI) and chlorophyll stress (e.g. red-edge position (REP),

photochemical reflectance index (PRI)). Studies on post-harvest changes in leaf spectra are rare (e.g., Richardson and Berlyn 2002; Foley et al. 2006). There are no studies which give details as to when crucial spectral properties of leaves such as vegetation indices significantly differ from values obtained immediately after harvest. Further, a complete understanding of this dehydration process and its implication on various spectral measurements remain to be established (Horler et al., 1983; Richardson and Berlyn, 2002; Foley et al., 2006).

Table 2.1 Articles where leaf spectral reflectance was measured in laboratory after collecting specimen from the plant.

Time gap between leaf sample collection & spectral measurement	References
15 min	Asner (1998), Kumar and Skidmore (1998).
1 hour	Cochrane (2000)
2 hours	Schmidt and Skidmore (2001); Cho and Skidmore (2006)
4 hours	Vaiphasa et al. (2005), Skidmore and Knowles (1996)
6 hours	Horler et al. (1983)
10 hours	Ramsey III and Jensen (1996)
12 hours	Clark et al. (2005)
24 hours	Hunt and Rock (1989)
same day	Zarco-Tejada et al. (2005)
immediate after harvest but no time specification	Peñuelas et al. (1994); Blackburn, (1998a)
not mentioned	Gao (1996); Blackburn (1998b); Carter and Knapp (2001); Gitelson et al. (2002); Gong et al. (2002); Sims and Gamon (2002)

The main objective of this study was to investigate the nature of post-harvest spectral changes for green leaves and its implications for widely used vegetation spectral indices in order to determine a “safe” period of time within which spectral properties remain significantly unchanged. Leaf specimens of eleven species were harvested and spectral measurements were made at different time intervals. Statistical analyses were subsequently carried out in order to determine the time when various vegetation indices become significantly different from their initial values.

2.2 Materials and method

2.2.1 Collection and preservation of leaf specimens

Mature leaf specimens of eleven species (Table 2.2) were collected in July 2005 in Enschede, The Netherlands. After detachment from the plant, the

leaves of each species were randomly divided into eleven sets and placed in marked plastic sample bags. Each of these bags, 121 in total had an adequate number of leaves for a successful spectral measurement. The sample bags were immediately taken to the laboratory and stored in the dark at room temperature (±25˚C), without applying any extra preservation and handling techniques. In addition to examine responses for individual species, they were also grouped using their leaf structure (e.g., thickness and protection mechanism) to examine each group's response to dehydration.

Table 2.2 List of species used in the experiment with different leaf types.

Species	Leaf type	Group
Abies grandis	Needle leaf	2
Acer pseudoplatanus	Large leaf with medium thickness	2
Betula pendula	Medium leaf with medium thickness	2
Fagus sylvatica	Medium size with glossy surface	2
Ilex aquifolium	Thick cuticle layered	4
Pinus nigra	Needle leaf	3
Quercus robur	Large leaf with medium thickness	2
Robinia pseudoacacia	Small leaf, soft and fragile	1
Thuja orientalis	Gymnosperm	3
Rhododendron sp.	Large leaf with thick cuticle layer	4
Grass (c4)	Thin leaf	1

2.2.2 Collection of leaf spectra

The first sets of spectral measurements were conducted within thirty minutes from the time of field collection and were labelled as base readings (t_0). Subsequent measurements (using a new bag each time) were made after 1, 2, 3, 4, 6, 8, 12, 24, 36 and 48 hours from the time of field collection. The interval between measurements was shorter initially with the assumption that changes would be faster during this period. Thus for every species we had eleven readings at different time intervals. The spectra were measured in a laboratory (i.e., dark room, ±25˚C) following the method described by Vaiphasa et al. (2005) in order to avoid ambient light sources unrelated to the true spectral signal of the leaves.

A GER 3700 (Geophysical and Environmental Research Corporation, Buffalo, New York) spectroradiometer measured the reflectance spectra. The GER 3700 is a three dispersion grating spectroradiometer using Si and PbS detectors with a single field of view. The wavelength range is from 325 nm to 2500 nm, with sampling intervals of 1.5 nm between 325 nm and 1050 nm, 6.2 nm between 1050 nm and 1900 nm and 9.5 nm in the 1900 nm to 2500 nm range. The Full Width Half Maxima (FWHM) is 3 nm, 11 nm and 16 nm in the 325 nm to 1050 nm range, 1050 nm to 1900 nm range and 1900 nm to 2500 nm range respectively. Although the spectrometer records up to 647 bands, due to the high noise at the extreme short wavelength area only the spectral range between 400 nm

and 2500 nm was analysed, which contains 597 wavebands. The sensor, equipped with a 1.5 m long fiber optic cable (25˚ field of view) was mounted on a tripod and positioned 15 cm at nadir above the target leaves. A light source (Lowel Pro-Light with 14.5V/50W/3200K JCV halogen lamp), pointing at the centre of the leaf plate, was placed at 30 degrees off-nadir approximately 40 cm from the target.

For each species a single leaf layer was formed on top of a flat black plate covering the entire viewing area of the sensor. For species comprising small leaves and needles (Group 1 & 3) more than one leaf layer was required to cover the plate, but the plant material applied was the minimum required to achieve the objective of covering the plate. Twenty spectral measurements were obtained from each sample plate, and averaged to produce a single spectrum in order to reduce specular behaviour (Schmidt and Skidmore, 2001). Twenty such repetitions were made per bag; in other words fresh leaves were placed on the plate 20 times and 20 spectra obtained at each time period. The radiance data was converted to reflectance using scans of a white "Spectralon" reference panel. We used a Savitzky-Golay (Savitzky and Golay, 1964) second order polynomial least-squares function of five bands window to spectrally smooth our data (Kumar and Skidmore, 1998; Schmidt and Skidmore, 2004).

2.2.3 Data analysis

2.2.3.1 Use of indices

To quantify the variations in spectral signature over time six well known vegetation indices (Huete and Jackson, 1988; Qi et al., 1995) were adopted to detect stress. In addition, we also measured the absolute peak reflectance in near infra-red (NIR) (750 – 800 nm) as an indicator of the volume of intercellular space in leaves.

(i) Narrow band NDVI
Normalized Different Vegetation Index (NDVI) (Rouse et al., 1973) is the most popular vegetation index in remote sensing. With the advent of hyperspectral spectrometry various narrow band combinations have been assessed described by Mutanga and Skidmore (2004) (Eq 1).

$$NDVI = \frac{(R_{833} - R_{680})}{(R_{833} + R_{680})} \qquad \text{Eq.1}$$

(ii) Red-Edge Position (REP)

The red edge is a unique feature of green vegetation resulting from two optical properties of plants - the chlorophyll absorption providing low red reflectance, and internal leaf scattering yielding high near infrared reflectance (Collins, 1978; Horler et al., 1983). Within this red edge region the point of maximum slope (or inflection point) is referred to red edge position (Filella and Peñuelas, 1994). Typically it occurs between 680 – 780 nm. Although it is principally sensitive to chlorophyll, the red-edge has been shown sensitive also to water, foliage mass and leaf area index (LAI) (Thomas and Gaussman, 1987; Curran et al., 1990; Curran et al., 1991; Danson and Plummer, 1995; Dawson and Curran, 1998). Two simple techniques for locating the REP were applied, (i) linear four-point interpolation technique (Guyot and Baret, 1988) and (ii) linear extrapolation technique (Cho and Skidmore, 2006).

Linear four-point interpolation technique

The linear four-point interpolation method (Guyot and Baret, 1988) assumes that the reflectance curve at the red edge can be simplified to a straight line centered near the midpoint between the reflectance in the near infra-red (NIR) at about 780 nm and the reflectance minimum of the chlorophyll absorption feature at about 670 nm. It uses four wavebands (670, 700, 740 and 780 nm), and the REP is determined by using a two-step calculation procedure:

Calculation of the reflectance at the inflection point

$$R_{re} = \frac{\left(R_{670} + R_{780}\right)}{2} \qquad \text{Eq.2}$$

where, R is the reflectance.

Calculation of the red edge wavelength or red edge position is according to Eq. 3

$$REP = 700 + 40\left(\frac{R_{re} - R_{700}}{R_{740} - R_{700}}\right) \qquad \text{Eq.3}$$

where, 700 and 40 are constants resulting from interpolation in the 700–740 nm interval.

Linear extrapolation technique

The technique is based on linear extrapolation of two straight lines (Eqs. 4 and 5) through two points on the far-red (680 to 700 nm) and two points on the NIR (725 to 760 nm) flanks of the first derivative

reflectance spectrum (FDR) of the red edge region (Cho and Skidmore, 2006). The REP is then defined by the wavelength value at the intersection of the straight lines (Eqs. 4 and 5).

Far-red line: $FDR = m_1\lambda + c_1$ Eq.4

NIR line: $FDR = m_2\lambda + c_2$ Eq.5

Where, m and c represent the slope and intercept of the straight lines. At the intersection, the two lines have equal λ (wavelength) and FDR values. Therefore, the REP, which is the λ at the intersection and is given by Eq. 6.

$$REP = \frac{-(c_1 - c_2)}{(m_1 - m_2)}$$ Eq.6

Four coordinate points (or wavebands) are required to calculate the REP by the linear extrapolation method; for instance, two bands near 680 and 700 nm to calculate m_1 and c_1 for the far-red line and two bands near 725 and 760 nm to calculate m_2 and c_2 for the NIR line.

(iii) Normalized difference water index

The normalize difference water index (NDWI) was developed to measure the liquid content in vegetation canopies and leaves which interact with the incoming radiation (Gao, 1996). NDWIs increase with higher LAI, showing its sensitivity to the total water amount in the stack. NDWI was calculated (Eq. 7) as described by Gao (1996).

$$NDWI = \frac{(R_{864} - R_{1245})}{(R_{864} + R_{1245})}$$ Eq.7

(iv) Moisture stress index

The moisture stress index (MSI) (Rock et al., 1986) is linearly correlated to both relative water content (RWC) and equivalent water thickness (EWT) of leaves (Hunt and Rock 1989). In addition RWC has been found to be correlated with leaf water content index (LWCI) (Hunt et al., 1987). MSI was calculated as described by Hunt and Rock (1989) (Eq. 8).

$$MSI = \frac{R_{1600}}{R_{820}}$$ Eq.8

(v) Simple Ratio Pigment Index

The simple ratio pigment index (SRPI) is based on carotenoid/chlorophyll ratio (Peñuelas et al., 1993; Peñuelas et al., 1995; Peñuelas et al.,

1995). Both carotenoids and chlorophyll absorb concurrently in the 300 to 500 nm ranges, but carotenoids do not absorb strongly in the red spectral area. Two narrow bands, one centered at 430 and another cantered at 680 nm, were used to calculate the index as described by Peñuelas et al. (1995) (Eq. 9).

$$SRPI = \frac{R_{430}}{R_{680}} \qquad \text{Eq.9}$$

(vi) Physiological/photochemical Reflectance Index

The physiological/photochemical reflectance index (PRI) (Gamon et al., 1992; Gamon et al., 1997; Sims and Gamon, 2002) is another widely used index related to carotenoid/chlorophyll ratio in green leaves. This index was originally developed for estimating changes in the xanthophyll pigment cycle, thereby deriving photosynthetic light use efficiency (Peñuelas et al., 1995; Gamon et al., 1997). PRI (Eq. 10) also compares the reflectance of red and blue region of the spectrum as it measures the reflectance on either side of the green hump around 550 nm.

$$PRI = \frac{(R_{531} - R_{570})}{(R_{531} + R_{570})} \qquad \text{Eq.10}$$

(vii) Highest absolute reflectance in NIR plateau

The highest absolute reflectance in NIR plateau between 740-1200 nm results from the high degree of intra- and inter leaf scattering. The optimum spectral region for sensing in the near-infrared region is situated between 750 – 800 nm (Tucker, 1979), which influence most of the indices that use the NIR region.

2.2.4 Statistical analysis

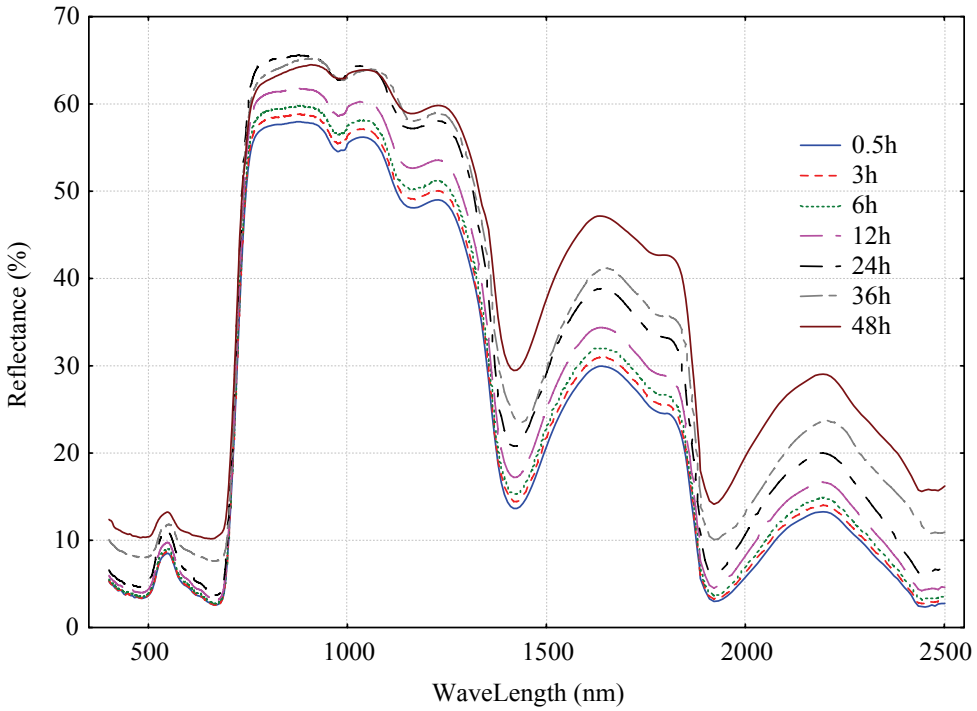

Figure 2.1 Changing nature of reflectance spectra of *Betula pendula* leaves, from immediately after collection (0.5 h) through 48 hours after collection.

For each species, we performed ten two sample two-tailed *t-test* to examine the differences in mean index value between initial (t_0) and the ten subsequent spectral measurements (t_1, t_2, ...t_{10}). We used this method to reveal the time at which indices became significantly different from the initial reading. The *t-test* was considered appropriate, as the data was confirmed to be normally distributed, and the sample size of two treatments was equal and large (n=20) (Moore and McCabe, 2003). The critical value was set at $\dot{\alpha}$ = 0.005 following a Bonferroni correction to account for the increased probability to reject the null hypothesis due to the multiple comparisons. Next, we investigated whether the changes of the indices over time differed between species using a two way ANOVA. To address this question we investigated the statistical significance of the interaction between species and time.

2.2.5 Histology

Electron microscopic scans of the cross section of leaves were made in order to visualize internal anatomical change to the leaves between different time periods. The scans were made using a cryo-scanning electronic microscope. For each species two leaves were examined within

two hours of collection and then after approximately 24 hours after collection.

Specimens were mounted in clamp holders and frozen in liquid nitrogen and subsequently placed in a dedicated cryo-preparation chamber (Oxford Instruments CT 1500 HF, Eynsham, UK). In this cryo-preparation chamber the specimen were fractured with a cold scalpel and freeze dried for 3 minutes at -90°C at 1 x 8-4 Pa to remove water vapour contamination. After 3 minutes specimens were sputter coated with a layer of 10 nm Pt at the same temperature. The sample was cryo-transferred into the field emission scanning microscope (JEOL 6300F, Japan) on a sample stage at -180°C. The analyses were performed at a working distance of 16 mm, with SE detection at 3.5 kV.

All images were recorded digitally (Orion, 6 E.L.I. sprl, Charleroi Belgium) at a scan rate of 100 seconds (full frame) at the size of 2528 x 2030, 8 bit. The images were optimized and resized for publication by Adobe Photoshop CS.

2.3 Results

2.3.1 Post-harvest changes in leaf spectra

Visually, most of the leaves remained unchanged during the first six hours. The first sign of wilting was visible in *Robinia pseudoacacia* and in the grass species. Subsequently other species started showing signs of desiccation within 12 hours with the exception of *Ilex aquifolium* and *Rhododendron* sp., which appeared unchanged after up to 48 hours of detachment.

Turning to the reflectance spectra, within the first few hours following the specimen collection, spectral changes were confined to the NIR and short wave infra-red (SWIR). For most species, NIR and SWIR reflectance increased with time. Within the first 24-36 hours, reflectance in the NIR region increased by 10-15 percent in *Robinia pseudoacacia, Betula pendula, Acer pseudoplatanus, Fagus sylvatica, Quercus robur* and grass species. After that period of time, NIR reflectance increment saturated and even decreased a little in some species (Figure 2.1). But for other species such as, *Ilex aquifolium* and *Rhododendron* sp. NIR reflectance kept increasing up to 48 hours. Changes in SWIR were somewhat more continuous, although the rate varied among species. A band by band two sample *t-test* between initial and subsequent time lapse measurements of *Betula pendula* (Figure 2.2) revealed the sensitivity of different spectral regions to dehydration.

2.3.2 Post-harvest changes in vegetation indices

The *t-test* results (Figure 2.4) revealed that, among the indices, NDWI and MSI were the first two indices which showed significant changes over

time for all species. They were followed by REPs, NDVI and LM-NIR, while PRI and SRPI were slowest to response after leaf detachment (Figure 2.4). REP extracted by the linear interpolation method showed higher

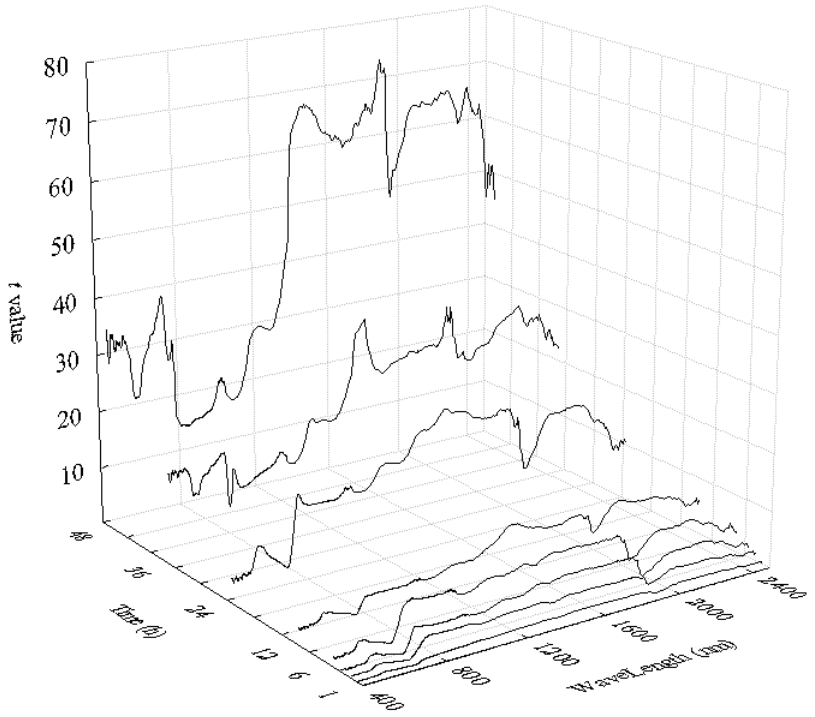

Figure 2.2 Plot showing the sensitivity of different spectral bands against dehydration calculated through band by band two sample *t-tests* between initial (t_0) and subsequent spectral measurements of *B. pendula* (critical $t_{\alpha = 0.005} = 2.845$).

sensitivity to time or leaf dehydration than the REP extracted using the linear extrapolation method. As depicted in Table 2.3, 6 species out the 11 have shown that significant changes took place earlier for the REP as calculated by the linear interpolation method compared to none for the REP calculated using the linear extrapolation technique.

The indices may be categorised into three groups according to the pattern of change. The first group consisting of the REPs, NDVI and LM-NIR showed a hump-shape pattern. The value of the spectral indices increased with time to a maximum point before started to decline (Figure 2.5). A third order polynomial curve determined the turning point for each index and species. We calculated the first derivative to localize the inflection point (Figure 2.5). The first derivative was calculated from the polynomial function and equated to zero (i.e., at the turning point the derivative function or rate of change equals zero). This process yielded a quadratic equation which was then solved for time using the quadratic

formula. The time taken by each index to attain its turning point differed among species (Table 2.4). The second group of indices consisting of NDWI, SRPI and PRI decreased with time in a linear fashion. A significant linear relationship was also observed between time taken for the REPs to reach the turning point and the time when SRPI or PRI became significantly different from their readings at t_0 (Figure 2.6). The only remaining index MSI showed a linear increasing trend.

Table 2.3 Time (in hours) at which the indices became significantly different from time t_0.

Species	Indices							
	REP (Guyot and Baret)	REP (Cho and Skidmore)	NDVI	NDWI	MSI	SRPI	PRI	LM-NIR
A. grandis	12	12	12	8	8	12	12	12
A. pseudoplatanus	8	12	8	6	8	8	12	8
B. pendula	8	12	12	8	6	8	12	8
F. sylvatica	8	8	12	6	8	12	24	8
I. aquifolium	24	24	24	12	12	24	24	12
P. nigra	12	12	12	8	8	12	12	8
Q. robur	8	12	12	6	8	12	24	8
R. pseudoacacia	6	8	8	6	6	8	8	6
T. orientalis	8	12	8	8	8	12	12	8
Rhododendron sp.	24	24	36	12	12	24	36	24
Grass (c4)	6	8	8	6	6	8	8	6

2.3.3. Influence of species on spectral change

The results of two-way ANOVA were used to investigate the influence of species on spectral change and revealed that there was a significant species effect on spectral changes when considering all the indices together $F(1, 80) = 1100$, $p < 0.000$. The result also revealed that a significant interaction did exist between species and time, $F(80, 64) = 10.0$, $p < .0001$. But when we used groups of species (Table 2.2) instead of individuals as predictor variables and indices of similar type as dependent variables, the interaction was only significant between species groups and time while using two water indices $F(6, 16) = 4.6$, $p < 0.0001$.

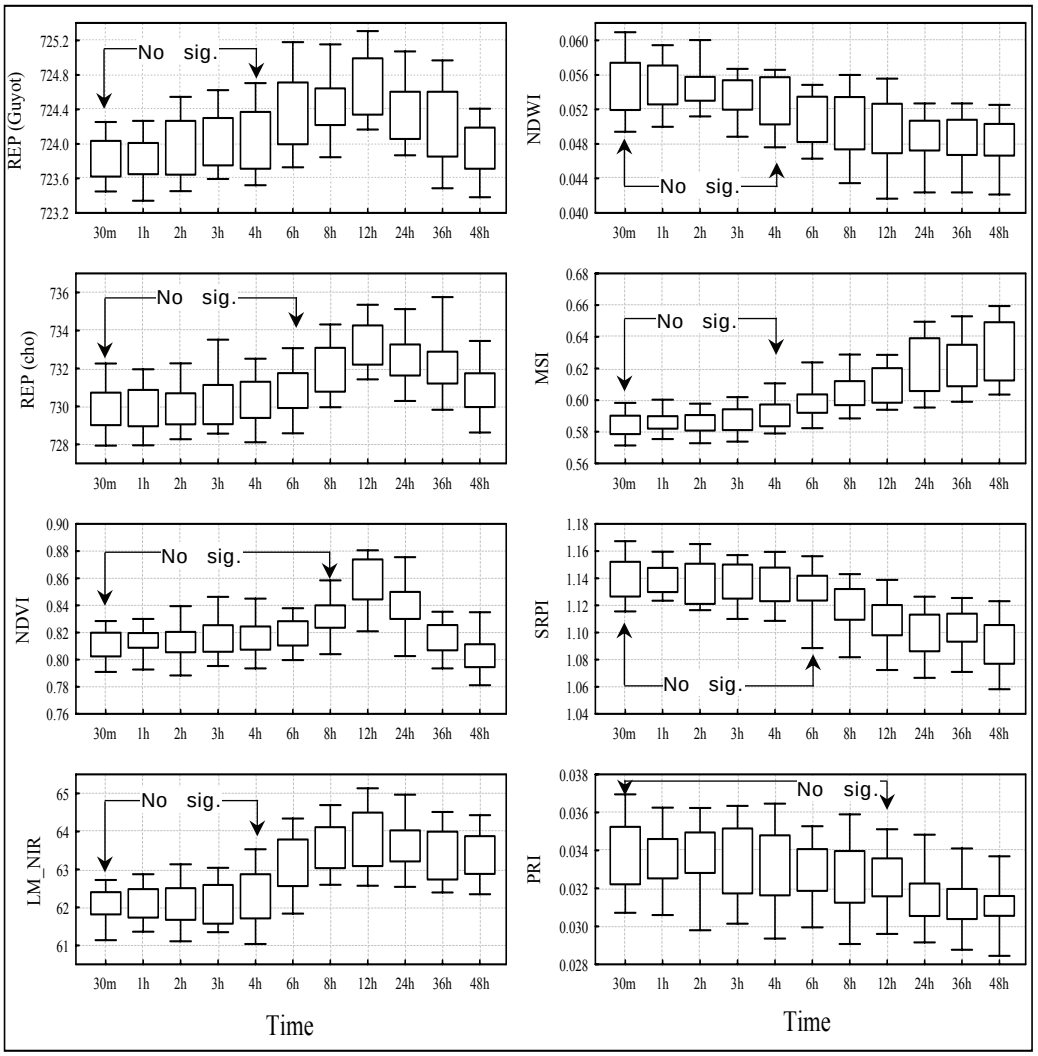

Figure 2.3 Changes of indices with progressive delay in the measurements in *B. pendula.* Arrows indicate time frame (h) within which no significant ($p<0.005$) differences of index values were observed from the initial readings.

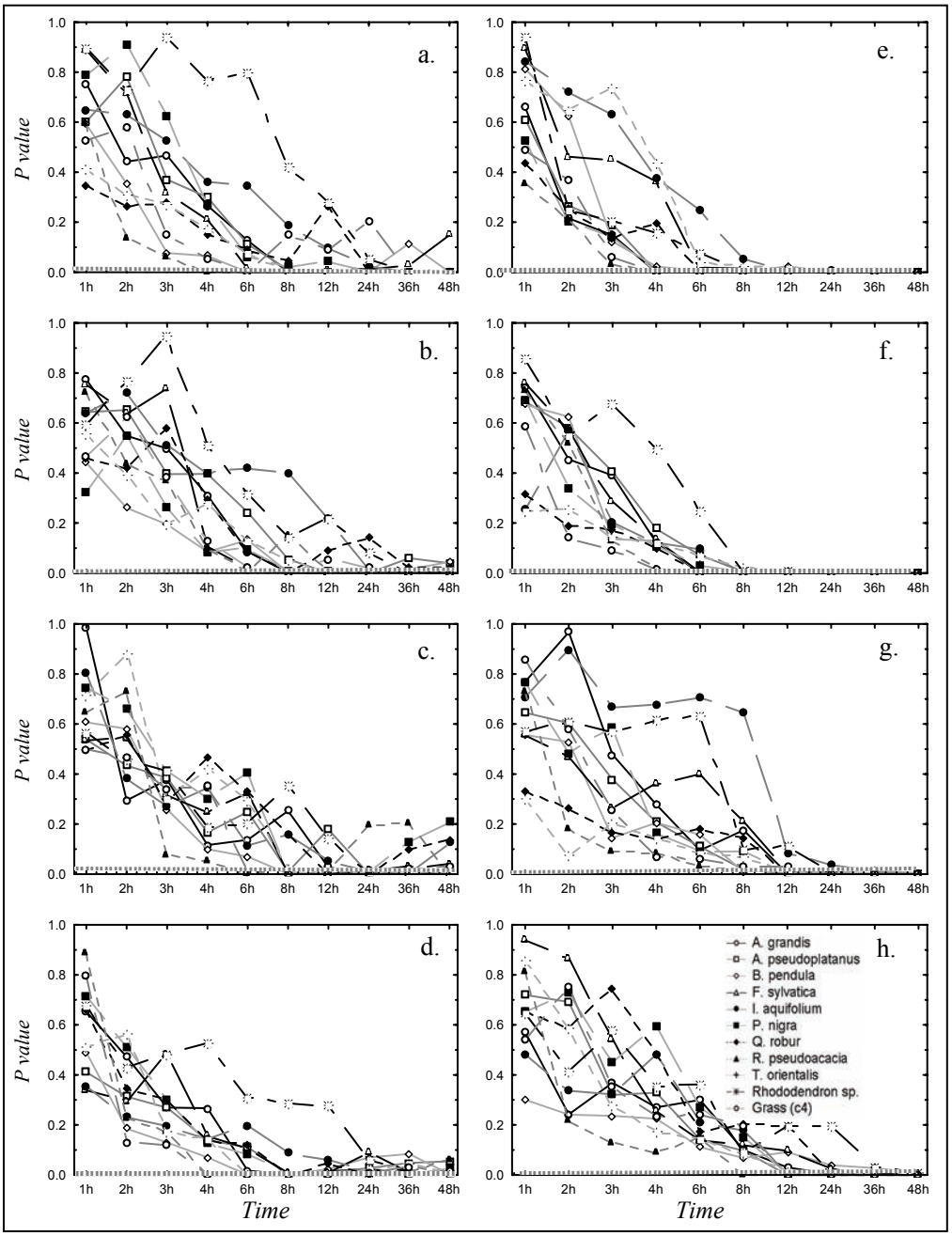

Figure 2.4 The figure shows the time at which indices in different species became statistically significant different from the base reading. Indices measured were: (a) REP (Guyot); (b) REP (Cho); (c) NDVI; (d) Local maximum in NRI; (e) NDWI; (f) MSI; (g) SRPI and (h) PRI. Dashed line shows the significant *p* level line.

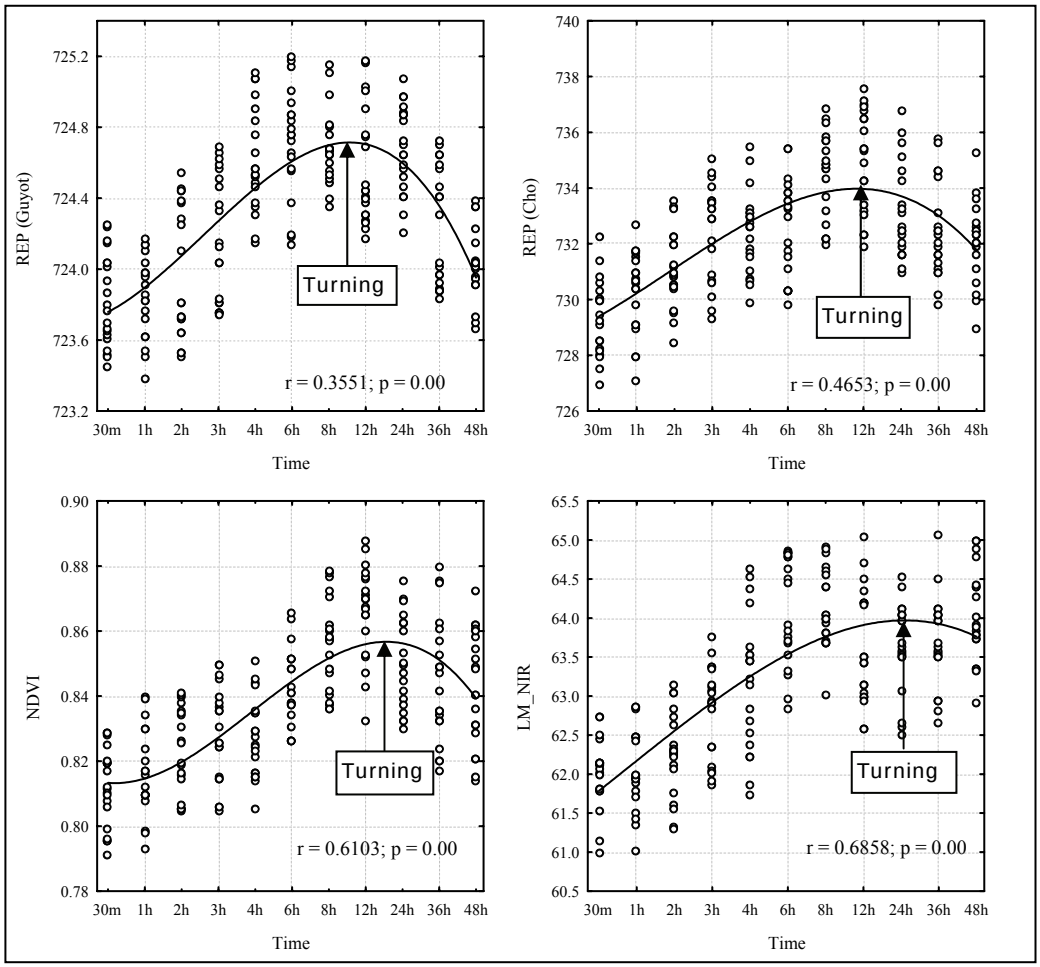

Figure 2.5 Figure shows the use of polynomial fit lines to calculate the inflection or turning points of the indices, at which the controlling factors shift their dominance, example from *B. pendula* leaves.

Table 2.4. The time taken by these indices to attain its turning points for different species.

Species	Time (h)			
	REP (Guyot)	REP(Cho)	NDVI	LM_NIR
Abies grandis	16	17	17	20
Acer pseudoplatanus	9.5	9	10	18
Betula pendula	11	12	14	25
Fagus sylvatica	18	20	18	36
Ilex aquifolium	30	28	36	42
Pinus nigra	20	18	20	38
Quercus robur	18	19	19	36
Robinia pseudoacacia	8	8	10	16
Thuja orientalis	19	20	24	40
Rhododendron sp.	34	35	38	48
Grass (c4)	9	10	10	15

2.3.4 Histology

Cross-sections of leaves produced by histological analysis depicted the changes between fresh and partly dried leaf specimens of different species. It is evident from cross-sections that the speed of dehydration and associated structural changes were different depending on a species

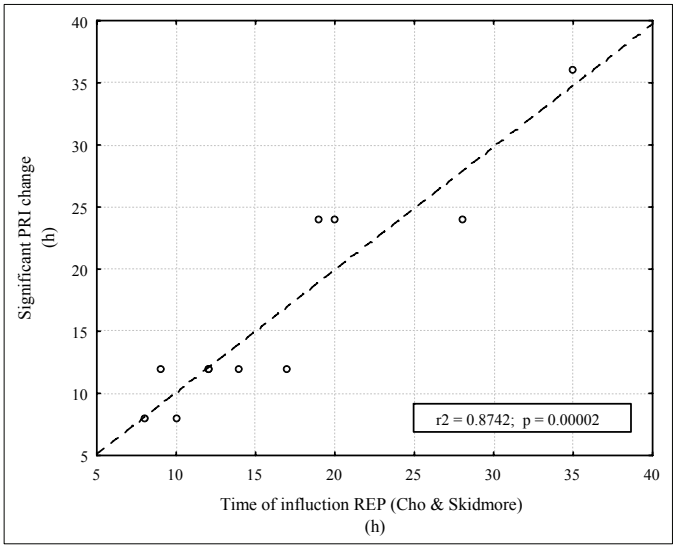

Figure 2.6 Figure shows the linear relationship between time at which PRI change significantly from t_0 reading and REP to reach the turning points for different species.

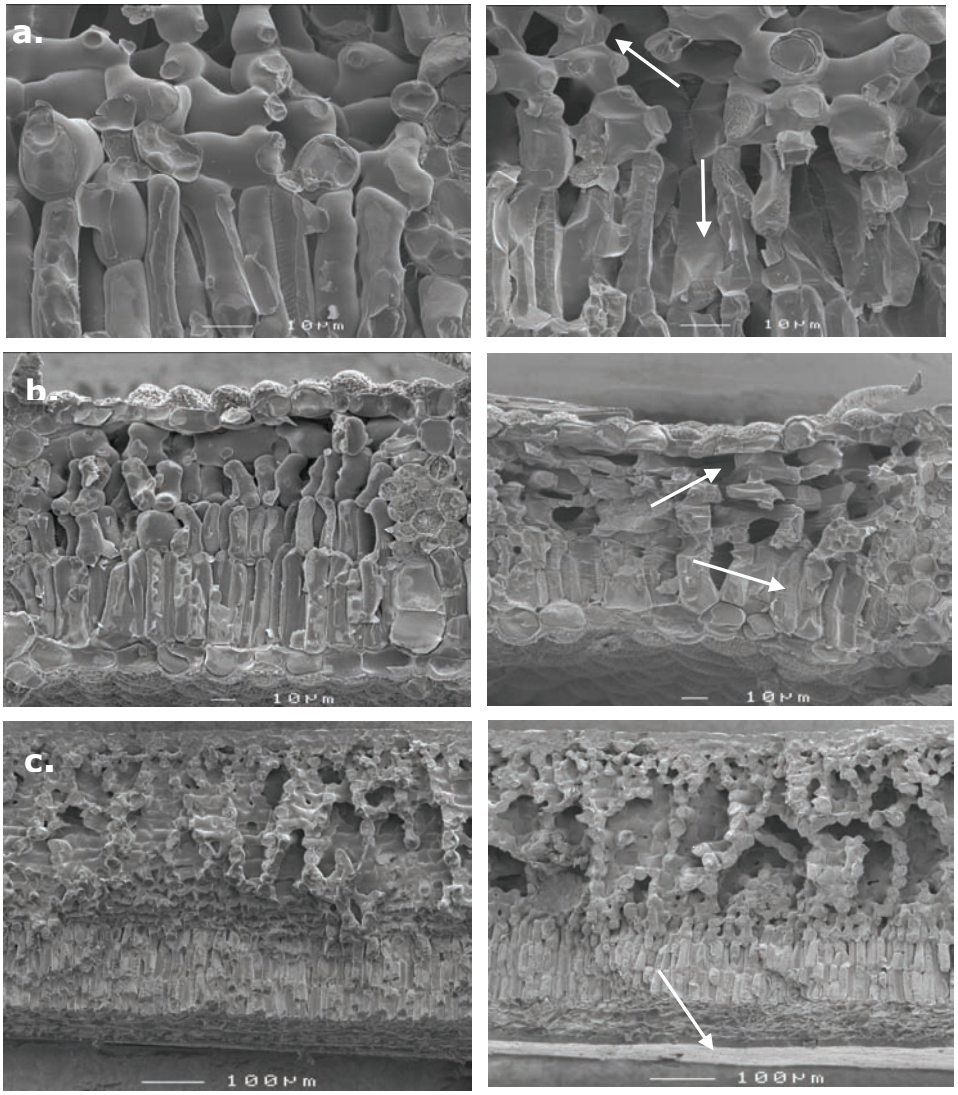

Figure 2.7 Leaf section produced by the histological analysis. Pictures on the left side are from within 2 hours of collection and picture on the right side are from approximately 24 hours after collection (a) *Fagus sylvatica* (b) *Robinia pseudoacacia* (c) *Ilex aquifolium*. Note the white arrows in the first two rows showing shrinkage and collapse of the mesophyll cells. In the third row the arrow indicates the thick protective layer of wax on the epidermis.

ability to withstand desiccation. As an example the sections of three species with different leaf structure are displayed in Figure 2.7; *Robinia pseudoacacia* with thin and fragile leaves, *Fagus sylvatica* with a thin protection of waxy layer on the epidermis and *Ilex aquifolium* with thick

and thick waxy protection on the epidermis. Both *Fagus sylvatica* and *Robinia pseudoacacia* showed visible change with appreciable shrinkage in cell walls (white arrow) and increased intercellular spaces due to the dehydration of cytoplasm compared with their fresh leaf structures. In *Robinia pseudoacacia,* the transformation was more prominent with the collapse of the spongy mesophyll layer causing a reduction in the overall leaf thickness. Meanwhile, only slight changes in the volume of the intercellular spaces could be observed for *Ilex aquifolium.* Across the species, changes were more prominent in the spongy mesophyll layer compared with the palisade mesophyll. Similar trends were observed for the other species (not shown in Figure 2.7).

2.4 Discussion

The study demonstrates that the spectral properties of harvested fresh leaves change significantly over time. However, the rate of change varies depending on plant species. Changes also varied considerably between different spectral region and or spectral indices.

Spectral measurements carried out within the first six hours after harvesting leaves from plants show no significant difference from the initial measurement, irrespective of the variations caused by different species (Table 2.3). Within this period of time, harvested leaves preserved the same spectral information content as from *in situ* measurements. Within this “safe” time period no vegetation indices changed significantly for any of the species. However, the use of improved preservation or handling, such as refrigeration or humidification may increase the “safe” time period for sampling.

The post-harvest effect on leaf spectra depends on the species (Table 2.3 and Figure 2.4). *Robinia pseudoacacia* and grass species proved to be the most sensitive to leaf detachment, as they showed significant changes in many indices within six hours. Most of the other broad leaf species (*Acer pseudoplatanus, Betula pendula, Fagus sylvatica* and *Quercus robur*) showed varied responses for different indices, though the “safe” periods of six hours was limited by the two water indices. The needle leaf (*Abies grandis, Pinus nigra*) and gymnosperm (*Thuja orientalis*) showed higher resistance to change and their “safe” period extended up to eight hours. Finally two broad leaf species protected by a thick cuticle (*Ilex aquifolium, Rhododendron sp*) showed the highest resistance to spectral change and show no significant changes up to twelve hours of detachment. The results confirm with earlier research which demonstrated that thicker leaves have higher protection against dehydration compared with the thinner leaves (Hunt and Rock 1989; Aldakheel and Danson, 1997; Richardson and Berlyn, 2002; Foley et al., 2006), though specific “safe” periods were not defined by these studies.

Band-by-band analysis (Figure 2.2) of reflectance spectra showed that post harvest spectral changes were initially confined to NIR and SWIR.

The visible region was more resistant to spectral change and that region did not vary significantly during the first 8 hours of the experiment. The increase in the NIR reflectance observed in this study may be due to shrinkage of the mesophyll cells and increase in the volume of the intercellular spaces resulting from post-harvest loss of water as revealed by the leaf cross sections (Figure 2.6). Gausman et al. (1970) shows that the NIR reflectance is positively correlated with the volume of the intercellular air space in the mesophyll layer of leaves and leaf dehydration increases NIR reflectance (Horler et al., 1983; Jacquemond and Baret, 1990; Carter, 1991). The loss of water may also account for the sensitivity of the SWIR which contains the major leaf water absorption bands (Curran, 1989; Aldakheel and Danson, 1997). Alternatively visible reflectance spectra are primarily controlled by the absorption of the pigment molecules and only later in the dehydration process pigments get damaged (Böttcher et al., 2001; Able et al., 2005).

Three groups of indices emerged from the study: the first group consists of REPs and NDVI; the second group includes the two water indices namely NDWI and MSI and the last group consists of the two photochemical indices SRPI and PRI. For the first group of indices, the "safe" periods varied widely from 6 hours to 24 hours depending on the species. It is interesting to note that although the REPs and NDVI are principally used for estimating leaf chlorophyll content and biomass (Chang and Collins, 1983; Curran et al., 1995; Clevers et al., 2002), they also appeared to be sensitive to changes in leaf water content confirming the results obtained by Horler et al. (1983). However, the results of this study suggest that REPs extracted by the linear extrapolation technique are less sensitive to leaf dehydration compared to the linear interpolation method. This may be attributed to the different bands used. The linear interpolation technique uses bands from the NIR side of the red edge and hence is more likely to have greater sensitivity to change of NIR reflectance. NDVI exhibit a longer "safe" period than the REP indices perhaps due to the saturation of NDVI above a certain leaf chlorophyll content (Seller, 1985; Gao et al., 2000). Furthermore, for NDVI and REPs a hump-shape pattern with a characteristic turning point (Figure 2.5) may be attributed to the change of dominance in the leaf property controlling the spectral reflectance, i.e., from leaf water content to pigment content. Shifts in the REP towards shorter wavelength have been associated with decrease in the leaf chlorophyll content (Horler et al., 1980; Boochs et al., 1990).

The two water indices were the most sensitive to leaf detachment for all species and defined the limiting factor for a "safe" period during which spectral reflectance measurements may be made. This result of water indices sensitivity are consistent with the change found in the original reflectance spectra, which showed a faster change in spectral regions that are related to the changes in the mesophyll tissue as a result of water loss.

Photochemical indices (SRPI and PRI) were least sensitive to change when leaves were detached because of the initial lack of movement in the visible part of the spectrum. The sensitivity of these indices depends on the ratio between leaf chlorophyll and carotenoid content (Peñuelas et al., 1995; Sims and Gamon, 2002) and the loss of chlorophyll results in a decrease in the SRPI and PRI, as chlorophyll generally declines at a faster rate than carotenoid when plants are under stress or water loss (Merzlyak et al., 1999; Sims and Gamon, 2002; Minekawa et al., 2005). This early loss of chlorophyll compared to carotenoid may be responsible for the delayed decrease in the values of SRPI and PRI (Figure 2.3). This loss of chlorophyll may also be the cause for a significant linear relationship (Figure 2.6) between time taken for the REPs to attain the turning point and the time when SRPI or PRI became significantly different from their t_0 readings.

2.5 Conclusion

The results of this study show that the spectral properties of fresh leaves change significantly over time from the time of harvest. A “safe” period to perform spectral measurement, irrespective of variations caused by species, was found to be six hours, though leaf samples must be stored in plastic bags and cool dark conditions. However, the rate of change in spectral indices differs due to the varying leaf structure of different species. Although leaf dehydration influences reflectance across the whole spectrum, the effects are more noticeable for NIR and SWIR compared with visible spectrum. Among the indices, the two water indices were most sensitive and in all species they defined the minimum “safe” period.

Acknowledgments

This study was financially supported by Nuffic and ITC. Thanks are also due to Jelger Kooistra for his support during laboratory measurements.

In chapter 2 it was shown that the laboratory measurements of leaves taken within six hours maintain the leaf's spectral characteristics similar to in situ measurements. In subsequent chapters (chapter 3, 4 and 5), "safe" time limit for laboratory measurements was respected.

In this chapter (chapter 3), laboratory measurements of leaf spectra from twenty-six tree species were used to investigate into various band selection procedures for species discrimination. The results identified that few spectral regions contain high information for species discrimination, and most of the bands were selected within those regions.

Chapter 3

Spectral regions for maximizing species discrimination

This chapter based on
Md. Istiak Sobhan, Chaichoke Vaiphasa, Andrew K. Skidmore
(Submitted after review)
Spectral regions for maximizing species discrimination.
Remote Sensing of Environment

Abstract

With imaging spectroscopy remote sensing of vegetation at a species level became possible. Various authors have tried to identify wavebands with the highest discriminating potential between vegetation types and species. However, these studies failed to recommend general waveband combinations which can replicate results across environments. This failure has been mostly attributed to the presence of information redundancy between bands of close proximity. To overcome this problem, this study identified spectral ranges able to discriminate between species. We used laboratory level leaf spectra of 26 tree species and four different commonly used discriminating techniques (Mann-Whitney U test, Principal Component Analysis, Stepwise Discriminant Analysis and a Genetic Neural Network based wrapper feature selection approach) to locate the dominant discriminating bands. It was found that these 4 spectral discrimination techniques selected bands from seven narrow regions of the spectrum (500-540, 630-650, 680-710, 740-760, 1280-1380, 1610-1680 and 2075-2175 nm) where discrimination between species is maximal. We tested the power of discrimination of the selected regions and the replicability of our findings. Discrimination strength was measured by comparing means of spectral distances (Bhattacharya distances) calculated between bands from the selected regions and bands from the whole spectrum. The result showed that the mean distances calculated from selected regions are significantly higher (p <0.05) for 315 species combinations (out of a total of 325). The reliability of the finding was confirmed by three independent data sets, which showed similar results. It is concluded that redundancy in hyperspectral vegetation spectra makes exact band selection very difficult, because in a narrow spectral range all the bands within carry similar information which facilitate the discrimination between species. This finding can play an important role when designing new broad band sensors specific for species mapping or “choosing” bands from adjustable airborne hyperspectral sensors.

Keywords: Spectroscopy, spectral region; U-test; Principal Component Analysis; Stepwise Discriminant Analysis; wrapper feature selection.

3.1 Introduction

With the advent of imaging spectroscopy, the qualitative and quantitative remote sensing of vegetation received a significant impulse. The high spectral resolution of hyperspectral images started to yield quality information about vegetation health, its chemical content and biomass (Curran, 1989; Curran et al., 1992; Peñuelas et al., 1997; Todd et al., 1998; Kokaly and Clark, 1999; Mutanga et al., 2003; Mutanga and Skidmore, 2004; Mutanga et al., 2004). The combination of this high spectral resolution with fine spatial resolution enabled scientists to start discriminating and mapping ecosystems and even species (Bajjouk et al., 1996; Gong et al., 1997; Cochrane, 2000; Schmidt and Skidmore, 2001; Kokaly et al., 2003; Schmidt and Skidmore, 2003; Silvestri et al., 2003; Thenkabail et al., 2004; Clark et al., 2005; Ramsey III et al., 2005; Vaiphasa et al., 2005). But to achieve the goal of species level discrimination, spectra collected from communities or ecosystems are not enough. A much finer resolution is necessary to detect, map and understand the spectral variations between species.

Various authors have successfully used leaf level reflectance spectra to discriminate between species (Cochrane, 2000; Yamano et al., 2003; Clark et al., 2005; Vaiphasa et al., 2005), though some claim that the leaf reflectance of different species is highly correlated due to their similar chemical composition (Portigal et al., 1997). Moreover, variations can occur within a species due to age differences, micro-climate, soil characteristics, precipitation, topography, phenology and a host of other environmental factors, including stresses (Gausman, 1985; Westman and Price, 1987; Carter, 1993; Carter, 1994; Portigal et al., 1997; Roberts et al., 1998; Gracia and Ustin, 2001; Smith et al., 2004). But as concentration of pigments and other bio-chemicals as well as leaf characteristics vary between species so does absorption and reflectance (Knipling, 1970; Asner, 1998; Martin et al., 1998; Schmidt and Skidmore, 2003).

The high spectral resolution of hyperspectral data is essential for capturing and discriminating subtle differences of the targets, but it also contains redundant information at the band level Bajwa et al. (2004), which makes computation difficult. To reduce this redundancy, scientists reduce the number of wavebands using a variety of techniques. Out of all these redundancy reduction techniques, one of the regular practices is band selection. In this method the highest discriminating bands are selected by using a number of discriminating statistics (e.g. principal component analysis, discriminant analysis)

Various authors (Cochrane, 2000; Schmidt and Skidmore, 2001; Schmidt and Skidmore, 2003; Thenkabail et al., 2004; Vaiphasa et al., 2005) have successfully used these methods to select informative bands in hyperspectral data and discriminate vegetation types or species. (Bajwa et al., 2004) also tried to identify bands for measuring soil electric

conductivity (EC) and cover canopy characteristics. While they became successful in discriminating vegetation types or species using their own spectral data, they failed to come up with a comparable list of wavebands. The cause of this discrepancy might be due to the high redundancy of information within nearby bands and/or utilization of different algorithms.

The present study evaluates the result of different waveband selection procedures by using laboratory quality reflectance spectra of 26 tree species. We compare the performance of different discrimination procedures and propose specific regions of the spectrum with the highest discriminating property.

3.2 Materials and method

3.2.1 Collection of leaf samples

Branches from sunlit top tree canopies with mature leaf were collected in July 2004 and immediately after detachment from the trees they were placed in sample bags and stored in a cool box to reduce transpiration. The samples were then taken to the laboratory for spectral reflectance measurements where all measurements were conducted within two hours from the time of field collection to avoid water loss and change of leaf properties. Twenty six tree species from 10 families had their spectral reflectance measured (Table 3.1).

3.2.2 Collection of Spectra

In the laboratory, leaves were separated from the branches and stacks of leaves (± 4 layers) were randomly spread on top of a flat black plate. The spectral response of each leaf plate was recorded 20 times. The plate was rotated 45˚ horizontally after every fifth recording in order to average the bi-directional reflectance distribution function (BRDF). Two leaves stacks were randomly formed from collected branches of every tree and from each stack of leaves one sample spectrum were measured. The conversion of spectral responses from radiance to reflectance was achieved internally by software associated with the spectrometer using a “Spectralon” white reference panel. The whole operation was conducted under laboratory conditions (i.e. dark room, ±25˚C) in order to avoid ambient light sources unrelated to the true spectral signal of the leaves.

Table 3.1 Twenty six tree species used for the laboratory reflectance measurement.

No.	Trees	Family	No. of spectral samples
1	*Fraxinus excelsior*	Oleaceae	63
2	*Fraxinus ornus*	Oleaceae	37
3	*Tilia cordata*	Malvaceae	60
4	*Populus alba*	Salicaceae	20
5	*Populus nigra*	Salicaceae	20
6	*Salix alba*	Salicaceae	40
7	*Salix cinerea*	Salicaceae	41
8	*Salix elaeagnos*	Salicaceae	60
9	*Salix purpurea*	Salicaceae	41
10	*Carpinus betulus*	Betulaceae	19
11	*Carpinus orientalis*	Betulaceae	20
12	*Ostrys carpinifolia*	Betulaceae	41
13	*Fagus sylvatica*	Fagaceae	20
14	*Quercus pubescens*	Fagaceae	20
15	*Juglanns regia*	Juglandaceae	21
16	*Robinia pseudacacia*	Leguminosae	40
17	*Ficus carica*	Moraceae	20
18	*Prunus avium*	Rosaceae	44
19	*Malus sylvestris*	Rosaceae	78
20	*Pyrus pyraster*	Rosaceae	21
21	*Sorbus aria*	Rosaceae	64
22	*Acer campestre*	Sapindaceae	41
23	*Acer monospessulanum*	Sapindaceae	41
24	*Acer obtusatum subsp. Obtusatum*	Sapindaceae	39
25	*Acer pseudoplatanus*	Sapindaceae	20
26	*Ailanthus altissima*	Simaroubaceae	41

A GER 3700 (Geophysical and Environmental Research Corporation, Buffalo, New York) spectroradiometer was used to measure the reflectance spectra. The GER 3700 is a three dispersion grating spectroradiometer using Si and PbS detectors with a single field of view. The wavelength range is 325 nm to 2500 nm, with sampling intervals of 1.5 nm between 325 nm and 1050 nm, 6.2 nm between 1050 nm and 1900 nm and 9.5 nm in the 1900 nm to 2500 nm range. The Full width

half Maxima (FWHM) is 3 nm, 11 nm and 16 nm in the 325 nm to 1050 nm range, 1050 nm to 1900 nm range and 1900 nm to 2500 nm range respectively. Although the spectrometer records up to 647 bands, but due to high noise in the extreme short wavelength area only the spectral range between 400 nm and 2500 nm was analysed, which contains 597 wavebands. The sensor, equipped with a 1.5 m long fibre optic cable (25˚ field of view) was mounted on a tripod and positioned 20 cm above the target leaves at the nadir position. A light source (Lowel Pro-Light with 14.5V/50W/3200K JCV halogen lamp), pointing at the centre of the leaf plate, was placed at 30 degree off-nadir. The spectral measurement procedure we followed is comparable with various earlier works (Ramsey III and Jensen, 1996; Cochrane, 2000; Clark et al., 2005; Vaiphasa et al., 2005).

3.2.3 Discrimination procedure

Four techniques were applied to measure the spectral discrimination between the 26 tree species (Table 3.1). From every technique the ten best discriminating bands were selected for further analysis. Only normal reflectance spectra were used for the analysis, because, as expected, continuum removed spectra produced similar results and failed to improve discrimination between species (Schmidt and Skidmore, 2003).

3.2.3.1 U-test

The reflectance spectra associated with the 26 tree species (Table 3.1) were statistically analyzed to determine whether the variance of reflectance between tree species was greater than within tree species. This can be tested with the Mann–Whitney U-test (Schmidt and Skidmore, 2003). The hypothesis tests that between all pairs of tree species there is no significant difference between the median reflectance of each individual waveband. Stated formally, the null hypothesis for n tree species and I spectral bands per reflectance measurement is:

$H_0 : \eta n^{(i)} = \eta n + 1^{(i)}$

where, ηn is the median reflectance for vegetation type number n = 1, 2, 3. . .(n-1), and I = 1, 2, 3. . .I is the spectral band. The number of possible pairs from n tree species, i.e. the set of combinations of 2 out of n is the binominal coefficient: $\left(\frac{n}{2}\right) = \frac{n!}{(n-2)!.2!}$. Therefore, the hypothesis is tested 325 times for all possible combination of 26 species. The null hypothesis was tested at significance level of ȡ = 0.00015 (to correct for the Bonferroni effect, 0.05/325). The alternative hypothesis is that the reflectance medians are not equal:

$H_1 : \eta n^{(i)} \neq \eta n + 1^{(i)}$

The motivation to use U-test is that it is a non-parametric test which does not assume a normal distribution of the sample sets and that is why the difference in median was tested instead of mean. It was also assumed that the unequal number of samples per species (Table 3.1) does not influence this test method, as the number of samples is large (20 and above) (Lehmann, 1998)

3.2.3.2 Principal Component Analysis (PCA)

The principal components transformation is a multivariate statistical technique that selects uncorrelated linear combinations (eigen vector weights or loadings) of variables in n-dimensional space in such a way that each successively extracted linear combination, or principal component (PC), has a smaller variance. PCA wavebands were computed using factor loadings (or eigen vectors) of each of the bands and multiplying the factor loadings with their respective wavebands reflectivity (Thenkabail et al., 2004).

3.2.3.3 Stepwise Discriminant Analysis

Stepwise Discriminant Analysis (SDA) is the feature selection method that repeats the addition and removal of a feature at each step. This process allows us to find the best subset with which satisfactory discrimination performance can be obtained.

Discriminant function analysis is used to determine which variables discriminate between two or more naturally occurring groups. The stepwise procedure is "guided" by the respective *F* to enter and *F* to remove values. The *F* value for a variable indicates its statistical significance in the discrimination between groups. In this study we used two different procedures to compute the *F* value:

Wilk's lambda (Λ)

Wilk's lambda is a multivariate test. Its value ranges between 0 and 1, with values close to 0 indicating the group means are different and values close to 1 indicating the group means are not different. Wilk's Lambda (Λ) can then be converted to an F value (Klecka, 1980).

$$F_{[t(k-1);ms-v)]} = [(1 - \Lambda^{1/s})/\Lambda^{1/s}][(ms - v)/t(k-1)] \qquad \text{Eq.1}$$

where:
t = the number of independent variables
k = the number of treatments
$m = (2kn - t - k - 2)/2$
$s = [(t^2(k - 1)^2 - 4)/(t^2 + (k - 1)^2 - 5)]^{1/2}$
$v = (t(k - 1) - 2)/2$

Mahalanobis distance

Mahalanobis distance is a measure of the distance between two points in the space defined by two or more correlated variables. Mahalanobis distance, D^2, is a generalized measure of the distance between two groups. When Mahalanobis distance is the criterion for variable selection, the Mahalanobis distances between all pairs of groups are first calculated. The distance between groups 1 and 2 is defined as

$$D_{12}^2 = (n-g)\sum_{i=1}^{p}\sum_{j=1}^{p} w_{ij}^{-1}\left(\overline{X}_{i1} - \overline{X}_{i2}\right)\left(\overline{X}_{j1} - \overline{X}_{j2}\right) \qquad \text{Eq.2}$$

where, p is the number of variables in the model, $\overline{X}_{i1}$ is the mean for the i^{th} variable in Group 1, $\overline{X}_{i2}$ is the mean for the i^{th} variable in Group 2. w_{ij}^{-1} is an element from the inverse of the within-groups covariance matrix.

The variable that has the largest D^2 for the two groups that are closest (have the smallest D^2 initially) is selected for inclusion. The corresponding F statistic is

$$F = \frac{(n-1-p)n_1 n_2}{p(n-2)(n_1+n_2)} D_{1,2}^2 \qquad \text{Eq.3}$$

This F value can be used for variable selection. At each step the variable chosen for inclusion is the one with the largest F value.

3.2.3.4 Wrapper feature selection approach

The wrapper approach is a feature selection algorithm that combines the strength of a traditional search algorithm (e.g. sequential forward selection, branch and bound technique, genetic search, etc.) with the capability of a classifier (e.g. nearest neighbour classifier, maximum likelihood classifier, etc.) (Siedlecki and Sklansky, 1989; John et al., 1994; Kohavi and John, 1997; Kavzoglu and Mather, 2002; Yu et al., 2002; Vaiphasa, 2003). In this study, the search mechanism of the wrapper tool was based on a genetic algorithm, and its classifier was a nearest neighbour classifier. The algorithm was applied to select the best band combination out of the total of 597 bands. The algorithm was initialized with the following genetic search parameters: crossover rate = 50%; mutation rate = 1%. The maximum number of iterations was fixed at 1000 and the method for classification was the Spectral Angle Mapper (SAM). Following the USGS guideline (Anderson et al., 1976), the optimizing criterion chosen at the 80% level was adequate for the

difficulties of discriminating trees at species level (i.e. Level III or IV of the USGS classification standard).

3.2.4 Finding the important regions

After selecting bands by using the above discrimination procedures, we pooled results in a frequency plot. Based on the distribution and frequency of occurrence we grouped the bands to form spectral regions with maximum frequency of occurrence and tested the power of separability by using randomly selected bands within those regions.

3.2.5 Testing Procedure

Two different testing procedures were performed to calculate the ability of the selected regions to discriminate species and test the replicability of our findings.

To test the strength of our selected regions for discrimination between species, we performed paired t-tests on Bhattacharya distances (Bhattacharya, 1943), which is a spectral separability measurement procedure. Two data sets were generated, the first consisted of ten randomly selected wavebands from the selected regions of the spectra (at least one band from each region) and the second of ten randomly selected wavebands from the entire spectrum. Bhattacharya distance between the spectra was calculated for each pair of two species using those ten selected bands.

We iterated the process 1000 times and a one tailed Student's t-test was performed on each pair of Bhattacharya distances based on the following hypothesis:

H_0: $\mu_1 = \mu_2$
H_A: $\mu_1 > \mu_2$

Where, μ_1 = mean of Bhattacharya distances calculated from wavebands collected from selected regions and μ_2 = mean of Bhattacharya distances calculated from wavebands collected from the whole spectrum. The significance was examined at the probability level of $P<0.05$. The process was repeated for all the species combinations (325).

Our findings were compared with the results from three independent data sets to determine whether similar bands would emerge. Two leaf level laboratory data sets (unpublished) consisting of three herbs and thirteen shrubs species and one canopy level data set of field spectra (Schmidt and Skidmore, 2003) from salt marsh species were used. All three sets of data were collected using similar spectrometer (GER 3700) with same band number and spectral range. We performed same discriminating algorithms on these data sets to compare the result.

3.3 Results

3.3.1 U-Test

Twenty six species means 325 possible species pairs. A pair of species (*Acer campestre* and *Carpinus orientalis*) was selected to illustrate the statistical comparison between species. Figure 3.1 shows the median spectra for the two species. The shaded areas indicate the reflectance wavelengths where the two species have a statistically significant difference in median reflectance.

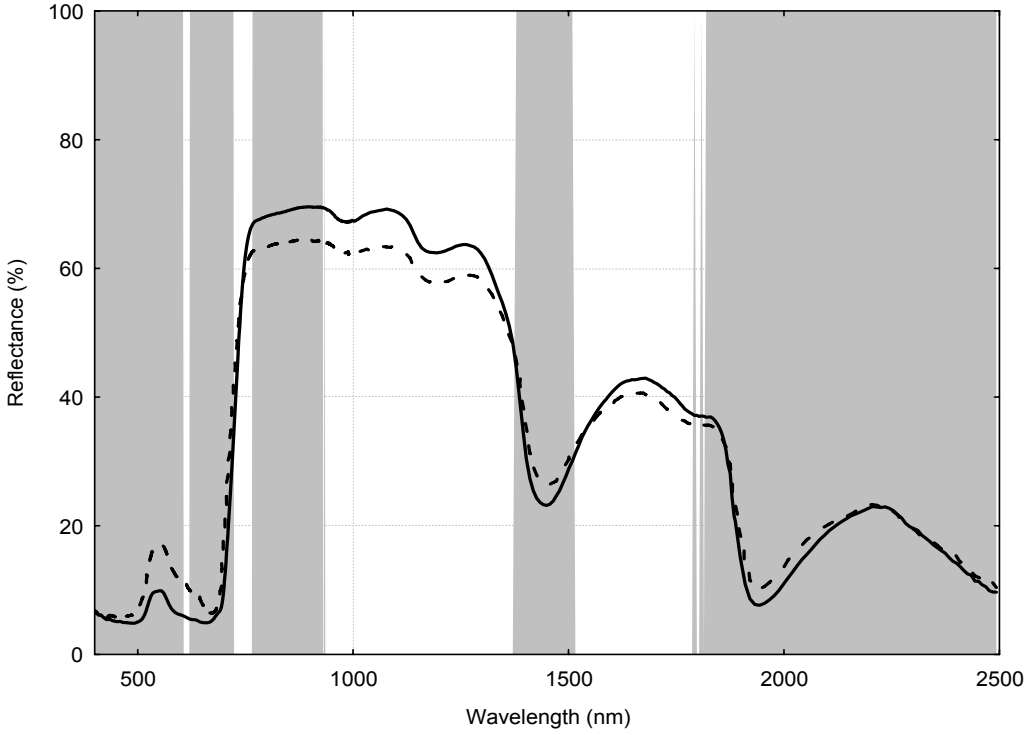

Figure 3.1 Median spectrum for *Acer campestre* (smooth line) and *Carpinus orientalis* (dashed line). Wavelengths with statistically significant difference between the two spectra are shaded grey.

The histogram in Figure 3.2 summarizes the result of all possible species combination pairs and indicates the frequency of species pairs with a statistically significant difference per wavebands. The significant level for the U-test was ά = 0.00015. From Figure 3.2 it can be seen that, for example at 601 nm, 275 species pairs (out of a possible 325) have a statically significant differences in reflectance. The median reflectance spectrum of *Acer campestre* is plotted on the histogram to visualize the position of the main features of a typical leaf reflectance curve.

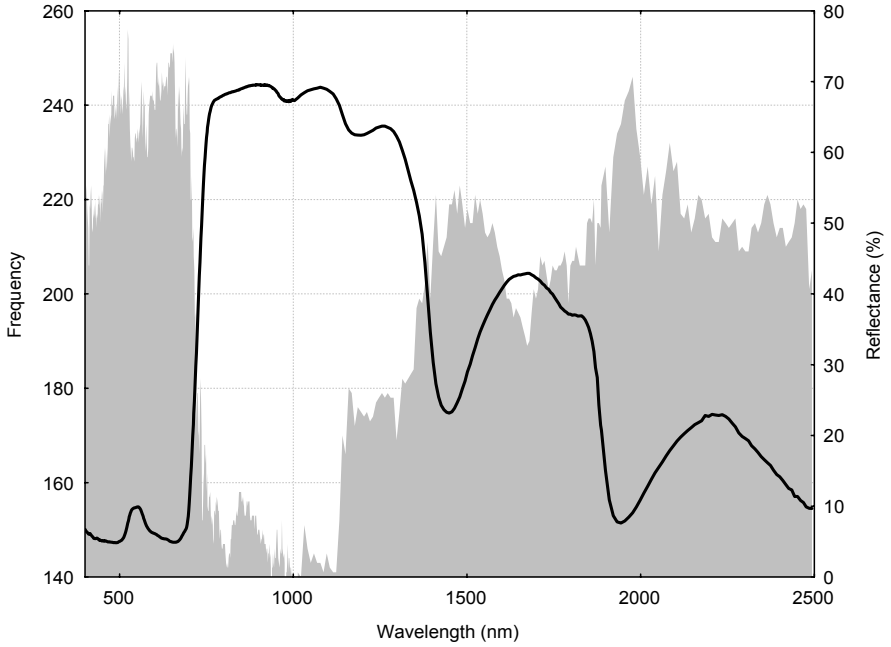

Figure 3.2 Frequency plot of statistically significant differences using the U-test with significance level of ȧ = 0.00015, between the field reflectance median of 26 tree species at every band. The median reflectance curve of *A. campestre* is displayed to indicate typical vegetation reflectance features.

No single waveband managed to discriminate between all the species. The maximum frequency obtained was 280 in wavebands at 513 and 643 nm while the minimum frequency was 197 obtained in waveband at 941 nm. Out of 597 wavebands more than 550 bands showed a discrimination frequency of over 200. The highest frequency was observed in the visible range of the spectrum, and relatively low frequencies were noted for the infra-red plateau (Figure 3.2).

To select bands for further analysis, bands were chosen from the highest local maxima (frequency). The ten selected wavebands were 494, 513, 642, 660, 697, 750, 1141, 1386, 1621 and 2155 nm.

3.3.2 Principal component analysis

In all the tree species the first five principal components (PCs) explained more than 95% of the variability. PC wavebands were computed using factor loadings (or eigen vectors) of each of the bands, and wavebands which provide the highest factor loadings are listed for PC1 – PC5 (Table 3.2). In some cases the target variability (95%) was reaches even with first three or four PCs and hence fourth and fifth PCs were not included.

Table 3.2 PCs showing wavebands with highest factor loadings[a]

Species	PC1	PC2	PC3	PC4	PC5
Acer campestre	741.28	647.48	691.37	700.16	1954.57
Acer monospessulanum	1378.64	516.3	673.79	1855.35	417.84
Acer obtusatum subsp. Obtusatum	741.28	675.25	684.04	531.93	691.37
Acer pseudoplatanus	1600.73	1297.08	684.04	422.08	2104.59
Ailanthus altissima	451.58	2165.76	1297.08	745.69	1666.88
Carpinus betulus	741.28	1402.39	423.49	681.11	527.66
Carpinus orientalis	742.75	1288.73	1394.51	2347.02	2094.22
Prunus avium	1378.64	650.4	767.78	2125.19	650.4
Fagus sylvatica	1370.65	907.98	1653.98	698.69	2083.79
Ficus carica	742.75	691.37	2382.78	2114.92	
Fraxinus excelsior	1378.64	503.57	697.23	684.04	2282.44
Fraxinus ornus	1288.73	2356.04	2125.19	692.83	2185.72
Juglanns regia	747.16	1614.29	689.9	1634.32	2165.76
Malus sylvestris	757.46	476.82	688.43	1647.46	2145.58
Ostrys carpinifolia	744.22	694.3	686.97	2073.31	1887.13
Pyrus pyraster	1362.62	742.75	681.11	1640.91	2094.22
Populus alba	744.22	684.04	2020.12		
Populus nigra	739.81	512.05	697.23	1288.73	2030.86
Quercus pubescens	1370.65	503.57	760.41	704.56	2185.72
Robinia pseudacacia	1362.62	892.87	2114.92	1660.45	2234.73
Salix alba	744.22	698.69	1370.65		
Salix cinerea	1338.31	694.3	735.4	2165.76	2273
Salix elaeagnos	710.43	637.27	1976.63		
Salix purpurea	1370.65	646.02	1954.57	2155.69	1614.29
Sorbus aria	745.69	1123.31	1627.68	2215.29	1679.62
Tilia cordata	1370.65	797.31	697.23	2319.66	685.5

[a] For each principal component, the band that provides the highest factor loadings is listed.

The red edge wavebands (around 740-750 nm) dominated the first principal component with 50% frequency of occurrence (13 out of 26 species), followed by the near infrared (NIR) around 1280-1380 nm with 42% frequency of occurrence (11 out of 26). The visible part of the spectral bands dominated in second and third principal components, particularly red wavebands around 680 nm appeared in large numbers in the third principal component. In the fourth and fifth principal components short wave infrared (SWIR) bands dominated (Table 3.2).

The frequency plot in Figure 3.3 summarizes the results of the principal component analysis for band selection and indicates the frequency of occurrence of wavebands with the highest factor loadings in different PCs. Though they were distributed widely along the axis of the wavelengths, several clusters were clearly visible; forming three clusters in the visible (around 510, 640 and 680 nm), two in the red edge slope (690 and 740 nm) and three more in NIR and SWIR (1300, 1650 and 2100 nm).

3.3.3 Stepwise discriminant analysis

Two different statistical methods were utilized to select wavebands which yielded sets of bands very similar to each other though not completely the same (Table 3.3). The differences are found mostly in their relative entry position during the discrimination process and the strength of discrimination shown by that particular band. Both methods picked bands not only from similar regions of the spectra but also in close proximity. For example, in the red-edge region of the spectrum the Wilk's lambda based procedure selected bands of 682 and 753 nm whereas the procedure which used Mahalanobis distance selected bands of 683 and 759 nm.

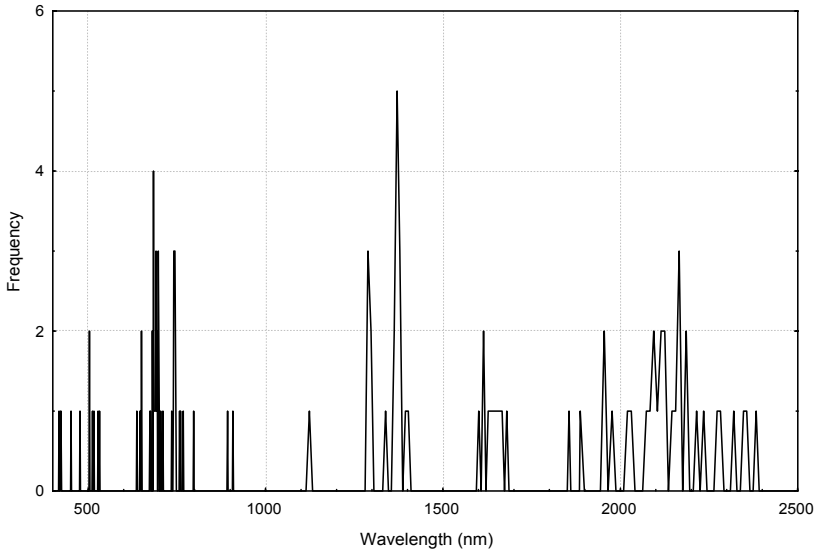

Figure 3.3 Frequency of occurrence of wavebands with highest factor loading in different PCs.

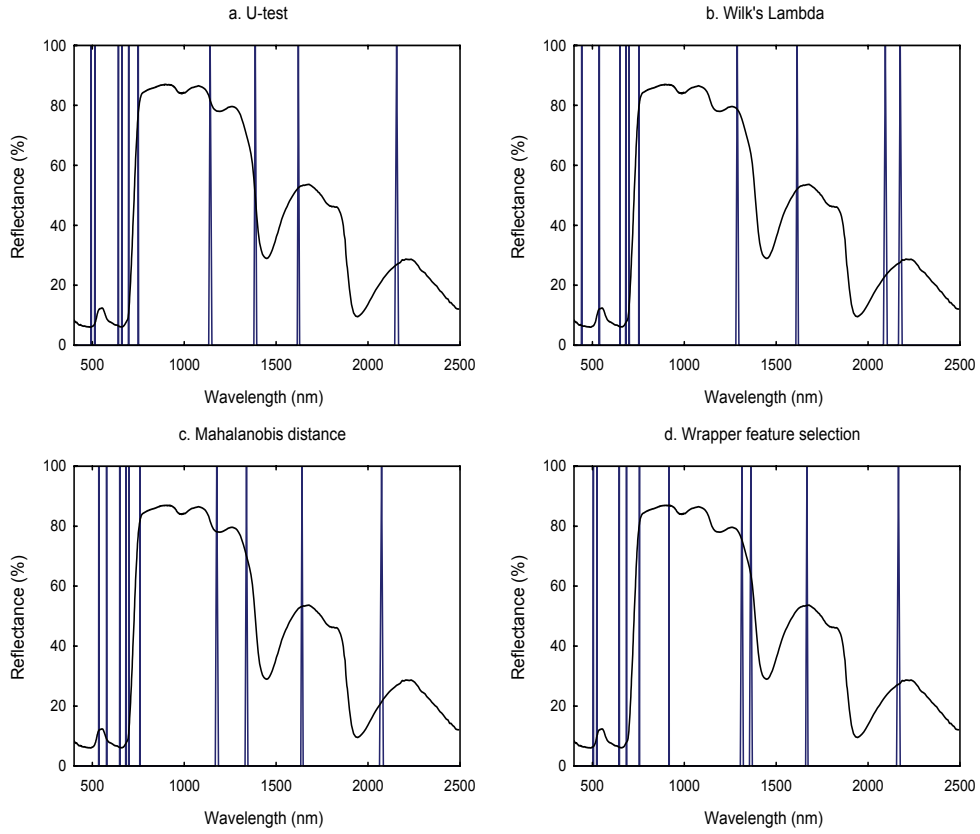

Figure 3.4 Wavebands selected by using different discriminating procedures; a. U-test, b & c. SDA (Wilk's lambda and Mahalanobis distance respectively), d. wrapper feature selection. The median reflectance curve of *A. campestre* is displayed to indicate typical vegetation reflectance features.

3.3.4 Wrapper feature selection

The wrapper feature selection algorithm was applied to search for the (sub)-optimal spectral band combination. The best combination found by the wrapper tool consisted of ten spectral wavebands at 504, 524, 646, 686, 756, 917, 1313, 1363, 1667 and 2165 nm (Figure 3.4). These ten bands managed to classify the entire spectral sample set with an 83% level of classification accuracy, by using the spectral angle mapper classifier algorithm.

Table 3.3 Ten best wavebands entered in two (Wilk's lambda and Mahalanobis distance) different statistical procedures under stepwise discriminant analysis. Corresponding statistics showed the strength of discrimination.

Step	Wilk's lambda			Mahalanobis distance		
	Band entered	Wave length (nm)	Statistic	Band entered	Wave length (nm)	Statistic
1	31	441	0.164	200	683	0.001
2	555	2094	0.021	128	578	0.116
3	99	537	0.008	492	1641	0.562
4	562	2175	0.006	98	535	1.129
5	247	753	0.005	553	2073	1.694
6	177	650	0.003	211	698	3.685
7	488	1614	0.001	451	1338	4.666
8	212	700	0.001	177	649	4.898
9	445	1288	0.000	252	759	5.397
10	199	682	0.000	432	1177	5.429

3.3.5 Finding the important regions

The wavebands which were selected with the four spectral discrimination methods (U-test, PCA, SDA and Wrapper feature selection) were merged together in order to determine their frequency of occurrence. In the frequency plot (Figure 3.5), distribution of these bands along the spectral axis formed several distinct clusters. In the visible spectral range, three clusters were formed from where most of the bands were selected. The wavelength ranges of these regions were 500 – 535, 630 – 650 and 680 – 710 nm. In the red edge region, wavebands formed clusters at both ends of the slope, e.g. at the base around 700 – 710 and around the shoulder 740 – 770 nm. Other clusters were located in the FNIR and SWIR segments of the spectrum and the wavelength ranges of these regions were 1280 – 1380, 1610 – 1680 and 2075 – 2175 nm. The selected regions with highest concentration of discriminating bands are shown in Table 3.4.

3.3.6 Testing Procedure

For all the species combinations (325), the mean of the Bhattacharya distances calculated from wavebands collected from selected regions were higher compared with the mean of Bhattacharya distances calculated from wavebands collected from the whole spectrum. Out of a total of 325 species combinations, 315 or 97% had statistically significant differences (higher) in mean Bhattacharya distances at $P<0.05$ (Table 3.5).

Tests with three independent data sets produced similar results and most of the wavebands selected were within the ranges we found with our original data set (Figure 3.6) except more bands in NIR for canopy level salt-marsh vegetation spectra.

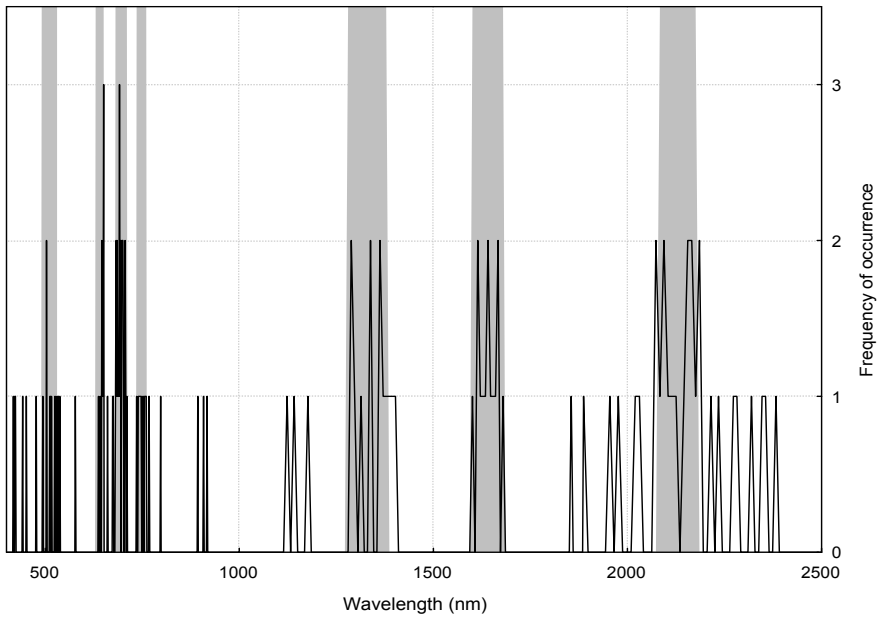

Figure 3.5 Selected regions (in gray) where discriminating wavebands occurred most frequently.

3.4 Discussion

Use of imaging spectroscopy in species discrimination is widespread both in the laboratory as well as in field campaigns (Cochrane, 2000; Schmidt and Skidmore, 2001; Yamano et al., 2003; Clark et al., 2005; Vaiphasa et al., 2005). The high spectral resolution is useful for capturing and discriminating subtle physico-chemical differences of the targets, but it contains redundant information at band level (Bajwa et al., 2004). This redundancy generates an enormous number of independent variables creating difficulties to run regular statistical procedures. Various authors have tried different kinds of data reduction techniques on hyperspectral data, but replicability has been a major problem.

In this paper we used four different data reduction techniques to identify important sections of the spectrum for discriminating tree species. The best discriminating wavebands using band selection techniques (Mann-

Table 3.5 Probability associated with Student's t-test between Bhattacharya (B) distances, calculated from two sets of ten randomly selected wavebands. The first set of B distances was calculated from wavebands collected from selected regions and the second set of B distances was calculated from wavebands collected from the whole spectrum. Bold types show the probabilities which were statistically not significant.

Species	1	2	3	4	5	6	7	8	9	10	11	12	13	14	15	16	17	18	19	20	21	22	23	24	25	26
1		0.000	0.000	0.000	0.000	0.000	0.000	0.000	0.000	0.000	0.000	0.000	0.000	0.000	0.000	0.000	0.000	0.000	0.000	0.000	0.021	0.000	0.000	0.000	0.016	0.000
2			0.000	0.000	0.000	0.000	0.000	0.000	0.000	0.000	0.000	0.000	0.000	0.000	0.000	0.000	0.000	0.000	0.000	0.000	0.040	0.000	0.000	0.000	0.000	0.000
3				0.000	0.013	0.000	0.000	0.000	0.000	0.000	0.000	0.001	0.000	0.008	0.020	0.000	0.000	0.000	0.000	0.000	0.000	0.000	**0.063**	0.000	0.000	0.000
4					0.000	0.000	0.000	0.000	0.000	0.000	0.000	0.000	0.000	0.000	0.000	0.000	0.000	0.000	0.000	0.000	0.000	0.000	0.000	0.000	0.013	0.000
5						0.000	0.000	0.000	0.000	0.007	0.000	0.000	0.000	0.000	0.000	0.000	0.000	0.000	0.000	0.000	0.000	0.001	0.000	0.000	0.000	0.022
6							0.000	0.000	0.000	0.000	0.000	0.000	0.000	0.000	0.000	0.000	0.000	0.000	0.000	0.000	0.000	0.000	0.000	0.000	0.000	0.000
7								0.000	0.000	0.000	0.000	0.000	0.000	0.000	0.000	0.000	0.000	0.000	0.000	0.000	0.000	0.000	0.000	0.000	0.000	0.000
8									0.000	0.000	0.006	0.002	0.000	0.000	0.000	0.000	0.000	0.000	0.000	0.000	0.000	0.000	0.000	0.037	0.000	0.000
9										0.000	0.000	0.005	0.000	0.000	0.000	0.000	0.000	0.000	0.000	0.000	0.000	0.000	0.001	0.000	0.000	0.000
10											0.004	0.001	0.000	0.000	0.000	0.000	0.000	0.000	0.000	0.000	0.000	0.000	0.000	0.000	0.000	0.000
11												0.000	0.000	0.000	0.000	0.000	0.000	0.000	0.000	0.000	0.000	0.000	0.000	0.000	0.000	0.000
12													0.000	0.000	0.000	0.000	0.000	0.000	0.000	0.000	0.000	0.004	0.090	0.025	0.000	0.000
13														0.000	0.000	0.000	0.000	0.000	0.000	0.000	**0.069**	0.000	0.002	0.000	0.000	0.000
14															0.000	0.000	0.000	0.000	0.000	0.000	0.000	0.000	0.000	0.000	0.000	0.000
15																0.000	0.000	0.000	0.000	0.000	0.000	0.000	0.018	0.000	0.003	0.000
16																	0.000	0.000	0.000	0.000	0.000	0.000	0.002	0.000	0.000	0.000
17																		0.000	0.000	0.000	0.011	0.000	**0.097**	0.000	0.000	0.000
18																			0.000	0.000	0.000	**0.085**	0.002	0.000	**0.051**	0.000
19																				0.000	0.000	**0.303**	**0.095**	0.000	0.019	0.000
20																					0.000	0.000	0.000	0.000	0.000	0.000
21																						**0.160**	**0.076**	0.000	0.000	**0.055**
22																							0.020	0.000	0.000	0.000
23																								0.000	0.000	0.000
24																									0.000	0.000
25																										0.000
26																										

Whitney U-test, principal component analysis, stepwise discriminant analysis and a genetic neural network based wrapper feature selection approach) may be identified from Figure 3.3 and 3.4. The methods we used not only find wavebands independently but they are also complimentary to each other. The Mann-Whitney U test looks at each individual band separately to find the band level differences in each single pair of species combination. Whereas, stepwise discriminant analysis and wrapper feature selection processes consider the whole spectrum to identify the most discriminating bands. While these three methods take into account the variability of reflectance between different species, principal component analysis only regards the internal variability of reflectance within species.

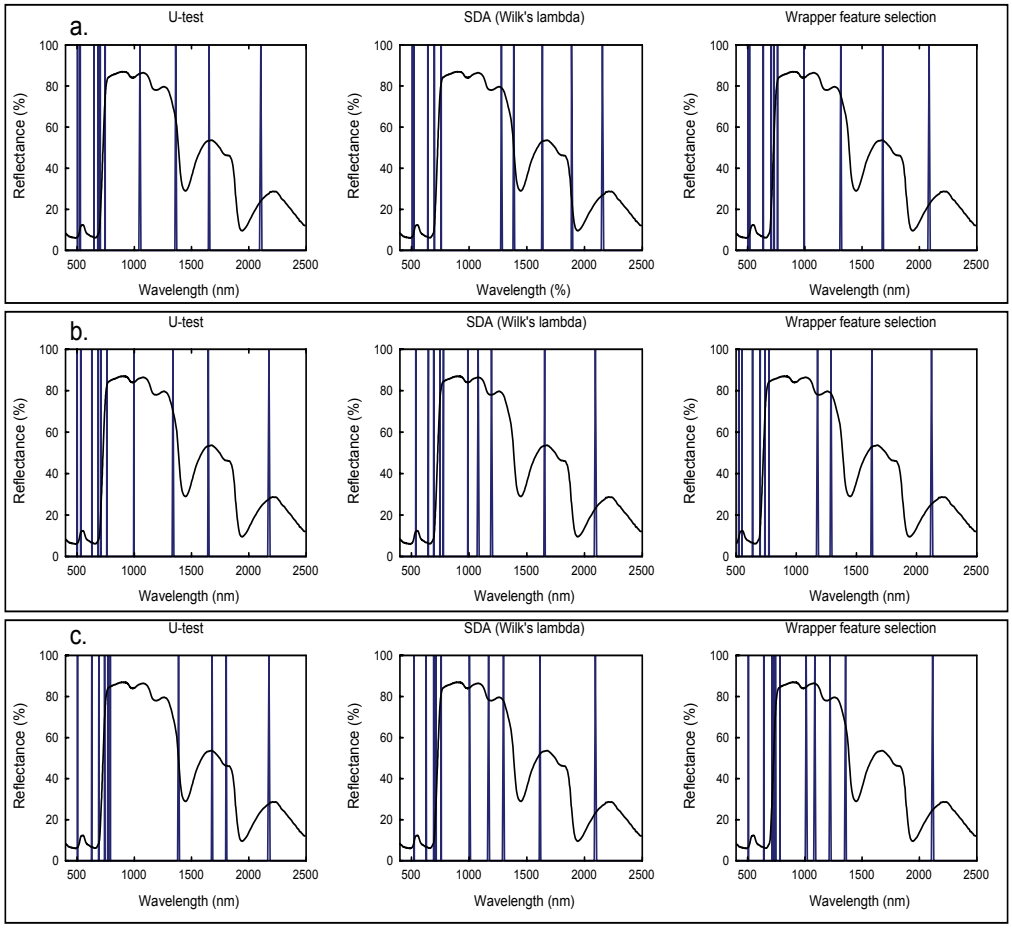

Figure 3.6 Wavebands selected using a similar discrimination procedure (u-test, SDA and Wrapper feature selection) but on different data sets. a. laboratory data of three herb species, b, laboratory data of thirteen shrub species and c. field data of salt marsh vegetation. The median reflectance curve of *A. campestre* is displayed to indicate typical vegetation reflectance features.

With the Mann-Whitney U-test we found that all 325 possible species pairs have significant differences (at ά= 0.00015) for many wavebands (Figure 3.2). This result not only indicates the potential to discriminate these species spectrally but also provides information about the bands discriminating best. The histogram (Figure 3.2) that serves as a guideline to select wavebands shows the highest frequency of significant differences in the visible, FNIR and SWIR and lowest ability to discriminate in the infrared plateau. Subsequently other methods for selecting discriminating bands followed a similar trend.

Table 3.6 Comparison of selected bands between previous studies and this study used for species discrimination.

Vaiphasa et al., (2005)	4 bands	720, 1277, 1415, and 1644 nm
Thenkabail et al., (2004)	22 bands	495, 555, 655, 675, 705, 735, 885, 915, 985, 1085, 1135, 1215, 1245, 1285, 1445, 1675, 1725, 2005, 2035, 2235, 2295 and 2345 nm
Bajwa et al., (2004) Only used Visible-NIR spectroscopy		Entropy : 627–684 Derivative : 690–705, 740–756 & 810-825 ANN : 530-550, 690-710, 740-750 PCA : 690-710 and several green bands.
Schmidt and Skidmore, (2003)	6 bands	404, 628, 771, 1398, 1803, and 2183 nm
Thenkabail et al., (2002)	12	490, 520, 550, 575, 660, 675, 700, 720, 845, 905, 920, 975
Cochrane, (2000)		Tree shape : 697-733 and 842-950 nm Branch shape : 692-713 nm
This study	7 regions	500–535, 630–650, 680–710, 740–770, 1280–1380, 1610–1680, 2075–2175

The result clearly illustrates the relative importance of using different parts of the spectrum for species discrimination. As leaf level reflectance spectra are controlled by two factors, firstly the morphology (e.g., internal and external leaf structure)(Verdebout et al., 1994) and secondly the leaf bio-chemical properties (e.g., water, photosynthetic pigments, structural carbohydrates and other secondary macromolecules) (Asner, 1998), the result could lead us to hypothesize that the spectral responses of leaf pigment and other bio-chemical properties contain more spectral information for discrimination than the information from leaf morphology. This may be because of similarities in tree leaf structure and our experimental design in which a stack of leaves (± 4 layers) was randomly spread on top of a flat black plate to collect the spectra.

A relative comparison with other studies (Table 3.6) shows that although our result does not coincide fully with their findings but a general trend does exist. Moreover, these differences largely remain confined to the wavebands of the NIR plateau.

Table 3.7 Selected regions and their importance for vegetation.

Wavelength (nm)	Band position	Importance for vegetation
500 – 535	Green	Blue absorption and upward slope to the green peak, sensitive to chlorophyll & carotenoid (Blackburn, 1998).
630 – 650	Red	Absorption pre-maxima, chlorophyll a, b (Blackburn, 1998).
680 – 700	Red edge	Start of the rapid change of slope (red edge), total chlorophyll, LAI, moisture stress (Blackburn, 1999; Datt, 1999).
740 – 760	Red edge	End of rapid change of slope (red edge), chlorophyll & nitrogen (Johnson et al., 1994; Yoder and Pettigrew-Crosby, 1995)
1280 – 1380	FNIR	Reflectance peak 2 in FNIR and downward slope to moisture absorption, starch (Curran et al., 1992)
1610 – 1680	SWIR	Reflectance peak 1 of SWIR, sensitive to lignin, tannin, starch and cellulose (Elvidge, 1990; Yoder and Pettigrew-Crosby, 1995; Kokaly and Clark, 1999)
2075 – 2175	SWIR	Reflectance peak 2 of SWIR, sensitive to lignin, sugar, protein (Curran et al., 1992; Yoder and Pettigrew-Crosby, 1995)

When we pooled all the selected bands from our four previously described methods (Figure 3.5), the distribution pattern along the wavelength axis forms several clusters. These clusters demonstrate, (1) the obvious power of discrimination of those spectral regions irrespective of selection algorithm or method and (2) different methods may not identify exactly the same bands, but a similar discriminating band does exist within close proximity. We selected seven narrow spectral ranges (Table 3.4), which included the maximum number of selected bands. These selected spectral regions have important vegetation characteristics (Table 3.7) as established by various authors.

We received very strong support for our spectral region concept while testing the power of discrimination of the selected regions. In all species combinations wavebands chosen from the selected regions produced higher spectral separability (Table 3.5 showed that in 97% of the species combinations selected regions produced significantly higher separability (Bhattacharya distances)). This result demonstrates clearly the value of these selected regions when discriminating between spectra. Moreover, the result also reveals the information sharing within the selected region. We picked bands randomly from the selected regions but still they managed to perform similarly.

The results of the replicability test (Figure 3.6) show that independent data sets for leaf spectra (Figure 3.6, a and b) generate a similar set of bands, which supports our findings. Spectra from canopy level data

(Figure 3.6, c) finds more bands in the NIR plateau, even though they also selected bands from our selected regions. These extra bands in NIR region were largely expected in canopy level data because of their additional canopy (structural) information and sensitivity of NIR reflectance to canopy properties. This result also indicates that the region of NIR plateau needs to be added when working with canopy spectra.

3.5 Conclusion

This study aimed to evaluate the result of four waveband selection procedures and came up with common regions in the spectrum with better discriminating properties. Our results have shown that:

(i) With the high spectral resolution of imaging spectroscopy, discrimination at species level is possible.
(ii) Redundancy in hyperspectral vegetation data makes exact waveband selection difficult, but still bands from narrow ranges appeared in all methods.
(iii) Seven spectral regions, which yield the highest discriminatory properties, were identified.
(iv) The information carried by these spectral regions which facilitate the discriminate between species is shared by all the bands within.
(v) Tests with independent data sets have proved the replicability and reliability of these selected regions.

This finding is important in solving the “dimensionality problem” of hyperspectral data because it reduces the computational effort when using statistical procedures. Moreover, the results may also assist in the design of new broad band sensors specific for species mapping or for “choosing” bands from adjustable airborne hyperspectral sensors.

Acknowledgements

This study was financially supported by Nuffic and ITC. Thanks are also due to Henk van Oosten for his support in programming.

In the preceding chapter the possibilities of using band selection techniques as well as identifying those spectral regions allowing discrimination between plant species were investigated. In the following chapter (chapter 4), the usefulness of spectral matching techniques for species discrimination is explored. Moreover, the band selection processes (chapter 2) draw some criticism for not utilizing the full potency of hyperspectral imaging. However, spectral matching techniques is utilize the full spectral resolution and hence the full strength of hyperspectral measurement. Results of this study highlighted the effectiveness of different spectral matching algorithms to differentiate between species and compared their performances.

Chapter 4

Spectral similarity measures for plant species discrimination

Md. Istiak Sobhan, Andrew K. Skidmore, Freek D. van der Meer
(In preparation)

Abstract

Plant species discrimination is an important and evolving aspect of vegetation imaging spectrometry. In this study, we investigated the use of spectral similarity measures (matching algorithms) to discriminate plant species spectra. In addition, we investigated the comparative performance of these measures to distinguish plant spectra collected both under laboratory conditions and from an image. Four different similarity measures were used in this study: (i) spectral correlation measure (SCM), (ii) spectral angle mapper (SAM), (iii) spectral information divergence (SID), and (iv) a combination of SAM and SID. Two statistical algorithms, relative spectral discriminatory probability (RSDPB) and relative spectral discriminatory power (RSDPW), were also used to measure species discriminability for multiple species and to compare the relative performance of the similarity measures. Laboratory spectra of six plant species, representing herb, shrub and tree (two each), and HyMap image spectra of three different plant covers were used to perform the discrimination. For the laboratory spectra, four different spectral configurations (full: 400 nm to 2500 nm, visible: 400 nm to 700 nm, NIR: 700 nm to 1300 nm, and SWIR: 1300 nm to 2500 nm) were chosen to examine the relative discriminatory power of the spectral regions. The spectral similarity analysis showed that dissimilarities were much larger between species groups (i.e., herb, shrub and tree) than within species groups. Greater affinity was found between the leaf spectra of trees and shrubs than with the leaf spectra of herbs. The different spectral configurations did not provide much difference in information regarding relative discrimination. However, it was possible to distinguish trees from shrubs by using the SWIR region of the spectra. Comparative performance analysis showed that the combined SAM and SID similarity measure outperformed all other spectral matching algorithms in discriminating species, while SAM and SID followed a similar trend. Comparative performance analysis revealed that SID performed significantly better (z = 3.35) than SAM in classifying a HyMap image.

Keywords: spectroscopy; species discrimination; similarity measures

4.1 Introduction

Discrimination of plant species is an important requirement for sustainable ecosystem management. Proper discrimination between species is necessary to map and monitor the spatial distribution of certain species, but this was not possible using traditional multispectral images of only moderate spatial resolution. However, the scenario changed with the advent of imaging spectroscopy. Not only did the high spectral resolution of hyperspectral images start to yield quality information about vegetation health and chemical content (Curran, 1989; Curran et al., 1992; Peñuelas et al., 1997; Todd et al., 1998; Kokaly and Clark, 1999; Mutanga et al., 2003; Mutanga and Skidmore, 2004), but the continuous narrow bands of spectral reflectance from the visible (400 nm) through to the SWIR (2500 nm) range of the electromagnetic spectrum also started to provide discrimination at the individual species level (Cochrane, 2000; Schmidt and Skidmore, 2001; Yamano et al., 2003; Clark et al., 2005; Vaiphasa et al., 2005).

Plant species discrimination has been highlighted as being one of the benefits of using hyperspectral data. But this discriminating ability of hyperspectral sensors depends largely on inter-species and intra-species spectral variability (Nagendra, 2002). As different plant species respond differently to energy in the electromagnetic spectrum (Verbyla, 1995), remotely sensed data of high spectral resolution can in theory be used to distinguish between these species. However, Price (1994) and Portigal et al. (1997) demonstrate that the leaf reflectances of different species are highly correlated because of their similar chemical composition, and hence are not unique. Moreover, variations can also occur within a species owing to age differences, micro-climate, soil characteristics, precipitation, topography, phenology, and a host of other environmental factors, including stress (Gausman, 1985; Westman and Price, 1987; Carter, 1993, 1994; Portigal et al., 1997; Roberts et al., 1998; Gracia and Ustin, 2001; Smith et al., 2004). However, as biochemical and leaf characteristics have wider variations between species than within species, so too have absorption and reflectance (Knipling, 1970; Asner et al., 1998; Martin et al., 1998; Schmidt and Skidmore, 2003), making discrimination possible.

In vegetation spectroscopy or hyperspectral remote sensing, various techniques have been developed to determine the differences between separate plant spectra. In most cases, vegetation indices are applied to spectra to compare their specific differences. Converting spectra into indices also reduces the high dimensionality of the hyperspectral data, facilitating computation. However, the high spectral resolution of hyperspectral data is also essential for capturing and discriminating subtle differences between the target species (Bajwa et al., 2004). A quantitative comparison of two or more surface reflectance data in imaging spectroscopy should be able to preserve more of this subtle but important spectral information that is particularly vital for vegetation

discrimination. Quantitative comparison is primarily carried out using matching or similarity techniques (Kruse et al., 1993). Algorithms of this kind try to find spectral similarity or dissimilarity between two spectra, and are generally used to compare one known (from the spectral library) with one unknown.

Two broad groups of spectral similarity measures have been developed: deterministic or empirical measures and stochastic measures. Deterministic measures include spectral angle, Euclidian distance, and cross-correlation of spectral vectors, and mostly use the geometrical characteristics of the spectra. In contrast, stochastic measures such as spectral information divergence consider the spectral band-to-band variability as a result of uncertainty incurred by randomness. They model the spectrum as a probability distribution so that the spectral properties can be further described by statistical moments of any order (Chang, 2000). Although similarity measures are extensively used in geological and particularly mineralogical studies, they have seldom been used in vegetation spectroscopy. Except for the spectral angle mapper (SAM), which has become a mainstream classifier (Ben-Dor and Levin, 2000; Bakker and Schmidt, 2002; Schmidt et al., 2004; Clark et al., 2005; Mundt et al., 2005), similarity measures have been used in vegetation discrimination to only a very limited extent. Moreover, apart from Du et al. (2004) and van der Meer (2006), little or no information is available on the overall performances of these spectral matching techniques in plant species discrimination or on their comparative advantages and disadvantages.

The aim of this study was to discriminate species by using four similarity measures to measure spectral dissimilarities among the different species. In addition, we also investigated the relative performances of these similarity measures in terms of plant species discrimination. The performances of two similarity measures (SAM and spectral information divergence (SID)) as classifiers to discriminate species in a hyperspectral image were compared. To achieve the objective spectral reflectance, data were derived from laboratory measurements of leaves, as well as extracted from HyMap hyperspectral images.

4.2 Materials and method

4.2.1 Collection of leaf samples

Fully sunlit mature leaves were collected from six species, representing tree, shrub and herb (two each) (Table 4.1), from Majella National Park, Italy, in July 2005. Immediately after detachment from plants, the leaves were placed in plastic sample bags and stored in a cool box to reduce transpiration. The samples were then taken to the laboratory for spectral reflectance measurements, and all measurements were conducted within

two hours of field collection to avoid water loss and change in leaf properties.

Table. 4.1 Species used to collect spectra in the laboratory.

Type	Species	Family
Herb	*Cichorium intybus*	Asteraceae
	Origanum vulgare	Lamiaceae
Shrub	*Crataegus monogyna*	Rosaceae
	Prunus spinosa	Rosaceae
Tree	*Acer campestre*	Aceraceae
	Fagus sylvatica	Fagaceae

4.2.2 Collection of spectra

To avoid ambient light sources unrelated to the true spectral signal of the leaves, the spectra were measured in a laboratory (i.e., dark room, ±25°C) following the method described by Cochrane (2000), Clark et al. (2005) and Vaiphasa et al. (2005). For each species, a single leaf layer was formed on top of a flat black plate covering the entire viewing area of the sensor. As most of the species used in this study produce small leaves, more than one leaf was required to cover the plate. Twenty spectral measurements were obtained for each plate and averaged to produce a single spectrum in order to reduce any specular behaviour. The plate was rotated 45° horizontally after every fifth recording in order to reduce the effect of the bidirectional reflectance distribution function. Twenty such spectra were obtained per species. The radiance data were converted to reflectance, using scans of a white Spectralon reference panel. We used a Savitzky-Golay (Savitzky and Golay, 1964) second-order polynomial least-squares function of a five-band window to spectrally smooth our data (Kumar and Skidmore, 1998; Schmidt and Skidmore, 2004). The average reflectance spectra of the six different species collected in the laboratory are shown in Figure 4.1.

A GER 3700 (Geophysical and Environmental Research Corporation, Buffalo, New York) spectroradiometer measured the reflectance spectra. The GER 3700 is a three dispersion grating spectroradiometer using Si and PbS detectors with a single field of view. The wavelength range is from 325 nm to 2500 nm, with sampling intervals of 1.5 nm between 325 nm and 1050 nm, 6.2 nm between 1050 nm and 1900 nm, and 9.5 nm between 1900 nm and 2500 nm. The full-width half maxima are 3 nm, 11 nm and 16 nm in the 325 nm to 1050 nm range, 1050 nm to 1900 nm range, and 1900 nm to 2500 nm range, respectively. Although the spectrometer records up to 647 bands, because of the high noise in the extreme short wavelength area only the spectral range between 400 nm and 2500 nm, which contains 597 wavebands, was analysed. The sensor, equipped with a 1.5 m long fibre optic cable (25° field of view) was mounted on a tripod and positioned 15 cm at nadir above the target leaves. A light source (Lowel Pro-Light with 14.5V/50W/3200K JCV

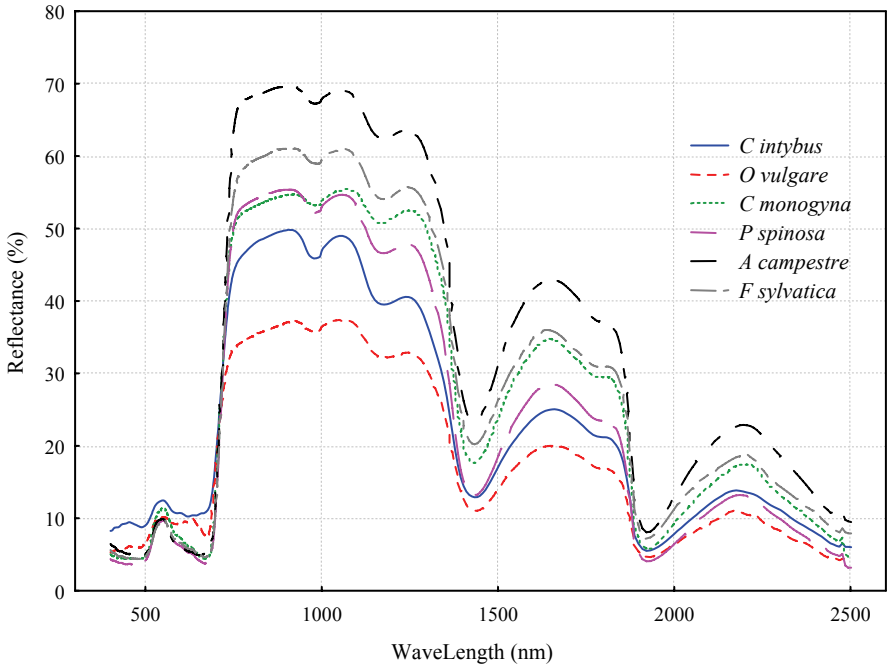

Figure 4.1 Average reflectance spectra of six species collected from laboratory measurement.

halogen lamp) pointing at the centre of the leaf plate was placed at 30° off-nadir, approximately 40 cm from the target.

4.2.3 Collection of spectra from Image

Spectral signatures of known pixels were collected from airborne HyMap hyperspectral data obtained on 4 July 2005 from Majella National Park, Italy. The HyMap sensor comprised 126 wavebands operating over the wavelength range 436 nm to 2485 nm, with average spectral resolutions of 15 nm (436 nm to 1313 nm), 13 nm (1409 nm to 1800 nm) and 17 nm (1953 nm to 2485 nm). The spatial resolution of the data was 4 m. The images were collected at solar noon. The solar zenith and azimuth angles for the image strips ranged from 30° to 33.7° and from 111.5° to 121°, respectively. The image strips were atmospherically and geometrically corrected. The atmospheric correction was carried out using ATCOR4-r (rugged terrain). ATCOR4 is based on the MODTRAN-4 radiative transfer code. The average reflectance spectra of the three different species collected from the HyMap image are shown in Figure 4.2.

4.2.4 Spectra similarity measures

To discriminate plant spectra, four different similarity measures were used, two representing the deterministic model, namely (i) spectral correlation measure (SCM) and (ii) spectral angle mapper (SAM), and two representing the stochastic model, namely (iii) spectral information divergence (SID) and (iv) a combination of SAM and SID. The comparative performance of these similarity measures was also investigated. Laboratory spectral similarity measurements were performed in four different spectral configurations: all 597 bands, the visible range (400 um to 700 nm), the NIR to red range (700 um to 1300 nm), and the SWIR range (1300 um to 2500 nm).

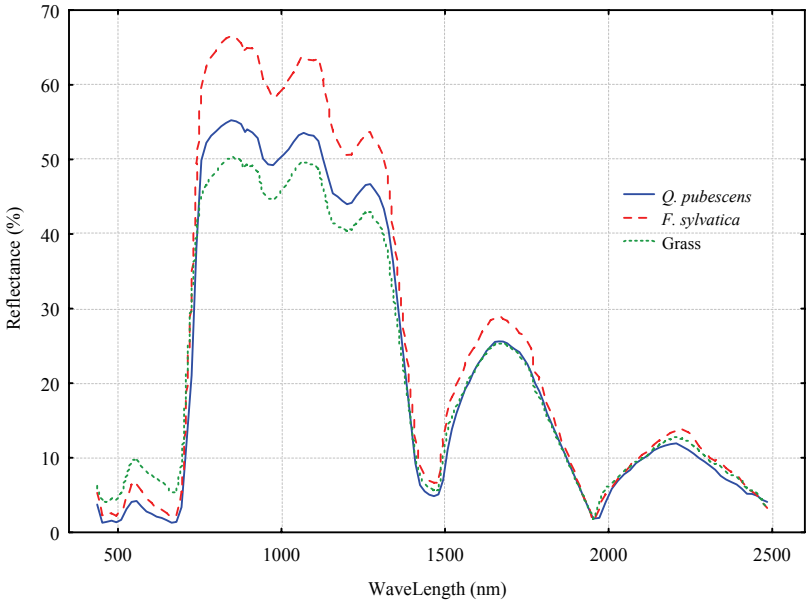

Figure 4.2 Average reflectance spectra of three species extracted from HyMap image.

4.2.4.1 Spectral correlation measure (SCM)

SCM (van der Meer and Bakker, 1997) calculates the correlation coefficient of the spectral signatures $\boldsymbol{s}_i = (s_{i1}, \ldots\ldots, s_{iL})^T$ and $\boldsymbol{s}_j = (s_{j1}, \ldots\ldots, s_{jL})^T$ and is defined as:

$$r_{si,sj} = \frac{n\sum_n^n s_i s_j - \sum_1^n s_i \sum_1^n s_j}{\sqrt{\left[n\sum_1^n s_i^2 - \left(\sum_1^n s_i\right)^2\right]\left[n\sum_1^n s_j^2 - \left(\sum_1^n s_j\right)^2\right]}} \qquad \text{Eq. 1}$$

where n is the number of spectral bands.

SCM takes into account the relative (overall) shape of the spectrum as well as the spectral match. This means that the resulting statistic matches the individual absorption features and the often found decline to longer and shorter wavelengths at the long and short ends of the spectrum of the reflectance values (i.e., differences in albedo) (van der Meer, 2006).

4.2.4.2 Spectral angle mapper (SAM)

SAM is the most popular and widely used spectral similarity measure in hyperspectral remote sensing. It calculates spectral similarity by measuring the angle between the spectral signature of two samples, $\boldsymbol{s}_i$ and $\boldsymbol{s}_j$ (Yuhas, 1992; Kruse et al., 1993). The measure determines the similarity between two spectra by calculating the spectral angle between them, treating them as vectors in a space with dimensionality equal to the number of spectral bands used (Kruse et al., 1993). This technique is relatively insensitive to illumination and albedo effects because the angle between two vectors is invariant with respect to the length of the vectors (Kruse, 1997). SAM between two spectral signatures $\boldsymbol{s}_i = (s_{i1}, \ldots\ldots s_{iL})^T$ and $\boldsymbol{s}_j = (s_{j1}, \ldots\ldots s_{jL})^T$ can be defined as:

$$SAM(s_i, s_j) = \cos^{-1}\left(\frac{\sum_{l=1}^{L} s_{il} s_{jl}}{\left[\sum_{l=1}^{L} s_{il}^2\right]^{1/2}\left[\sum_{l=1}^{L} s_{jl}^2\right]^{1/2}}\right) \quad \text{Eq. 2}$$

Another popular deterministic similarity measure in remote sensing is the Euclidean distance (ED):

$$ED(s_i, s_j) = 2\sin\left(\frac{SAM(s_i, s_j)}{2}\right) \quad \text{Eq. 3}$$

However, when the angle produced between two spectra is very narrow in SAM(s_i, s_j), ED(s_i, s_j) and SAM become virtually the same. As this applies in the case of two vegetation spectra, we did not consider ED in this study.

4.2.4.3 Spectral information divergence (SID)

SID (Chang, 2000) derives from divergence theory and calculates the probabilistic behaviours between spectral signatures (Chang, 2003; van der Meer, 2006). Compared with SAM, which examines the geometrical characters between two spectral signatures or pixel vectors, SID computes the discrepancy between the probability distributions produced by the spectral signatures. Consequently, SID might be more effective than SAM in capturing the subtle spectral variability (Chang, 2003) natural to plant spectra. SID between two spectral signatures can be defined as:

$$SID(r_i, r_j) = D(r_i \| r_j) + D(r_j \| r_i) \quad \text{Eq. 4}$$

where

$$D(r_i \| r_j) = \sum_{l=1}^{L} p_l D_l(r_i \| r_j) = \sum_{l=1}^{L} p_l (I_l(r_i) - I_l(r_j)) = \sum_{l=1}^{L} p_l \log(p_l / q_l) \quad \text{Eq. 5}$$

and

$$D(r_j \| r_i) = \sum_{l=1}^{L} q_l D_l(r_j \| r_i) = \sum_{l=1}^{L} q_l (I_l(r_j) - I_l(r_i)) = \sum_{l=1}^{L} q_l \log(q_l / p_l) \quad \text{Eq. 6}$$

calculated from the probability vectors $\boldsymbol{p} = (p_1, p_2, \ldots\ldots p_L)^T$ and $\boldsymbol{q} = (q_1, q_2, \ldots\ldots q_L)_T$ for the spectral signatures of s_i and s_j, where $p_k = s_{ik} \Big/ \sum_{l=1}^{L} s_{il}$ and $q_k = s_{jk} \Big/ \sum_{l=1}^{L} s_{jl}$. So the self-information provided by $\mathbf{r}_j$ for band *l* is defined by $\boldsymbol{I}_l(\mathbf{r}_j)$ = -log q_l and similarly $\boldsymbol{I}_l(\mathbf{r}_i)$ = -log p_l. According to information theory, $D(r_i \| r_j)$ in Eq. 5 is called the relative entropy of $\mathbf{r}_j$ with respect to $\mathbf{r}_i$, which is also known as the Kullback-Leibler information measure (Kullback, 1959).

4.2.4.4 SID-SAM mixed measure

The SID-SAM mixed measure proposed by Du et al. (2003, 2004) to increase discriminability makes two similar spectra even more similar and two dissimilar spectra more distinct. Although the measurement can be implemented in two versions (as described in Eqs 7 and 8), but because of their similar and closely related outputs, we only used the tangent of the SAM version in our analysis.

$$SID(TAN) = SID(s_i, s_j) \times \tan(SAM(s_i, s_j)) \quad \text{Eq. 7}$$

$$SID(SIN) = SID(s_i, s_j) \times \sin(SAM(s_i, s_j)) \quad \text{Eq. 8}$$

4.2.5 Measurements for discriminability

Spectral similarity measures calculate similarity or dissimilarity between two pixel vectors or two spectral signatures, but these paired discrimination procedures alone are not enough to discriminate more than two pixel vectors or spectral classes. Moreover, as different similarity measures use different units of measurement, it is impossible to evaluate their performance without comparable statistics. Therefore, in order to discriminate a set of spectral classes of different plant species or to determine the relative performance of the measures described above, two statistical algorithms, (i) relative spectral discriminatory probability (RSDPB) and (ii) relative spectral discriminatory power (RSDPW), were used.

Table 4.2 Similarity score produced by SCM algorithm between species pairs. Full and NIR spectral ranges are shown in the upper right half of the table and visible and SWIR ranges in the lower left half of the table.

			C intybus	*O vulgare*	*C monogyna*	*P spinosa*	*A campestre*	*F sylvatica*
					Full spectral range			
visible range	Herb	*C intybus*		0.99508	0.98216	0.98793	0.97816	0.98339
		O vulgare	0.88270		0.98276	0.98701	0.97416	0.98041
	Shrub	*C monogyna*	0.77206	0.68711		0.99488	0.99730	0.99819
		P spinosa	0.79210	0.71246	0.99806		0.99275	0.99572
	Tree	*A campestre*	0.79316	0.60944	0.93734	0.94311		0.99606
		F sylvatica	0.79904	0.70946	0.99277	0.99497	0.95433	
					NIR range			
SWIR range	Herb	*C intybus*		0.97464	0.94325	0.98314	0.95933	0.96348
		O vulgare	0.99461		0.96397	0.97665	0.96193	0.97096
	Shrub	*C monogyna*	0.99519	0.99469		0.98425	0.99372	0.99489
		P spinosa	0.99704	0.99584	0.99839		0.99252	0.99324
	Tree	*A campestre*	0.99685	0.99485	0.99746	0.99652		0.99844
		F sylvatica	0.99376	0.99620	0.99646	0.99600	0.99742	

Table 4.3 Similarity score produced by SAM algorithm between species pairs. Full and NIR spectral ranges are shown in the upper right half of the table and visible and SWIR ranges in the lower left half of the table.

			C intybus	*O vulgare*	*C monogyna*	*P spinosa*	*A campestre*	*F sylvatica*
					Full spectral range			
visible range	Herb	*C intybus*		0.05592	0.12421	0.11769	0.14658	0.13222
		O vulgare	0.13039		0.12764	0.13763	0.16078	0.14545
	Shrub	*C monogyna*	0.24563	0.24781		0.0752	0.04994	0.04206
		P spinosa	0.24040	0.23836	0.02235		0.07829	0.06224
	Tree	*A campestre*	0.15492	0.21565	0.14196	0.13756		0.03408
		F sylvatica	0.17459	0.19682	0.08194	0.07835	0.08419	
					NIR range			
SWIR range	Herb	*C intybus*		0.04456	0.052139	0.04081	0.06406	0.05691
		O vulgare	0.05219		0.061338	0.07097	0.08875	0.08013
	Shrub	*C monogyna*	0.06274	0.04982		0.03207	0.03494	0.02793
		P spinosa	0.09336	0.07271	0.047595		0.02648	0.02154
	Tree	*A campestre*	0.03450	0.04752	0.04799	0.08508		0.01332
		F sylvatica	0.05134	0.04150	0.04746	0.07895	0.03370	

4.2.5.1 Relative spectral discriminatory probability (RSDPB)

RSDPB calculates the relative capability of all spectra to be discriminated from others. In general, the higher the probability, the better is the capability of a set of spectra to be discriminated from others. Let $\{s_k\}_{k=1}^{K}$ be *K* spectral signatures in the set Δ, which can be considered as a database, and **t** be any specific target spectral signature to be identified using Δ (Chang, 2003). The definition of the RSDPB of all $\mathbf{s}_k$ in Δ relative to **t** is:

$$P_{t,\Delta}(k) = \frac{m(t,s_k)}{\sum_{j=1}^{L} m(t,s_j)} \qquad \text{For } k = 1, \ldots\ldots, K \qquad \text{Eq. 9}$$

where $\sum_{j=1}^{L} m(t,s_j)$ is the normalization constant and $m(t,s_k)$ is any of the previously defined spectral similarity measures. $\sum_{j=1}^{L} m(t,s_j)$ is defined as the sum of all similarity measures in an endmember matrix and $m(t,s_k)$ is the sum of all similarity measures for the target spectrum ***t*** relative to the other spectra s_k.

4.2.5.2 Relative spectral discriminatory power (RSDPW)

RSDPW lies in calculating how well one spectral vector can be distinguished (discriminated) from another spectral vector, relative to a reference spectral vector (Chang, 2003; van der Meer, 2006). Given *m*(.,.) is a spectroscopy measurement, ***d*** is the reference spectral signature, and s_i and s_j are the spectral signatures or pair of pixel vectors, the RSDPW of *m*(.,.) represented by $RSDPW_m$ (s_i,s_j;***d***) is:

$$\Omega(s_i,s_j;d) = \max\left\{\frac{m(s_i,d)}{m(s_j,d)}, \frac{m(s_j,d)}{m(s_i,d)}\right\} \qquad \text{Eq. 10}$$

4.2.6 Use of similarity measure as classifier

We also tested the performance of two similarity measures (SAM and SID) as classifiers and classified a small subset of a HyMap image of Majella National Park, Italy, composed of beech and oak forest and grassland vegetation. We used threshold values for angle and divergence to assign the pixels to a specific class. We calculated the overall accuracy of the classification, kappa coefficients ($\hat{K}$) and *z* statistics between the two classifiers.

4.3 Results

4.3.1 Similarity of spectra within and between species

The ability of hyperspectral sensors to determine plant species depends largely on inter-specific and intra-specific spectral variability, so it was imperative to check the similarity values within and between species.

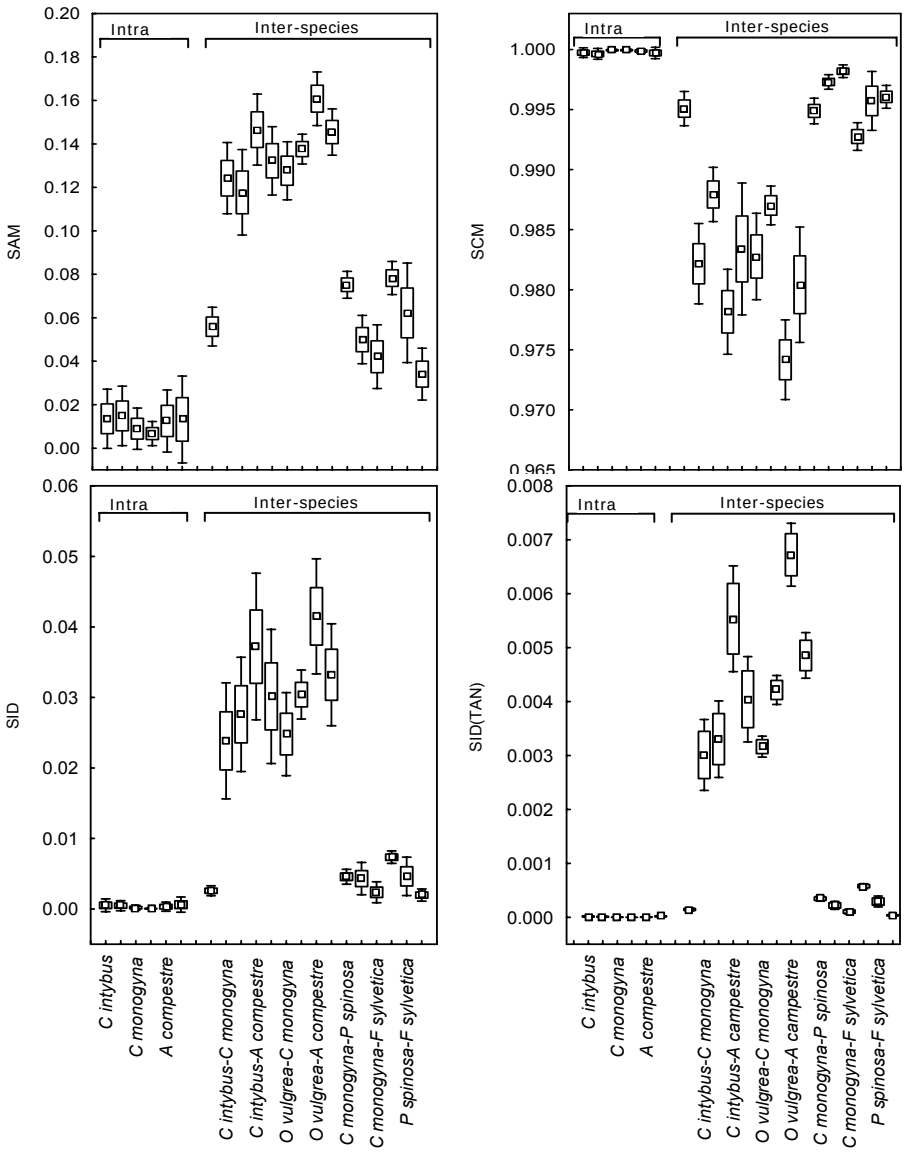

Figure 4.3 Differences of values in intra and inter-species setting using three different similarity measures.

Spectral similarity within a species was significantly higher than that between different species (Figure 4.3). It is also evident from Figure 4.3 that, compared with the leaf spectra of herbs, the leaves of shrubs and trees are more similar.

Table 4.4 Similarity score produced by SID algorithm between species pairs. Full and NIR spectral ranges are shown in the upper right half of the table and visible and SWIR ranges in the lower left half of the table.

			C. intybus	*O vulgare*	*C monogyna*	*P. spinosa*	*A. campestre*	*F. sylvatica*
					Full spectral range			
visible range	Herb	*C intybus*		0.00259	0.02384	0.02760	0.03721	0.03014
		O vulgare	0.00794		0.02480	0.03041	0.04149	0.03320
	Shrub	*C monogyna*	0.02612	0.02508		0.00457	0.00431	0.00237
		P spinosa	0.02536	0.02341	0.00257		0.00735	0.00464
	Tree	*A campestre*	0.01019	0.02049	0.00995	0.00958		0.00198
		F sylvatica	0.01322	0.01628	0.00324	0.00306	0.00344	
					NIR range			
SWIR range	Herb	*C intybus*		0.00113	0.00163	0.00147	0.00343	0.00256
		O vulgare	0.00266		0.00289	0.00401	0.00660	0.00523
	Shrub	*C monogyna*	0.00484	0.00323		0.00052	0.00098	0.00055
		P spinosa	0.00898	0.00581	0.00148		0.00051	0.00027
	Tree	*A campestre*	0.00095	0.00196	0.00302	0.00658		0.00014
		F sylvatica	0.00178	0.00172	0.00303	0.00628	0.00068	

Table 4.5 Similarity score produced by SID(TAN) algorithm between species pairs. Full and NIR spectral ranges are shown in the upper right half of the table and visible and SWIR ranges in the lower left half of the table.

			C. intybus	*O vulgare*	*C monogyna*	*.P spinosa*	*A. campestre*	*F. sylvatica*
					Full spectral range			
visible range	Herb	*C intybus*		0.00015	0.00301	0.00330	0.00553	0.00404
		O vulgare	0.00105		0.00316	0.00421	0.00672	0.00485
	Shrub	*C monogyna*	0.00677	0.00652		0.00034	0.00022	0.00010
		P spinosa	0.00642	0.00585	0.00001		0.00057	0.00029
	Tree	*A campestre*	0.00170	0.00455	0.00144	0.00134		0.00004
		F sylvatica	0.00252	0.00337	0.00028	0.00025	0.0003	
					NIR range			
SWIR range	Herb	*C intybus*		0.00005	0.00009	0.00006	0.00022	0.00015
		O vulgare	0.00015		0.00018	0.00029	0.00059	0.00042
	Shrub	*C monogyna*	0.00031	0.00017		0.00002	0.00004	0.00002
		P spinosa	0.00085	0.00045	0.00007		0.00001	0.00001
	Tree	*A campestre*	0.00003	0.00010	0.00015	0.00056		0.00001
		F sylvatica	0.00009	0.00008	0.00015	0.00051	0.00002	

4.3.2 Spectral similarity

4.3.2.1 Laboratory spectra

Tables 4.2 to 4.5 show the similarity scores produced by the similarity measures SCM, SAM, SID and SID(TAN), respectively. These tabular scores were used to compute the RSDPB (Figure 4.4) and the RSDPW (Figure 4.5).

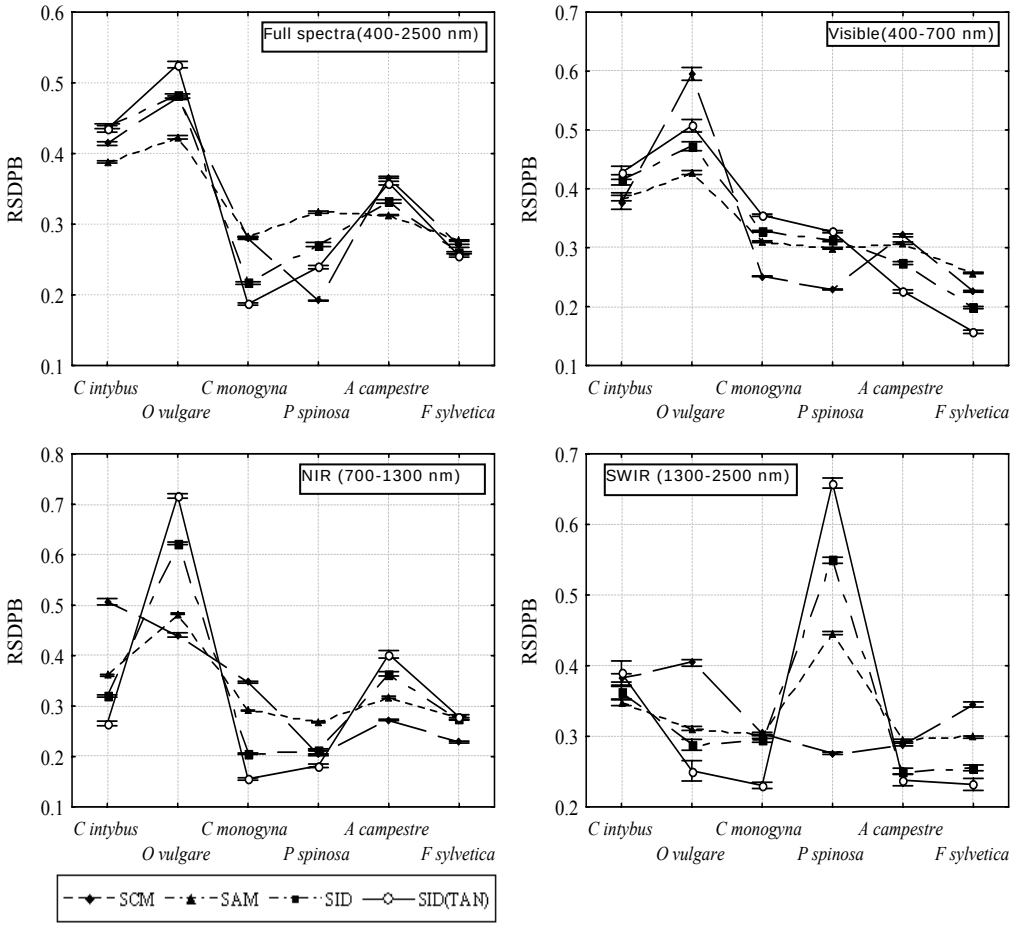

Figure 4.4 RSDPB result for the laboratory plant spectra of six species and three spectral similarity measures. Four different spectral configurations are shown in four graphs.

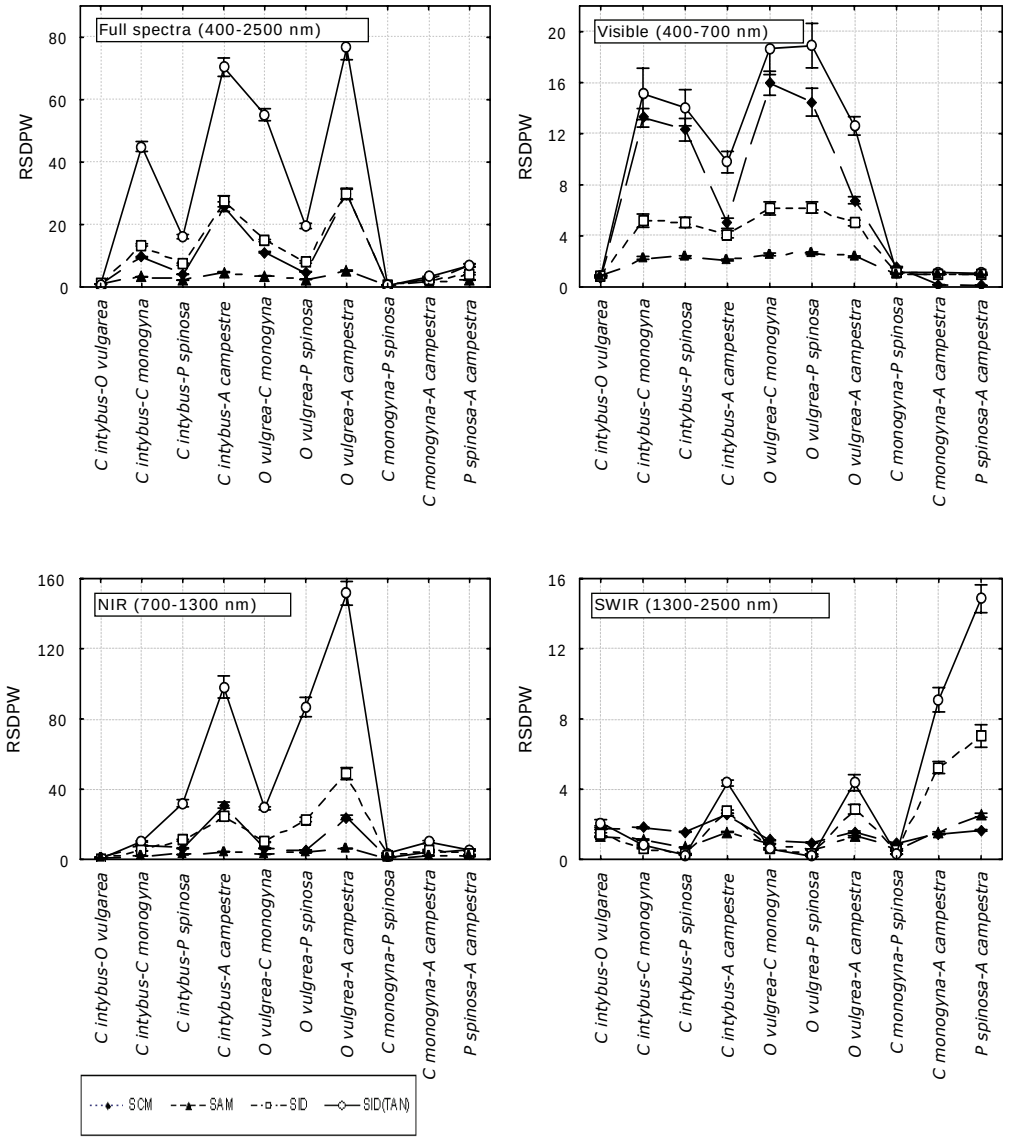

Figure 4.5 RSDPW result for the laboratory plant spectra using *Fagus sylvatica* as reference. Four different spectral configurations are shown in four graphs.

The RSDPB statistic (Figure 4.4) revealed that for the four spectral configurations the spectra from the two herb species showed greater discriminatory probability than the spectra from the trees and shrubs. Apart from the SWIR section, the different configurations did not provide much different information regarding relative discriminatory probability.

On a species-by-species basis, *Origanum vulgare* showed the highest separability. The two shrub species demonstrated the lowest separability in all configurations, except in the SWIR section, where they showed better separability. In particular, *Prunus spinosa* showed the highest separability of all species in the SWIR section. As regards the two tree species, *Acer campestre* showed higher discriminatory probability than *Fagus sylvatica*.

Fagus sylvatica was used as reference spectra to compute the RSDPW statistic (Figure 4.5) for the laboratory plant spectra (see Section 2). With reference to a tree leaf spectral vector, both herbs (*C. intybus* and *O. vulgare*) and shrubs (*C. monogyna* and *P. spinosa*) revealed low discriminatory power within the group in all spectral configurations. Both the trees and shrubs showed higher discrimination from herbs. However, except in the SWIR section, it was difficult to separate tree spectra (*A. campestre*) from the shrubs. As with the RSDPB, here too the SWIR section showed a pattern of discrimination very different from that of the other configurations.

For RSDPB, different measurements did not always show similar trends (Figure 4.4). SAM and SID followed a largely similar trend in all configurations. The performance of SID(TAN) was also linked to SAM and SID, but SID(TAN) showed higher discriminability than either SAM or SID for most of the species. SCM failed to produce the best discrimination for any species in the full spectral configuration, but in shorter spectral configurations it performed comparatively better. For RSDPW, in most of the combinations the SID(TAN) dissimilarity scores were more than twice as effective in terms of spectral discrimination (Figure 4.5). SID came second, except in the visible range, where SCM performed strongly.

4.3.2.2 Spectra from image

Spectra collected from the image produced consistent results similar to those found for the laboratory spectra. Figure 4.6 reveals that grass spectra are very dissimilar and can be easily discriminated from *Q. pubescens* and *F. sylvatica* spectra. The discrimination probabilities of the two tree species were much less prominent. For RSDPW, grass spectra were used as a reference to distinguish two tree species spectra. The SID(TAN) measure performed higher for both RSBPD and RSBPW.

4.3.3 Similarity measures as classifier

Because of the simplicity of the landscape, both algorithms performed very well as classifiers (Table 4.6). The outcome of the overall classification accuracy for the two algorithms (see Table 4.6) revealed that SID outperformed SAM as a classifier. Kappa coefficient ($\hat{K}$) values also supported SID's superiority. A *z* statistic (Table 4.6) between the two classifiers proved there was a significant difference in ($\hat{K}$) values for the two classified images, as the null hypothesis was rejected using the

normal curve deviate statistic (z) for α = 0.05 if z_t > 1.96 (i.e. $z_{\alpha=0.05}$ = 1.96).

Table 4.6 Comparison between the performances of two classifiers

	SAM	SID
Overall accuracy (%)	84.7102	91.0995
Kappa coefficient ($\hat{K}$)	0.7703	0.8672
z statistic	3.35016	

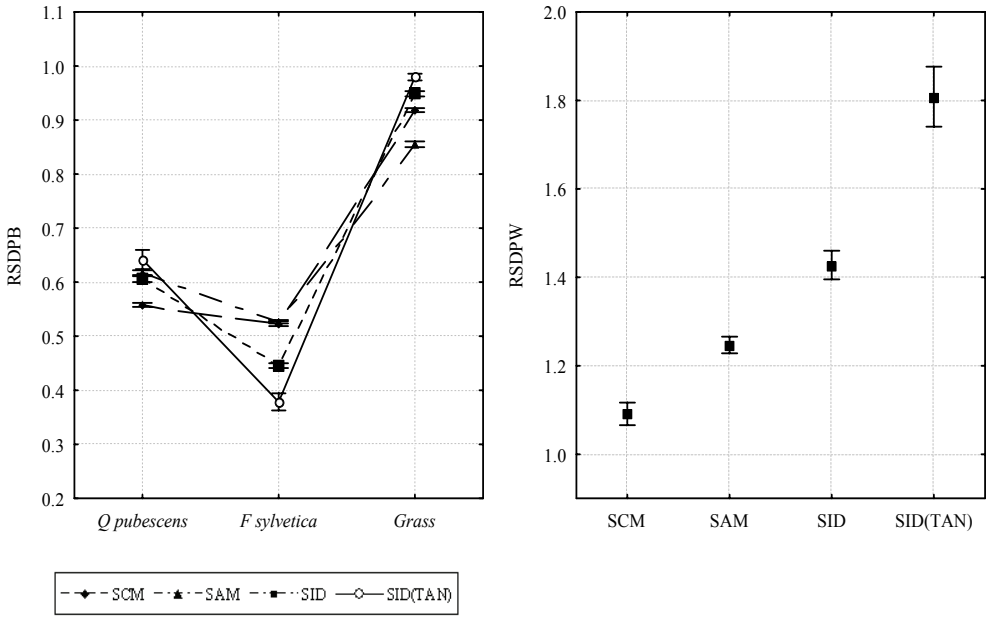

Figure 4.6 RSDPB & RSDPW results for the image derived plant spectra of three species and three spectral similarity measures. In RSDPW grass species has been used as reference endmember to calculated discriminatory power between *Q. pubescens* and *F. sylvatica*.

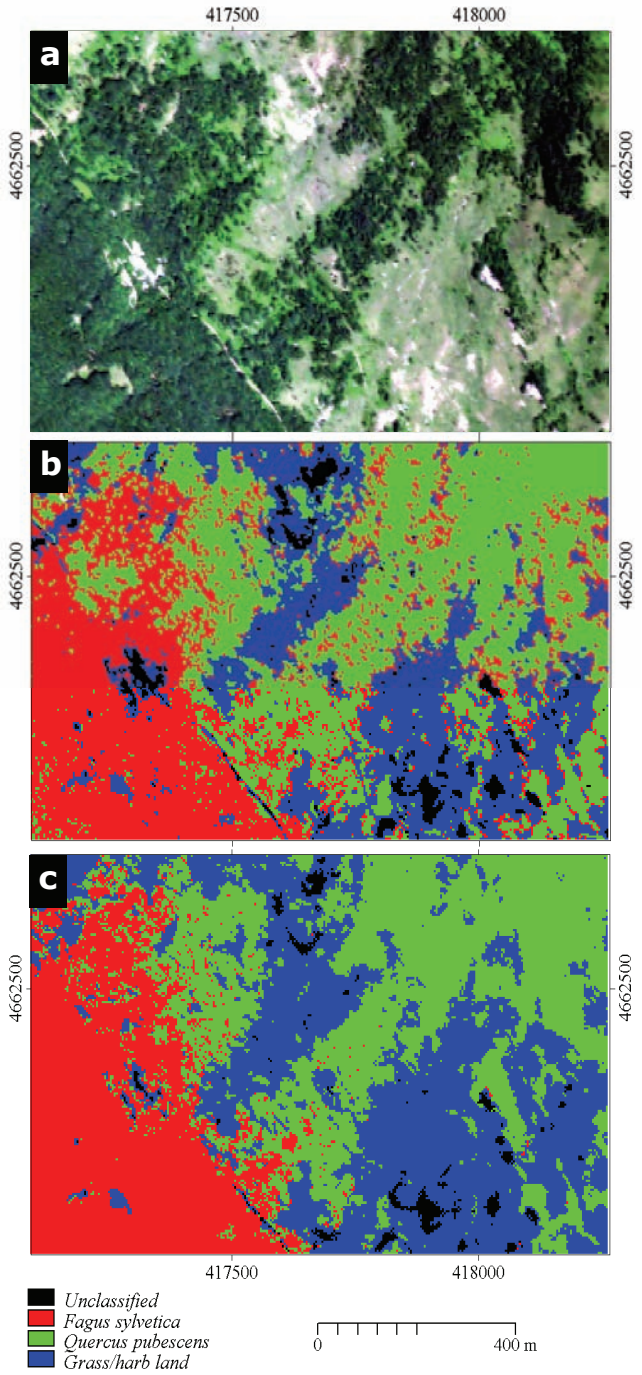

Figure 4.7 a. A true colour composite HyMap image from Majella National Park, Italy. b. Classified images of the same area using SAM. c. Classified image of the same area using SID.

4.4 Discussion

Spectral similarity measures were successful in discriminating species for laboratory-level leaf spectra, as well as image-level species endmember spectra (collected from the airborne HyMap hyperspectral image). From the results (Tables 4.2 to 4.5), it is evident that all four similarity measures managed to find dissimilarities between the spectra of different plant species, but from the tabular data it is not possible to infer the discrimination performance of individual species. Moreover, similarity measurements were performed in a pairwise manner, not in a multivariate set-up. To overcome the problem of pairwise measurements in a multiple species set-up, we used the RSDPB and RSDPW objective statistical algorithms. RSDPB revealed the degree of discrimination of individual species in relation to others. The results of RSDPB (Figure 4.4) revealed that both the herb species can be discriminated more accurately from shrub and tree species in the full, visible and NIR spectral configurations. In general, the discrimination probability followed the line of species types rather than individual species. This might be due to the differences in leaf structure of the species, since the leaf structures of herbaceous species differ from those of trees and woody shrubs. This was more evident since the two herb species had shown relatively higher separability from both the shrub and tree species, while the shrub and tree species had only minor differences between them. The results of RSDPW (Figure 4.5) revealed similar groupings, as relative discrimination between the two herbs (*C. intybus* and *O. vulgare*) and two shrubs (*C. monogyna* and *P. spinosa*) spectra showed very low probability of discrimination. In addition, discrimination of herb spectra from shrub and tree spectra remained very prominent. The differences between shrub and tree spectra appeared only when using the SWIR part of the spectra. The results from image spectra (Figure 4.6) also showed a relatively higher discrimination accuracy for grass spectra from the two tree species.

Use of different parts of the spectra did not reveal any significant differences in species discrimination, contradicting our expectations and earlier literature (Verbyla, 1995; Atkinson et al., 1997; Gong et al., 1997; Cochrane, 2000). The only exception was in the SWIR section, where both RSDPB and RSDPW showed very different discrimination probability from that in the rest of the spectra. Although not conclusive, it was apparent that the discriminatory scores (Figures 4.4 and 4.5) of full spectral configurations were a generalization or an average of the visible, NIR and SWIR sections, accommodating all the variations in discriminatory probability or power found in the three sections separately.

Comparing the performance of the four similarity measures was not easy, especially with regard to the RSDPB results (Figures 4.4 and 4.6). For most species, the mixed measure SID(TAN) worked better, but the results were not conclusive. SAM and SID followed a similar pattern in all

the configurations, but in general SID performed better than SAM in most cases. As far as the RSDPW statistics (Figure 4.5) are concerned, SID(TAN) significantly outperformed the other measures. The better performances of SID and SID(TAN) in discriminating plant spectra are consistent with the findings of Du et al. (2004). These authors argue that the information theory-based measures allow each spectrum or pixel vector to have a certain degree of spectral variation, which may be a better alternative to other empirical measures such as SCM or SAM. This is particularly true for plant spectra, which always have subtle variations because of various environmental factors. Despite the fact that SCM managed to discriminate among all the species, it failed to produce good results for many of them. As SCM is highly sensitive to the overall spectral shape (van der Meer and Bakker, 1997) and plant spectra are similar in shape (Portigal et al., 1997), this measure failed to provide the best variability between species. In shorter spectral ranges, SCM worked comparatively better than in the full spectral configuration. In general, however, reduction in band number did not really support any specific similarity measure, and their overall performances remained more or less unchanged from those in the full spectral configuration.

Using SAM and SID measures as classifiers produce visually similar outputs (although this was not unexpected as they were only tested on discriminating between three different spectral classes). However, as shown in Table 4.6, the overall accuracy and kappa coefficient of SID were higher. The z statistic also revealed that the classification performed by SID was significantly better than that by SAM.

4.5 Conclusion

This study applied four spectral similarity measures to discriminate the laboratory spectra of six plant species and the image spectra of three vegetation types. Two discriminatory statistical algorithms were used to evaluate the results produced by the similarity measures and determine their performance. The performances of similarity measures when used as classifiers were also tested. The following conclusions can be drawn from this study:

1. Spectral similarity measures were successfully used to discriminate species. Discriminations were more prominent along the line of species types (i.e., herb, shrub and tree) rather than for individual species.
2. Use of different parts of the spectra did not reveal any significant differences in species discrimination. The only exception was the SWIR section, where both RSDPB and RSDPW showed very different discrimination probability from that found in the rest of the spectral configurations.
3. The mixed algorithm SID(TAN) outperformed all the other similarity measures in spectral discrimination. SID(TAN) uses both SAM and SID to make similar spectra even more similar and dissimilar spectra

more distinct. SID came second, although SAM followed a very similar trend.

4. Compared with SAM, SID produces higher accuracy when used as a classifier.

Acknowledgements

Thanks are due to Bas Retsios and Harald van der Werff for programming support. This study was financially supported by Nuffic and ITC.

In Chapter 4, we examine the possibility of using several spectral matching techniques and compared their usefulness. In the following chapter (chapter 5) two of these spectral matching algorithms are used to measure the dissimilarities between species. However, the main objective of this chapter is the use of a phenological event (flowering) to enhance spectral discrimination between species. We hypothesized that flower pigment will enhance separability of species.

Chapter 5

Use of phenological events to increase species discrimination

Md. Istiak Sobhan, Andrew K. Skidmore, Moses A. Cho
and Herbert H. T. Prins
(In preparation)

Abstract

Phenology is a long-known physiological process of plants with a well-defined temporal pattern. Although remote sensing has traditionally been used to track the phenological changes of plant communities, their use in discriminating plant species is rather limited. In this study, we investigated the nature and magnitude of changes produced by a phenological event (i.e., flowering), for the purpose of maximizing species discrimination. Reflectance measurements were made of six herb species, both with and without flowers in the canopy. Spectral differences between the with-flower and without-flower stages were determined using two spectral similarity algorithms (i.e., spectral angle mapper (SAM) and spectral information divergence (SID)). Moreover, we used continuum-removed band depth analysis for the pigment absorption regions (400 nm to 550 nm and 551 nm to 725 nm) in order to examine the influence of floral pigment on the spectra. The results showed that, although species are separable at both stages, the magnitude of separation was significantly higher with flowers in the canopies. They also revealed that the major source of this enhanced discrimination originated from the visible part of the spectra. Band depth analyses also confirmed that more species pairs demonstrated higher separability in with-flower measurements. Our investigation into the change in image classification accuracy because of phenological differences revealed a significant difference between two dates (z = 5.4883), and the target species in flower showed much less confusion in the matrix. Finally, we conclude that flowering has a positive effect on discrimination between these species. Therefore, the discriminatory probability between two species can differ according to the time of the year.

Keywords: phenology; hyperspectral; species discrimination.

5.1 Introduction

Phenology is the study of the times of recurring natural phenomena. The word is derived from the Greek *Phainomai* (φαινομαι), meaning to appear or to come into view, and indicates that phenology is concerned principally with the dates of the first occurrence of natural events in their annual cycle. Examples include the dates of emergence of leaves and flowers, the first flight of butterflies, and the first appearance of migratory birds (Wikipedia, 2007). Ecological studies have demonstrated that vegetation phenology has a relatively well-defined temporal pattern (Goward, Tucker and Dye, 1985; Prins and Loth, 1988). For example, in deciduous vegetation and in many crops, leaf emergence tends to be followed by a period of rapid growth, then a relatively stable period of maximum leaf area, and subsequently the emergence of flowers and fruits (Zhang et al., 2003). Recent technological developments in remote sensing have generated a new field in phenological research that is concerned with the study of phenological cycles of whole ecosystems on a global scale.

As the changes in phenological stages can be observed at all different scales, ranging from field level to satellite sensing level, for obvious reasons they have attracted a lot of attention since the early days of remote sensing (Vinogradov, 1977; Boyer et al., 1988; Brisco, Brown and Manore, 1989; Moulin et al., 1997). Phenological studies conducted by means of remote sensing are divided primarily into two distinct divisions. Initial as well as most subsequent research concentrated on tracking phenological variability between different plant communities at varying scales, from ecosystem to country level (Goward, Tucker and Dye, 1985; Reed et al., 1994) and even at global scale (Justice et al., 1985; Zhang et al., 2003). The second and less studied side of plant phenology is the characterization of phenological patterns of individual species and the subsequent discrimination of these species by using the patterns (Turner et al., 2003; Underwood, Ustin and DiPietro, 2003). To make it easier to distinguish between species, most of the above studies have used either multitemporal images of two different phenological stages or images taken on dates when two species are at different phenological stages (Verbyla, 1995). The majority of the studies on plant phenology are based on the changing nature of the spectral characteristics of leaves during autumn senescence (Boyer et al., 1988; Miller et al., 1991; Rock, Lauten and Moss, 1993; Gitelson, Merzlyak and Lichtenthaler, 1996). However, with the arrival of imaging spectroscopy and hyperspectral sensors, the need has declined for multitemporal images for species discrimination purposes. The availability of images with high spectral and spatial resolutions has made it possible to discriminate species with single-date imaging (Everitt et al., 1992; Parker Williams and Hunt, 2002).

Various studies have demonstrated that discrimination at the individual species level can be achieved with a hyperspectral sensor without any

support from phenological events (Cochrane, 2000; Schmidt and Skidmore, 2001; Yamano, Chen and Tamura, 2003; Clark, Roberts and Clark, 2005; Vaiphasa et al., 2005). Price (1994), however, argues the case for the uniqueness of vegetation spectra, and hence the validity of using them for species discrimination. Everitt et al. (1992) document the fact that during flowering both common goldenweed (*Isocoma coronopifolia*) and Drummond goldenweed (*I. drummondii*) can be distinguished from associated plants and soil by using conventional colour aerial photography. Several other studies (Everitt et al., 1995; Lass et al., 2002; Hunt et al., 2003; Hunt et al., 2004; Parker Williams and Hunt, 2004) have also used phenological support to distinguish target species from others. However, most of these studies concentrate on discriminating leafy spurge (*Euphorbia esula*), an invasive species with distinct yellow-green coloured bracts. Ge et al. (2006) have also tried to characterize various canopy components of yellow starthistle (*Centaurea solstitialis*) while flowering, in order to simulate various flowering stages and investigate their influence on spectral regions. Although it is clear from the above that species discrimination is possible without the support of certain phenological episodes, quantitative analysis of the phenological impact on species discrimination is inadequate. Moreover, comparative analysis of discrimination between two species at different phenological stages is still lacking.

The main objective of this study was to investigate the nature and magnitude of changes produced by a phenological event, for the purpose of maximizing species discrimination. To achieve this objective, we used flowering as our target phenological event. Reflectance measurements were made of six herb species, with and without flowers in the canopy. The spectral differences between two separate phenological stages were determined using spectral similarity algorithms. We also hypothesize that, as flowers add pigment signatures to the plant spectra, discrimination would be concentrated largely in the visible part of the spectrum – even though we realise that flowers and pollinators have often co-evolved, leading to enhancement in parts of the spectrum not visible to the human eye. We have thus taken this visible part of the spectrum in quite broad terms.

5.2 Materials and method

5.2.1 Collection of samples

Fully bloomed whole-plant specimens of six herb species (Table 5.1) were collected during summer 2005 in Majella National Park, Italy. After detachment from the substratum, the plants were placed in plastic sample bags and stored in a cool box to reduce transpiration. The samples were then immediately taken to the laboratory for spectral reflectance measurements, and all the measurements were conducted

within two hours of field collection to avoid dehydration-related changes in leaf spectra.

Table 5.1 Species used to measure spectra in this experiment.

Species	Flower colour	Family
Centaurea sp.	Pink	Asteraceae
Cichorium intybus	Blue	Asteraceae
Daucus carota	White	Apiaceae
Galega officinalis	Pink	Fabaceae
Crepis biennis	Yellow	Asteraceae
Scabiosa columbaria	Blue-pink	Dipsacaceae

5.2.2 Collection of spectra

In the laboratory, specimens from the same species were bundled together in such a way that they formed a pure homogenous canopy similar to their natural state. We produced four such canopies (or bouquets) of specimens for each species. These bouquets were held vertically upright by a clamp and placed on the top of a flat black mat to minimize background reflectance. Fifty spectral measurements were obtained for each bouquet, but after every ten measurements they were averaged to produce a single spectrum in order to reduce specular behaviour (Schmidt and Skidmore, 2001). So from four bundles of specimens we constructed 20 spectra. The process was repeated after carefully pruning all the flowers from the plants to mimic the non-flowering stage. At the end, 40 spectra were obtained for each species, half with flowers and half without flowers in the canopy.

A GER 3700 (Geophysical and Environmental Research Corporation, Buffalo, New York) spectroradiometer measured the reflectance spectra. The GER 3700 is a three dispersion grating spectroradiometer using Si and PbS detectors with a single field of view. The wavelength range is from 325 nm to 2500 nm, with sampling intervals of 1.5 nm between 325 nm and 1050 nm, 6.2 nm between 1050 nm and 1900 nm, and 9.5 nm between 1900 nm and 2500 nm. The full width half maxima are 3 nm, 11 nm and 16 nm in the 325 nm to 1050 nm range, 1050 nm to 1900 nm range, and 1900 nm to 2500 nm range, respectively. Although the spectrometer records up to 647 bands, because of the high noise in the extreme short wavelength area, only the spectral range between 400 nm and 2500 nm was analysed, which contains 597 wavebands. The sensor, equipped with a 1.5 m long fibre optic cable (25° field of view) was mounted on a tripod and positioned 20 cm at nadir above the target canopy. A light source (Lowel Pro-Light with 14.5V/50W/3200K JCV halogen lamp) pointing at the centre of the target canopy was placed at 30° off-nadir, approximately 40 cm from the target. The radiance data were converted to reflectance, using scans of a white Spectralon reference panel. The whole operation was conducted under laboratory conditions (i.e., dark room, ±25°C) in order to avoid ambient light sources unrelated to the true spectral signal of the canopy. We used a

Savitzky-Golay (Savitzky and Golay, 1964) second-order polynomial least-squares function of a five-band window to spectrally smooth our data (Schmidt and Skidmore, 2004).

5.2.3 Data Analysis

5.2.3.1 Discrimination through similarity measures

The reflectance was analysed using two similarity measurement algorithms, namely (i) spectral angle mapper (SAM) and (ii) spectral information divergence (SID), to discriminate the species. These similarity measures were computed in four different spectral configurations: full spectral range (400 nm to 2500 nm), visible range (400 um to 700 nm), NIR range (700 um to 1300 nm) and SWIR range (1300 um to 2500 nm).

(i) Spectral angle mapper (SAM)
SAM is the most popular and widely used spectral similarity algorithm in hyperspectral remote sensing. It calculates spectral similarity by measuring the angle between the spectral signature of two samples, $\boldsymbol{s}_i$ and $\boldsymbol{s}_j$ (Yuhas, 1992; Kruse et al., 1993). The algorithm determines the similarity between two spectra by calculating the spectral angle between them, treating them as vectors in a space with dimensionality equal to the number of spectral bands used (Kruse et al., 1993). This technique is relatively insensitive to illumination and albedo effects because the angle between two vectors is invariant with respect to the length of the vectors (Kruse, 1997). SAM between two spectral signatures $\boldsymbol{s}_i = (s_{i1}, \ldots\ldots s_{iL})^T$ and $\boldsymbol{s}_j = (s_{j1}, \ldots\ldots s_{jL})^T$ can be defined as:

$$SAM(s_i, s_j) = \cos^{-1}\left(\frac{\sum_{l=1}^{L} s_{il} s_{jl}}{\left[\sum_{l=1}^{L} s_{il}^2\right]^{1/2} \left[\sum_{l=1}^{L} s_{jl}^2\right]^{1/2}} \right) \quad \text{Eq. 1}$$

(ii) Spectral information divergence (SID)
SID (Chang, 2000) derives from divergence theory and calculates the probabilistic behaviours between spectral signatures (Chang, 2003; van der Meer, 2006). Compared with SAM, which examines geometrical characters such as the angle between two spectral signatures or pixel vectors, SID computes the discrepancy between the probability distributions produced by the spectral signatures. Consequently, SID may be more effective than SAM in capturing spectral variability (Chang, 2003). SID between two spectral signatures can be defined as:

$$SID(r_i, r_j) = D\left(r_i \| r_j\right) + D\left(r_j \| r_i\right) \quad \text{Eq. 2}$$

where

$$D(r_i \| r_j) = \sum_{l=1}^{L} p_l D_l(r_i \| r_j) = \sum_{l=1}^{L} p_l \left(I_l(r_i) - I_l(r_j)\right) = \sum_{l=1}^{L} p_l \log(p_l / q_l) \quad \text{Eq. 3}$$

and

$$D(r_j \| r_i) = \sum_{l=1}^{L} q_l D_l(r_j \| r_i) = \sum_{l=1}^{L} q_l \left(I_l(r_j) - I_l(r_i)\right) = \sum_{l=1}^{L} q_l \log(q_l / p_l) \quad \text{Eq. 4}$$

calculated from the probability vectors $\boldsymbol{p} = (p_1, p_2, \ldots\ldots p_L)^T$ and $\boldsymbol{q} = (q_1, q_2, \ldots\ldots q_L)_T$ for the spectral signatures of s_i and s_j, where $p_k = s_{ik} \Big/ \sum_{l=1}^{L} s_{il}$ and $q_k = s_{jk} \Big/ \sum_{l=1}^{L} s_{jl}$. So the self-information provided by $\mathbf{r}_j$ for band *l* is defined by $\boldsymbol{I}_l(\mathbf{r}_j)$ = -log q_l and similarly $\boldsymbol{I}_l(\mathbf{r}_i)$ = -log p_l. According to information theory, $D(r_i \| r_j)$ in Eq. 2 is called the relative entropy of $\mathbf{r}_j$ with respect to $\mathbf{r}_i$, which is also known as the Kullback-Leibler information measure (Kullback, 1959).

The differences in similarity values generated from phenological changes and spectral configurations were compared statistically. Two sample *t* tests were used to ascertain whether discriminability between a species pair changes because of a phenological event. *t* tests were also used to detect the magnitude of changes caused by the flowering event in different parts of the spectra. A one-way ANOVA test was performed to test the significant difference ($p \leq 0.05$) of species separability when using different spectral configurations. In the case of significant differences in similarity values (i.e., spectral angle and SID value), the Bonferroni post hoc test was applied to identify which groups are significantly different.

5.2.3.2 Continuum removed band depth analysis

We hypothesized that during flowering the differences between the species would be more prominent in the visible part of the spectra because of enhanced absorption by floral pigments. Hence, to test this hypothesis in a more detailed manner, we used continuum-removed band depth analysis for the two known main pigment absorption features (between 400 um and 550 nm and between 551 and 750 nm) in the visible region. Continuum removal normalizes the reflectance spectra by applying a convex hull fitted over the top of the local maxima and allows comparison of individual absorption features (Kokaly, and Clark, 1999). After the application of continuum removal, band depth was calculated for each wavelength within the absorption features as described by Mutanga, Skidmore and Prins (2004) and Noomen et al. (2006), but only the maximum band depths for each absorption feature were used for this investigation (Figure 5.1). The band depth values were then used to compute *t* values between all species pairs, both with-flower and without-flower measurements. These series of with-flower and without-flower *t* values were then plotted against each other in a scatter plot to visualize

the relative discrimination. To reduce the error produced by multiple comparison, we used the *t* test with the Bonferroni adjusted significance level (ά = 0.003, with initial ά = 0.05/15 pairs of species).

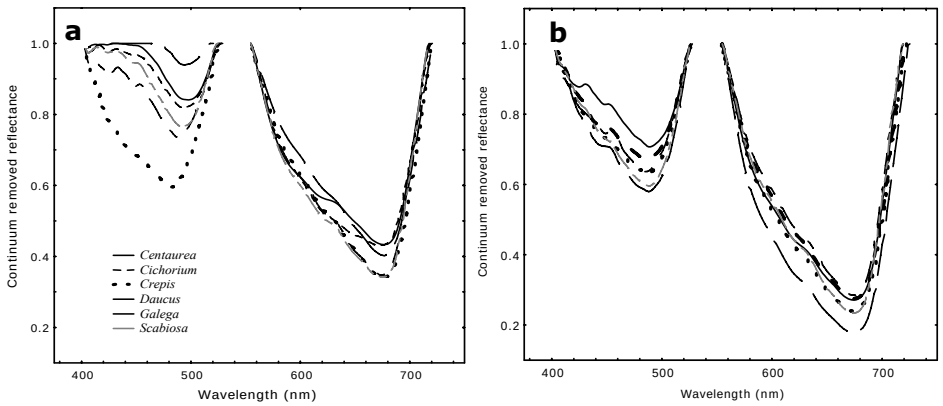

Figure 5.1 Continuum removed band depth profile for different plant species. (a) with-flowers; (b) without-flowers.

5.2.4 Effect of phenological differences on classification accuracy

Two HyMap hyperspectral images from the same area of Majella National Park, Italy, were used to investigate the effect of phenological differences on classification accuracy (detailed description of the image acquisition and pre-processing are provided in the next chapter). The two images were obtained on 15 July 2004 and 4 July 2005, respectively. Our main target species was Spanish broom (*Spartium junceum* L.), a shrub with bright yellow flowers, and we hypothesized that in blooming condition it could be well separated from another associated shrub species (i.e., *Prunus spinosa*) in the area., Although the two image acquisition dates were only two weeks apart but as the main blooming season for this species is late June (reflected in the image of 4 July), and the plants are virtually flowerless by mid-July (reflected in the image of 15 July). The ground covers between these two dates had not changed and therefore we used the same training and test field data set for classification and accuracy measurements. The SAM classifier was used to classify the images. We calculated the overall accuracy of the classification, kappa coefficients ($\hat{K}$) and *z* statistics between the two dates. Producer and user accuracies were also calculated for all cover classes.

5.3 Results

5.3.1 Visual differences in spectra

We measured the spectra of the flowers separately from those of the plants (Figure 5.2a) and they obviously differed greatly, especially in the visible and NIR regions of the spectra. Although reduced to a great extent, the effect of these flowers was still noticeable in the plant spectra measured with the flowers (Figure 5.2b and enlarged in the inset), and these differences between species were visible in the visible part of the spectra. In without-flower measurements, however, visual differences were non-existent.

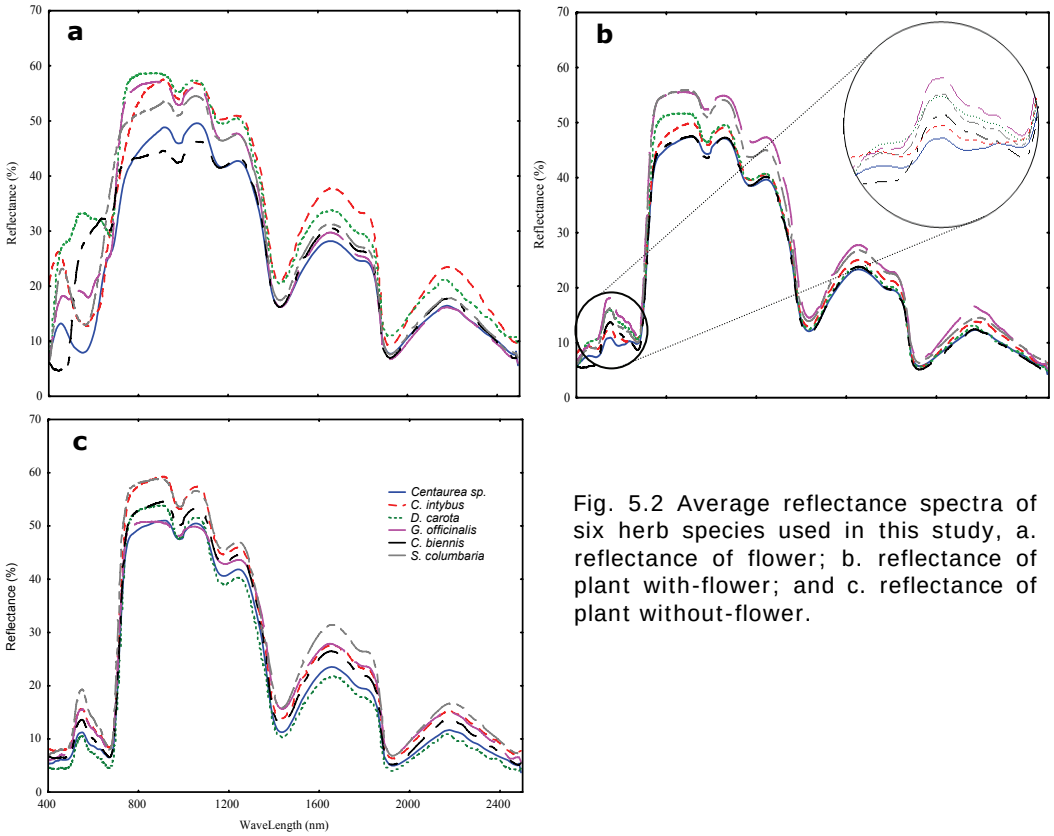

Fig. 5.2 Average reflectance spectra of six herb species used in this study, a. reflectance of flower; b. reflectance of plant with-flower; and c. reflectance of plant without-flower.

5.3.2 Comparison of discriminations

The results showed that all six species were spectrally separable by both algorithms and in both phenological conditions (Figure 5.3). However, there were large differences in the discriminatory values (i.e., spectral angle and spectral divergence) between with-flower and without-flower measurements. With-flower discrimination scores were almost twice as high as without-flower values, especially in the visible and full spectral ranges (Figure 5.3). A one-way ANOVA was used to test whether the discrimination scores produced by the different spectral configurations when discriminating species pairs were significantly different. These tests (Table 5.2) showed significant differences between the scores of these spectral configurations. A Bonferroni post hoc test on the ANOVA output showed that in with-flower measurements discriminations between species in all configurations were significantly different in both the SAM and the SID algorithms (i.e., full ≠ visible ≠ NIR ≠ SWIR). On the other hand, in without-flower measurements there was no significant difference

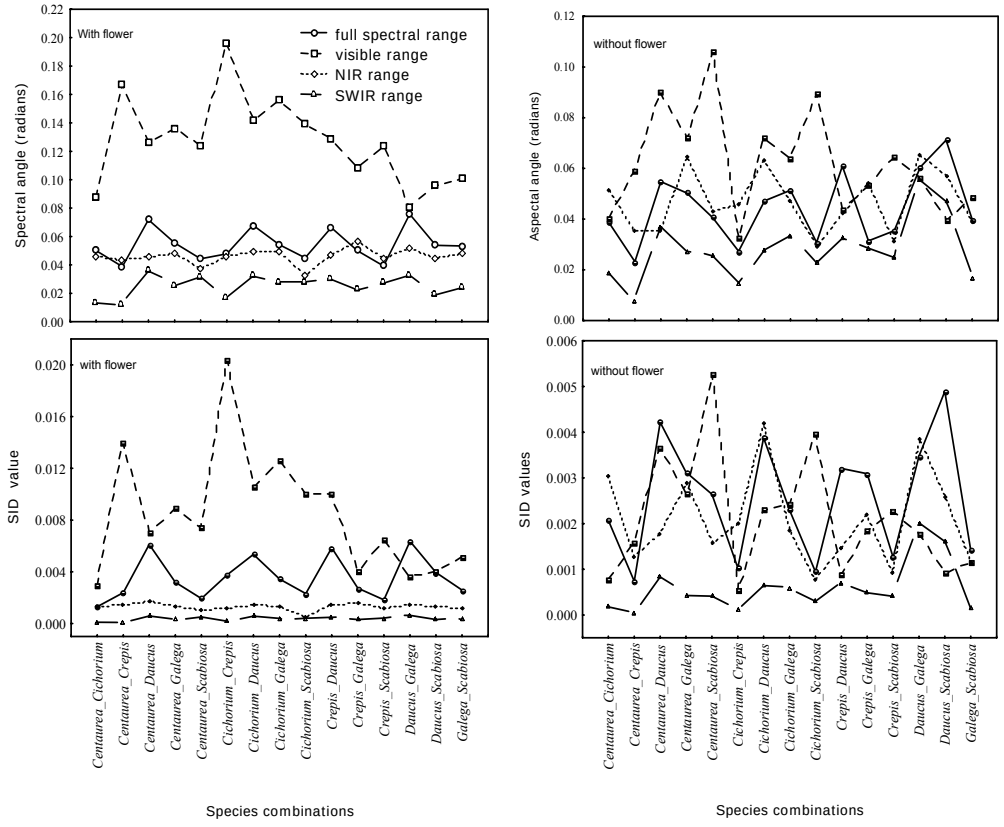

Figure 5.3 Discrimination scores produced by two spectral similarity measures (SAM and SID) while discriminating species pairs in two phenological conditions.

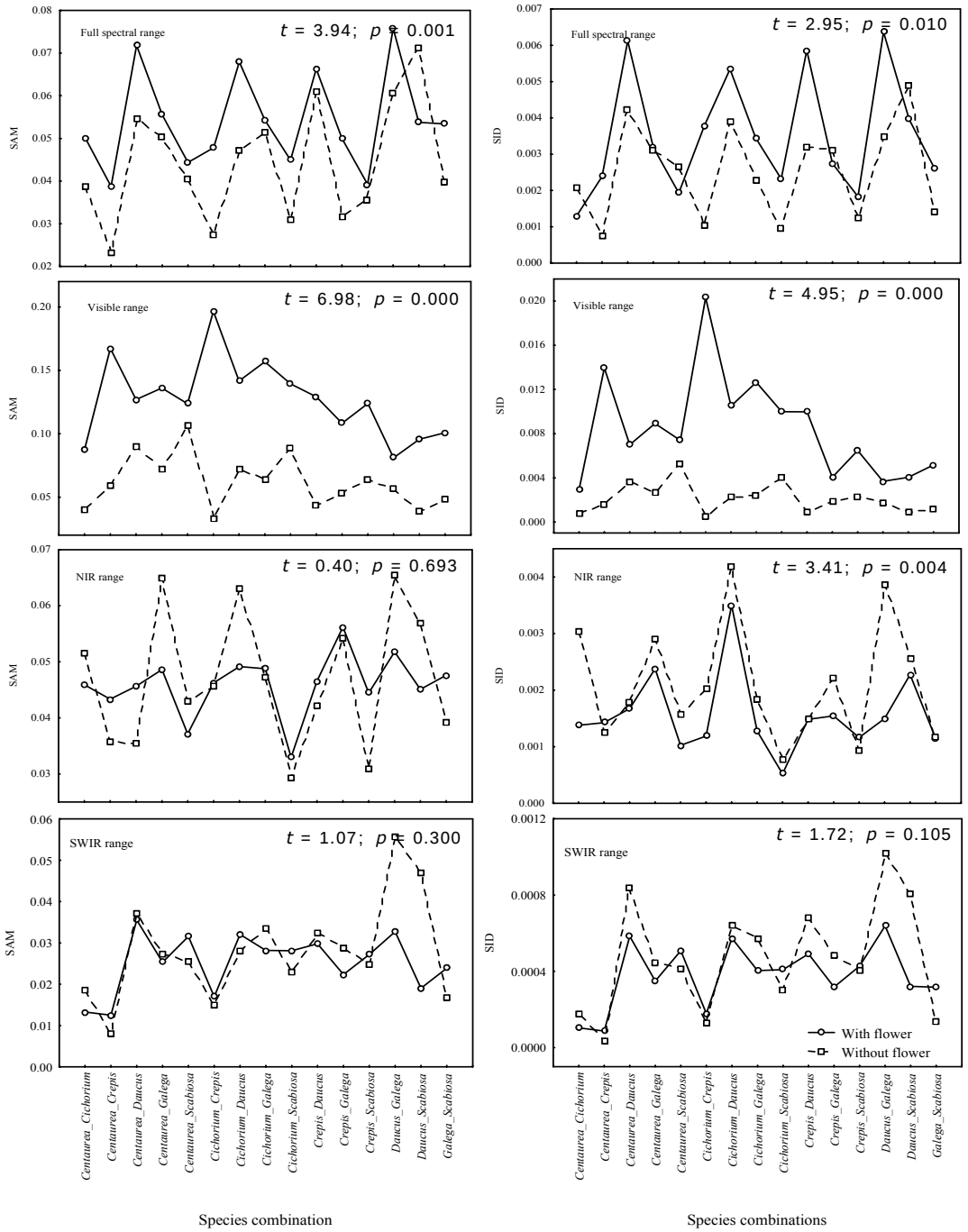

Figure 5.4 Comparisons of similarity measure values between with-flower and without-flower measurements in all four spectral configurations. *t*-test results showing the significance of their differences. Left column is for SAM and right column is for SID measurements.

between the full spectral configuration and the NIR (i.e., full = NIR ≠ visible ≠ SWIR) in the SAM algorithm and no significant difference between the full, visible and NIR (i.e., full = visible = NIR≠ SWIR) in the SID algorithm.

Table 5.2 ANOVA results showing the significance of difference between various spectral configuration groups while discriminating species.

Types of measurement	Source of Variation	*df*	*F*	*P-value*
SAM with-flower	Between groups	3	101.4537	0.00000
SAM without-flower	Between groups	3	12.54164	0.00000
SID with-flower	Between groups	3	26.6565	0.00000
SID without-flower	Between groups	3	7.847339	0.00018

The comparison of the similarity measure values or discrimination scores produced by the two different phenological scenarios was tested by conducting *t* tests for all four spectral configurations (Figure 5.4). In both algorithms, with-flower measurements obtained a significantly higher discrimination score in the full and visible spectral ranges. The differences were especially distinct in the visible part of the spectra. Whereas with the SID method a significant difference was found when using the NIR part as well, with the SAM method the two phenological conditions produced no significant difference in score when using the NIR and SWIR parts of the spectra.

5.3.3 Continuum removed band depth analysis

Band depth analysis in the blue (400 um to 550 nm) absorption area revealed that 11 species pairs demonstrated higher discrimination in with-flower measurements, compared with four in without-flower measurements (Figure 5.5). In the red absorption area, 13 pairs showed higher discrimination in with-flower measurements. However, band depth analysis in the blue area also revealed that two species pairs showed no significant discrimination between them (t > 3.234) in with-flower measurements, while three pairs showed no discrimination between them in the without-flower condition. The relevant numbers for the red area were three pairs and five pairs, respectively (Figure 5.5).

5.3.4 Classification accuracy

Compared with classification accuracy for the 2004 image (59%), overall classification accuracy for the 2005 image (71%) showed a significant increase. A z statistic (Table 5.3) between the two image dates proved that there was a significant difference in kappa coefficient ($\hat{K}$) values for the two classified images, as the null hypothesis was rejected using the normal curve deviate statistic (z) for α = 0.05 if z_t > 1.96 (i.e., $z_{\alpha=0.05}$ = 1.96).

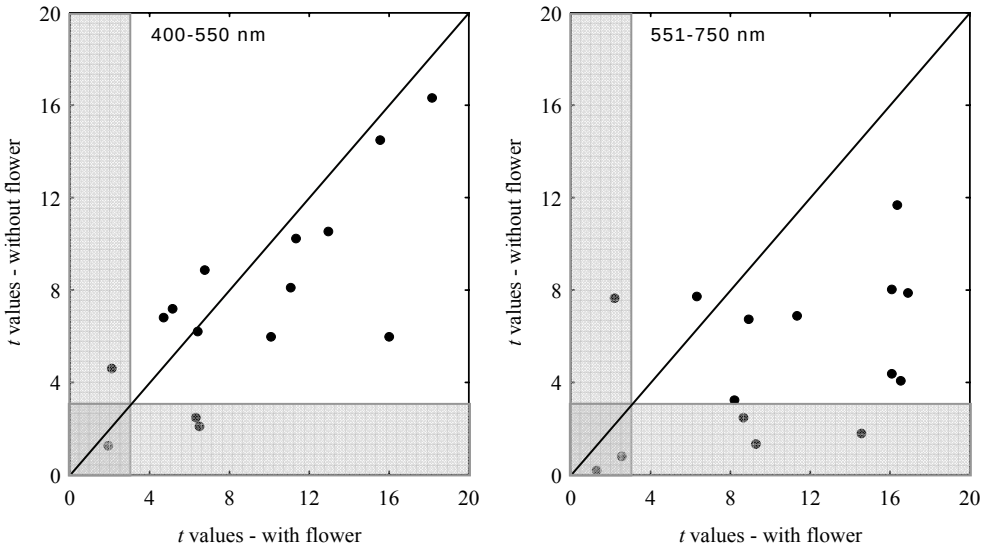

Figure 5.5 Scatter plot showing the comparative discriminability by band depth analysis. Shaded areas showing the critical level of *t* value (critical $t_{\alpha=0.003}$ = 3.234 at *df* = 14).

Table 5.3 Comparison of accuracy between 2004 and 2005 images.

	2004	2005
Overall accuracy (%)	59.2217	71.5938
Kappa coefficient ($\hat{K}$)	0.5343	0.6691
z statistic	5.4883	

Producer and user accuracies for the classified images (Table 5.4) revealed a substantial increase for our main target species, *Spartium junceum*, and other shrub covers. Other cover classes, however, remained largely unchanged.

Table 5.4 Producer and user accuracies of two classified images.

Class	2004		2005	
	Prod. Acc.	User Acc.	Prod. Acc.	User Acc.
Spartium	67.23	41.03	96.84	92.00
Oak	87.07	75.37	87.38	79.65
Mowed grassland	39.20	71.08	46.46	72.84
Road	65.85	95.29	49.32	78.26
Rocky area	86.76	71.52	89.62	79.17
Grass land	52.61	81.62	65.16	66.45
Shrub	51.70	68.42	70.59	78.29

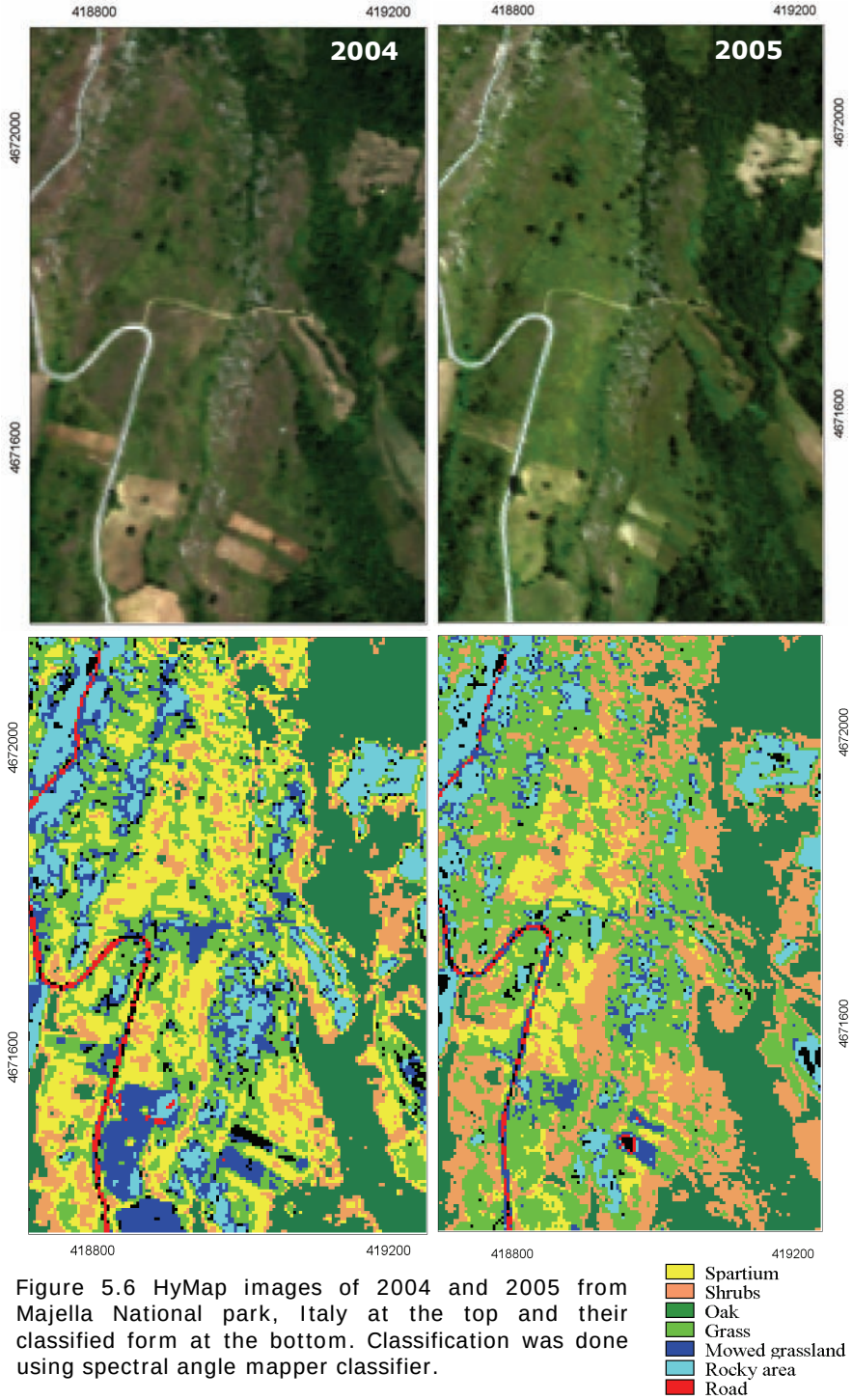

Figure 5.6 HyMap images of 2004 and 2005 from Majella National park, Italy at the top and their classified form at the bottom. Classification was done using spectral angle mapper classifier.

5.4 Discussion

Flowering is an important phenological event for all angiosperms. In this study, we used this phenological event to examine the possibility of enhancing species discrimination through spectral measurements. The results (Figure 5.4) showed that the impact of flowers on separability was significant in both the full spectral configuration and the visible range, thus confirming the findings of Everitt et al. (1992), who used the 630 um to 690 nm range to distinguish two flowering weed species from associate vegetation. However, the impact of flowering on species separability in the NIR and SWIR regions was not significant.

Figure 5.2a shows that, owing to the differences in flower colour, there was a high dissimilarity in reflectance in the visible spectral regions. This flower influence was visible even in the reflectance of plants with flowers (Figure 5.2b). Figure 5.3 supports this finding in a more structured way. Highest discrimination under blooming conditions was always found in the visual range. The increase in the magnitude of the dissimilarity scores of SAM and SID highlights the fact that the high discrimination in the visible range enhances the separability in the full spectral configuration. However, under non-blooming conditions, the NIR starts to play a more significant role in species separation. The ANOVA results (Table 5.2) failed to show any conclusive difference between the two phenological conditions, as both groups showed significant differences in different configurations. A post hoc Bonferroni test revealed that in the flowering stage the capabilities of all spectral configurations to discriminate species differed significantly. In the non-flowering measurements, however, the differences between configurations became less prominent, with the visible range losing its high discriminatory power. In other words, flowering exerted a big discriminatory influence on the studied species but this additional discriminatory power was concentrated almost entirely within the visible range of the spectrum. The two spectral similarity algorithms that we used in this study did not differ significantly in terms of the results produced.

Results of continuum-removed band depth analyses (Figure 5.5) revealed that most of the species pairs were more separable when flowering. The differences between the results derived from the blue and red absorption pits were not significant.

Classification accuracy showed a significant increase when flowers were in the canopy (2005), as compared with the non-flowering state (2004). Both overall accuracy and the kappa coefficient increased significantly (Table 5.3). Table 5.4, computed from the confusion matrix, gives more detailed insight into the changes. The increased accuracy of our target species, *Spartium junceum,* was very high. Both producer and user accuracies rose from 67% and 41%, respectively, to more than 90%. This also increased the accuracy of its associate shrub, *Prunus spinosa*. There are visual differences in the two classified images (see Figure 5.6),

with a big reduction in the area covered by *Spartium junceum.* This highlights the fact that the flowers of *Spartium junceum* change their spectral reflectance, reducing confusion with associated species. The results show that at different times of the year different species can have different discriminatory probabilities. Consequently, it is very important to know the phenological cycles of the species to be discriminated in order to schedule image acquisition to the best advantage.

5.5 Conclusion

Using hyperspectral remote sensing, the study evaluated the effect of phenological input in enhancing plant species discrimination. The conclusion is that phenological changes such as the emergence of flowers can be used to enhance species-level discrimination. However, the changes in the reflectance spectra attributable to flowering were largely confined to visible range. Band depth analyses also showed that the pigment absorption of all species in flower changed significantly, thus enhancing their separation. Study of the image classifications showed that it is important to know the exact time or phenological stage at which two different target species are most separable. This is essential for scheduling image acquisition to achieve better discrimination between target species.

In the three previous chapters we concentrated solely on the species discrimination primarily based on laboratory measurements. Whereas, in the next chapter (Chapter 6), sub-pixel unmixing technique were applied to discriminate species within the pixel.

The sub-pixel unmixing technique followed in this chapter used common shrub and tree species of the area as endmembers and provides the spatial distribution of studied species as well as the composition of these species per pixel.

Chapter 6

Mapping shrub and tree species richness from hyperspectral imagery using a matched filtering unmixing technique

This chapter based on
Md. Istiak Sobhan, Moses A. Cho, Andrew K. Skidmore
Fabio Corsi and Herbert H.T. Prins

Abstract

Re-colonization of natural vegetation in abandoned farmlands and pasture is the most important vegetation process taking place in the European Mediterranean region. Many studies have sort to capture the changing vegetation composition in these systems through field-based studies in order to enhance the sustainable management of biological diversity. But these studies are labour intensive and expensive, and cannot be extended over large areas. However, Hyperspectral imagery with high spatial and spectral qualities offers new possibilities to provide important information about vegetation composition that are indicative of successional stages. This study investigates the utility of spectral unmixing technique using airborne hyperspectral imagery for identifying shrub and tree species composition at pixel level. Airborne hyperspectral (HyMap) imagery and ground data were collected in the summer of 2005 from the Majella national park, Italy. Fourteen common shrub and tree species were utilized as endmembers to explore their composition and distribution in the study area. Ground locations were recorded with pure canopy cover of these species and their top-of-canopy reflectance were obtained from the HyMap images and used as endmember (image endmembers) in the unmixing process. Matched filtering, a partial spectral unmixing algorithm was used to determine the spectral abundance (degree of match) per pixel of these endmembers by creating a fraction image for each of them. These fraction images were aggregated together into a single map which illustrated the number and composition of shrubs and trees per pixel. Overall performance of this technique to predict number of species per pixel was good (r^2=0.83). The root mean square error (RMSE) between the observed and predicted number of species was slightly less than one species per pixel (i.e. RMSE = 0.73). However, species by species comparison between actual and predicted composition revealed an accuracy of 69%. We conclude that, unmixing technique with hyperspectral imagery can be useful for mapping species distribution at the sub-pixel level and may successfully replace the high labour intensive field investigation over large areas.

Keywords: Unmixing; Matched filtering; species richness; land abandonment; secondary succession.

6.1 Introduction

Throughout the history of human settlement in the European Mediterranean region, short-term land abandonment has occurred repeatedly which helps to characterize the landscape (Naveh and Lieberman, 1994; Fernández, Mora and Novo, 2004), but due to the changes in the socio-economic setting, a dramatic rural exodus and subsequent abandonment of agricultural and pastoral land have taken place in the second half of the last century (Naveh 1991; Lepart and Debussche, 1992; Bonet 2004). As a consequence, natural forest formation has taken place on former croplands and pastures, causing large scale transformation of the regional landscape (Tatoni, and Roche, 1994; Prévosto, and Curt, 2004). This re-colonization by natural vegetation in abandoned farmland is the most important vegetation process taking place in southern European Mediterranean region attracting huge scientific attention (Lepš, Osbornová-Kosinová and Rejmánek, 1982; Debussche and Lepart, 1992; Tatoni et al., 1994; Debussche et al., 1996; Ne'eman and Izhaki, 1996; Prins and Gordon, 2007).

This repeated cycle of land abandonment and re-colonization due to secondary plant succession creates the characteristic heterogeneity of the Mediterranean landscape (Barbero, Bonin and Quezel, 1990), which supports high species diversity (Ales et al., 1992). In most of the Mediterranean regions which receive higher precipitation, this process of succession from abandoned agricultural land to natural vegetation leads to the establishment of either oak or beech forest depending on the environmental backdrop with intermediate scrubby shrub formation (Saïd, 2001; Prévosto and Curt, 2004). However, interspecific interactions and environmental conditions (e.g., rainfall and soil water availability) determine the pathways or trajectory of this secondary succession (Bonet, 2004). Moreover, van der Putten et al., (2000) show that species diversity or richness in the initial or intermediate stages can play an important role in the succession process. However, Armesto and Pickett, (1985) argue that the species richness changes along the succession process itself. In other word, succession can also be viewed as a gradient in time where species turnover is partially a function of changing resources availability (Pickett, 1976; Tilman, 985). Meanwhile, Grime, (1979) and Carson and Barrett, (1988) projected that the increasing resources availability could also alter the trajectory of the succession. Therefore, there is quite some scientific debate on whether chronosequences can really be taken as equivalent to spatial sequences. Yet in this paper we will not delve into that.

Sustainable management of any ecosystem require a comprehensive understanding of species composition and distribution. Moreover, in areas with active succession processes, it is also important to identify the local trajectory of the succession and present state of vegetation within that trajectory. Monitoring the changes of species richness and particularly

examining the composition of certain species can make it possible to recognize the trajectory of succession of a specific area. A quantitative spatial and temporal approach is essential (van der Maarel, 1993) to monitor and understand this dynamic process and its possible consequences on local flora and fauna, such as, loss of open habitat grassland species (Verdú, Crespo, and Galante, 2000; Reidsma et al., 2006).

Remote sensing is instrumental in the characterisation of landscape heterogeneity (Turner, 1989; Quattrochi and Pelletier, 1991; Seixas, 2000; Kerr and Ostrovsky, 2003). Conventionally, landscape heterogeneity is characterised through image classification of broad vegetation types. Traditional methods of classification techniques such as maximum likelihood classifier determines vegetation classes at the pixel level (i.e., each pixel is assigned to a vegetation class). However, this kind of per pixel classification is problematic in a landscape where the individual vegetation communities are smaller than the pixel resolution of the sensor. In changing landscapes such as those in the Mediterranean, species composition vary at relatively short distances (Salvador, 2000). In such cases each pixel could consist of several vegetation communities (e.g., grass, shrubs and trees) or species (e.g., different species of trees and/or shrubs), which makes monitoring of species richness and or composition very challenging. The advent of sensors with both high spectral and spatial resolution has raised new expectations about the possibilities of spectrally discriminating species (Cochrane, 2000; Schmidt and Skidmore, 2003; Clark, Roberts and Clark, 2005) and thus improving the characterization of vegetation communities or species composition in highly heterogeneous landscapes.

Airborne hyperspectral imagery with continuous narrow bands of spectral reflectance from the visible (400 nm) through the short-wave infrared (2500 nm) range of the electromagnetic spectrum with high spatial resolution can provide much better accuracy in mapping vegetation communities or even individual species. But yet, conventional classifiers can only provide pixel level classification. To deal with this problem spectral unmixing was introduced. The technique is based on the assumption that the spectral reflectance of a given pixel is a linear combination of individual reflectance spectra (endmembers) of the reflective component materials on the ground (Adams, Smith and Johnson, 1985; Smith et al., 1990; Roberts, Smith and Adams, 1993). So each pixel retains the characteristic features of the individual component spectra. Spectral unmixing utilizes the high dimensionality of the hyperspectral imagery to produce a fraction image for each endmember, which shows the relative abundance of the endmember in a subpixel estimation (Adams et al., 1995). Different types of unmixing algorithms are available and used for mapping individual plant species or associations with mixed success (Roberts et al., 1998; McGwire, Minor and Fenstermaker, 2000; Parker Williams and Hunt, 2002; Robichaud et

al., 2007). But compared to other vegetation attributes, plant species composition is still the most difficult attribute to detect with remote sensing techniques (Lewis, 1998).

The objective of this study was to investigate the utility of the spectral unmixing technique using airborne hyperspectral imagery for identifying shrub and tree species composition at the pixel level in a semi-natural Mediterranean landscape, which in turn would provide spatial information on the ongoing succession process. In order to achieve the objective, we applied the matched filtering (MF) unmixing technique on a HyMap hyperspectral image from Majella National Park, Italy.

6.2 Materials and method

6.2.1 The study area

The study site is located in Majella National Park, Italy (42º14' - 42º50'N and 13º50' - 14º14'E), which covers an area of 74000 ha. The park extends into the southern part of Abruzzo, at a distance of 40 km from the Adriatic Sea. This region is situated in the massifs of the Apennines mountain range. The park is characterised by several mountain peaks, the highest being Mount Amaro (2794 m). More specifically, the study area (42º03'56 - 42º09'23N and 13º59'03 - 14º02'22E) is situated between Mounts Majella and Mount Morrone to the east and west, respectively. It covers an area of approximately 10 km x 4.5 km as shown in Figure 6.1. Average yearly precipitation is approximately 800 mm.

6.2.2 Field data collection

Field work was carried out from 16 to 29 June 2005. Field information was collected using two different methods, namely, (a) collection of endmember locations and (b) sampling for species composition.

We conducted several transect surveys in the east-west direction, from about 1800m elevation (pure beech, *Fagus sylvatica* stands) to about 400m elevation (pure oak, *Quercus pubescens* stands). Along these transects, GPS readings were collected for endmembers, where homogeneous canopy cover of more than 5 m by 5 m was found to keep the pixel reflectance as impervious as possible and minimize the influence of other species. Twenty different endmembers were collected for the study (Table 6.1). Out of which, fourteen were common shrub and tree species of the area and the rest were supporting endmembers to facilitate unmixing procedure and enhance the accuracy by minimizing fraction errors. We have limited our study to common shrubs and trees species of the study area, because of the difficulties associated with obtaining pure image endmember spectra from 4 m pixels.

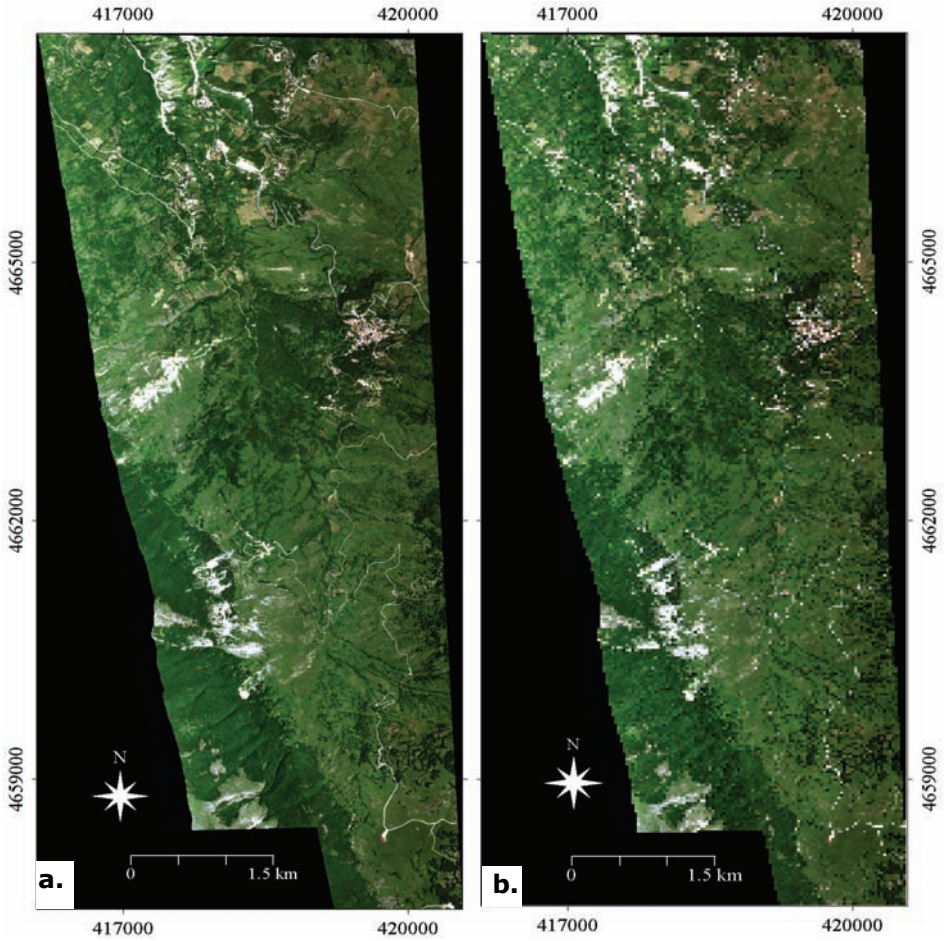

Figure 6.1 True colour composite of HyMap hyperspectral image for the study area, (a) with original 4 m pixel and (b) with re-sampled 30 m pixel.

Sampling for species composition was performed using a "random sampling technique" A GPS was used to locate the sample plots in the field. A 30 m x 30 m plot size was adopted in this study. Shrubs and tress were deemed visible and enlisted only if they coved greater than 5% of the sample plots. All field sample plots were aligned with the direction of the flight line. Nomenclature of the plant species follows Flora D'Abruzzo (Conti, 1998).

6.2.3 Image acquisition and pre-processing

6.2.3.1 Geometric and atmospheric correction

Airborne HyMap data of the study site were obtained on 4 July 2005. The flight was carried out by German Aerospace Research Centre and Space

Agency (DLR). The HyMap sensor comprised 126 wavebands, operating over the wavelength range 436–2485 nm, with average spectral resolutions of 15 nm (436–1313 nm), 13 nm (1409–1800 nm) and 17 nm (1953–2485 nm). The spatial resolution of the data was 4 m. The images were collected at solar noon. The specific study site was covered by two image strips, each covering an area of about 40 km x 2.5 km. The solar zenith and azimuth angles for the image strips ranged between 30–33.78 and 111.5–121.8 respectively. The image strips were geometrically and atmospherically corrected by DLR. The on-board navigation system used for geometric correction was a C-MIGITS II system, which has a dx-dy accuracy of 2.5m and dz accuracy of 3m. The atmospheric correction was carried out using ATCOR4-r (rugged terrain). ATCOR4 is based on MODTRAN-4 radiative transfer code. However, there were differences between the reflectance of similar pixels in the overlapping sections between image strips. Spectral calibration between strips was carried out using the empirical line method in Environment for Visualising Images (ENVI 4.2) software (Research System, Inc.) in order to minimize the differences. Ten image spectra collected from a reference strip (strip 2) and corresponding targets from its overlapping neighbour (strips 1) were used to compute a linear regression function for each channel. Using the regression functions, strip 1 was then adjusted to have a spectral response similar to that of strip 2. The spectra were collected from homogenous targets such as roads, agricultural fields, limestone quarry, and dense beech forest pixels.

6.2.4 Collection of endmember spectra from image

GPS readings of the endmembers were over-laid on the true colour composite HyMap image. A point region of interest (ROI) tool in ENVI 4.3 software (ITT Inc.) was used to collect image endmember spectra from the image (Gillespie et al., 1990; Adams, Smith, and Gillespie, 1993; Adams et al., 1995). The true colour composite image of the area was used to ensure that pixels outside the each species canopy were not collected, as (Ferrier, 1999) described that spectral unmixing is highly dependent on the quality of input endmembers. The number of pixels used for each endmember is shown in Table 6.1.

Table 6.1 Different endmembers used in this study.

Tree/Shrub endmembers	Number of endmember pixels	Supporting endmembers	Number of endmember pixels
Fagus sylvatica	94	Mowed grassland	135
Quercus pubescens	52	Tarmac road	116
Juglanns regia	10	Rocks	112
Robinia pseudoacacia	21	Tree shades	92
Acer campestre	30	Sparse grassland	93
Fraxinus excelsior	17	Thick grassland	110
Pinus nigra	35		
Tilia cordata	11		
Salix alba	19		
Rosa canina	17		
Spartium junceum	24		
Juniperus communis	11		
Crataegus monogyna	10		
Corylus avellana	17		

6.2.5 Per pixel assessment of shrubs and tree species

6.2.5.1 Resampling

Before performing the unmixing analysis of the original HyMap image with 4m pixels was resampled to 30m pixels to match with our field observations plot size with no spatial reference of species occurrence with the plot. This was necessary to ensure that the number of shrubs and trees found in the field plots were comparable with the predicted output from the unmixing process, though the endmember spectra were collected from 4m pixels.

6.2.5.2 Spectral unmixing process

Spectral unmixing is a way of determining the relative abundances of materials depicted in multi- or hyper-spectral imagery based on the materials spectral characteristics (Ferrier, 1999). The reflectance of each single pixel of an image is assumed to be a combination of the surface reflectance of each material (or endmember) present within the pixel (Adams, Smith, and Johnson, 1985; Adams, Smith, and Gillespie, 1993; Roberts, Smith, and Adams, 1993). Out of several available unmixing techniques, we used Match filtering method. Matched filtering finds the abundances of user-defined endmembers using a partial unmixing. The strength of the matched filtering process is that all of the endmembers in

the image need not to be known. This technique maximizes the response of the known endmember and suppresses the response of the composite unknown background, thus "matching" the known signature. It provides a rapid means of detecting specific materials based on matches to library or image endmember spectra. We ran the matched filtering algorithms using our selected image endmembers spectra. The un-mixing process uses the mean spectrum per species.

The partial unmixing technique applied in this study is based on a linear operator that minimizes the total energy in a hyperspectral image sequence while the response of the operator to the signature of endmembers is constrained to a desired constant level (Resmini et al., 1997; Jacobsen, Heidebrecht, and Nielsen, 1998).

Consider a finite set of observation spectral vectors (***r***1 … ***ri*** …. ***rq***) each of which are drawn from an area of interest in a hyperspectral image sequence. In this notation, the spatial position (*x*, *y*) of each of the pixel vectors is described by the subscript. Each of the *q* observations is an *l* by 1 vector ***ri***=(***ri***1…..***rik***….. ***ril***) *T* that has properties described by the linear mixture model (Eq. 1)

$$\mathbf{r}(x,y) = \mathbf{M}\,\alpha(x,y) + \mathbf{n}(x,y) \qquad \text{Eq. 1}$$

where **r**(x,y) is an *l* by 1 vector of observations at location (x,y) (*l* is the number of spectral bands), **M** is an *l* by *p* matrix with columns containing the endmember spectra for the *p* endmembers (**M** is constant for all (x,y)), α(x,y) is a *p* by 1 vector of abundance for the endmembers at location (x,y), and **n**(x,y) is an *l* by 1 vector of noise. In the model the noise is random with dispersion (or covariance) matrix σ2 **I** (**I** is the *l* by *l* unit matrix).

The results of the matched filtering appear as a series of gray-scale images (fraction images), one for each selected endmember (Boardman, Kruse, and Green, 1995). These floating point images provide a means of estimating relative degree of match to the reference endmember spectrum and approximate sub-pixel abundance. Moreover, these images also illustrate the spatial distribution of the corresponding endmember (Adams et al., 1995). In case of vegetation endmembers, the fraction or relative degree of match is proportional to the real abundance of canopy cover (Parker Williams, and Hunt, 2002). As match filtering minimize the response of composite unknown background, so the data histogram of background materials proximate around 0.0, whereas the target (endmember) data distribution occurs in the upper tail of the histogram, where 1.0 is a perfect match.

Although partial unmixing process does not necessarily require all possible endmembers within the image frame, too few endmembers can subset the unmodeled endmembers into the resulting fraction images,

creating the fraction error (Sabol, Adams, and Smith, 1992). To minimize these fraction errors, we added six supporting endmembers with the list of fourteen pure shrub and tree endmembers (Table 6.1) while running the unmixing procedure. Selection of these supporting endmembers was driven primarily because of their high cover percentage in the image.

6.2.5.2 Preparation of species composition map

The species composition map was produced by aggregating fraction images resulting from the unmixing process. During this aggregation process, we left out fraction images produced from the supporting endmembers, as their existence to minimize fraction error was already achieved and they were no longer necessary for further analysis. Harsanyi and Chang (1994) had demonstrated that an endmember appeared to be present in a pixel if it scores more than 0.1 in the relative degree of match. But we increased that threshold value to 0.2 to decrease the possibility of "false positive" response from some rare endmembers as reported by Boardman (1998). So in a specific pixel endmembers which scored above 0.2 were deemed to be present and those scored below 0.2 were considered absent. In other words, we counted the number of endmembers scored above 0.2 to get the species number in a pixel. As an example showed in Figure 6.2, seven endmembers scored above the threshold values of 0.2 and were considered to be present in that pixel. So the aggregated image illustrated the number and composition of shrubs and trees per pixel.

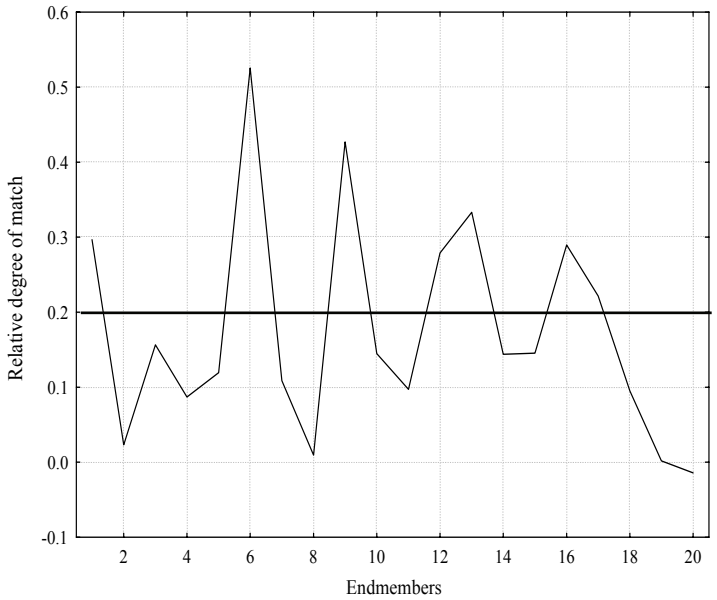

Figure 6.2 Spectral profile showing relative abundance of different endmembers per pixel. The line indicates the threshold (0.2) above which an endmember was considered present in the pixel.

6.2.6 Validation

Ground observations from 30 sample plots were used to evaluate the results. Correlations between these field plot data and corresponding pixel values for species number and compositions were assessed by calculating root mean square error (RMSE) between the observed and predicted number of species. We also used χ^2 "goodness of fit" to evaluate the null hypothesis Ho (that the prediction were consistent with observed) against the alternative H_A (that they were not are not consistent) and null hypothesis was rejected if $\chi^2 \geq \chi^2_\alpha$. The desired level of significance (ά) was fixed at 0.05. χ^2 was calculated by using Eq. 2.

$$\chi^2 = \sum_{i=1}^{k} \frac{(f_i - e_i)^2}{e_i} \qquad \text{Eq. 2}$$

where,

$f_i =$ observed species number for sample plot *i*

$e_i =$ expected species number for sample plot *i*

$k =$ number of sample plots

Moreover, we also compared species composition between field data and predicted output for each sample plot to investigate the under and over prediction for each individual species.

6.3 Results

6.3.1 Endmembers

Three non-vegetated endmembers (viz., Rock, road and mowed-grassland) were clearly distinct from the others (Figure 6.3). However, both road and mowed-grassland spectra had visible influence from characteristic vegetation spectra. Roads were too narrow to have a complete pure spectrum for 4m pixel while mowed-land had a vegetation signal. Tree shed spectrum produced the lowest reflectance as these dark pixel had very low illumination level. Rest of the spectra from tree and shrub species were difficult to differentiate visually in figure 6.3.

6.3.2 Spatial distribution of individual species and mapping species richness per pixel

The individual gray scale fraction images for each endmember species provided a good understanding of their spatial distribution pattern for that species. In Figure 6.4 two fraction images for *F. sylvatica* and *Q. pubescens* are presented as examples. The gray scale corresponds to the degree of match between sub-pixel abundance and reference

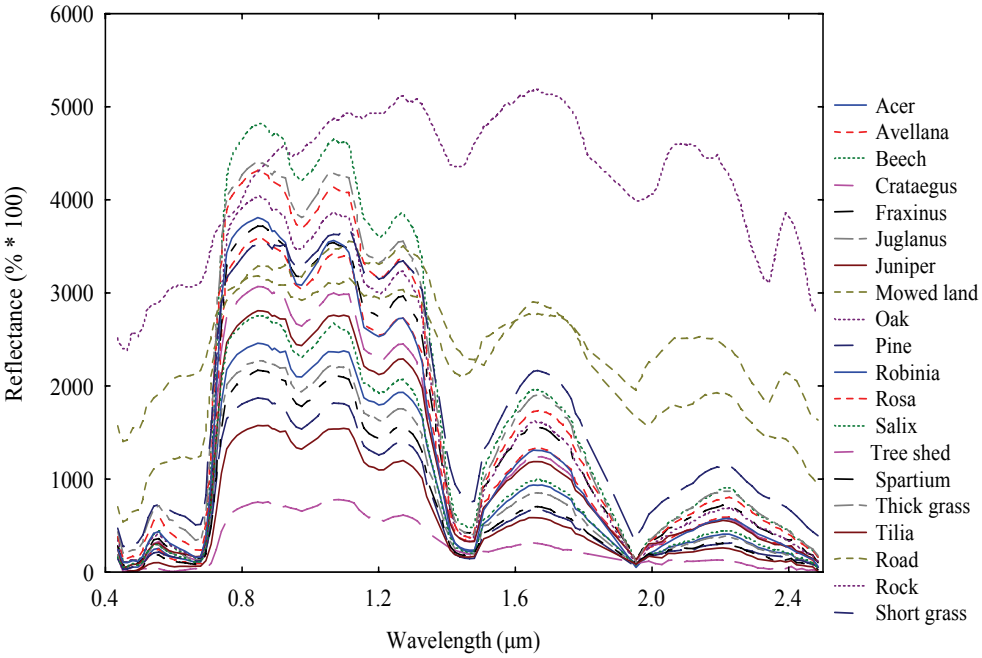

Figure 6.3 Average spectral reflectance of twenty endmembers used in this study

endmember. Black areas have zero or low values, so no match to the reference endmember, while brighter areas have higher MF score and higher match to the input endmember. Using a threshold value of 0.2, a present-absent binary image can be developed for all endmember species as shown in Figure 6.5.

The aggregated species richness map as shown in Figure 6.6 illustrates the number of shrub and tree species found per pixel. White areas are either out of the study image or grasslands having no or very low shrub/tree covers. Meanwhile, the red and orange pixels are with high shrub and tree species numbers. A large part of blue areas are comprised of Beech and Oak woodlands, which form monotypic stand in the study area.

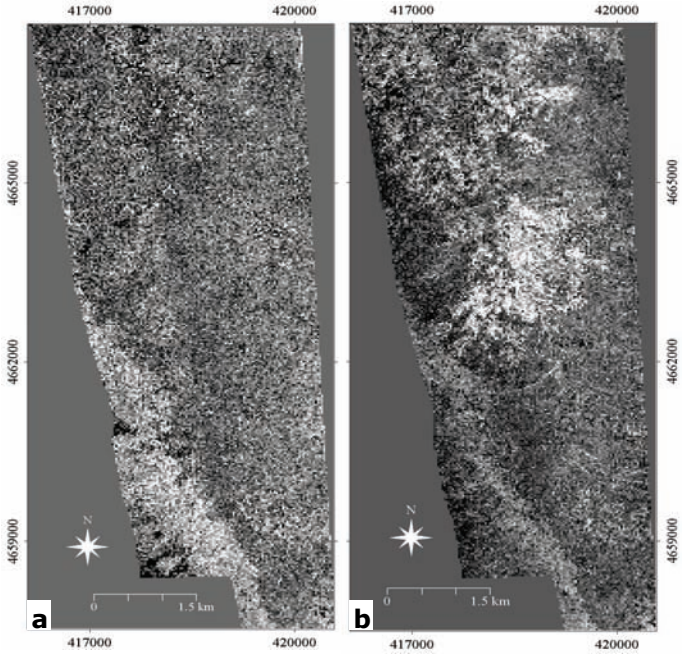

Figure 6.4 Examples of fraction images, (a) beech (*F. sylvatica*) and (b) oak (*Q. pubescens*)

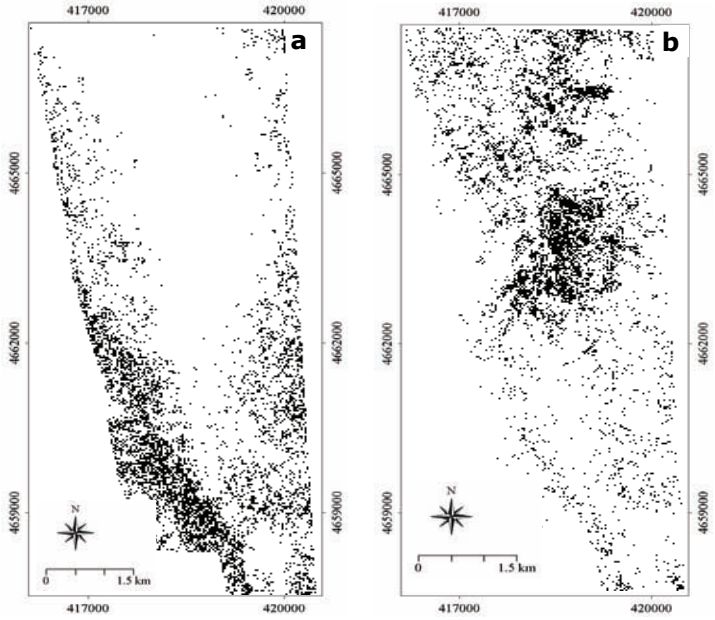

Figure 6.5 Present-absent binary images produced by slicing the fraction images shown in Figure 6.2 (a) beech (*F. sylvatica*) and (b) oak (*Q. pubescens*)

6.3.2 Comparison of unmixing results with field measurements

Overall performance of this technique to predict the number of species per pixel was satisfactory, because a scatterplot of species number (Figure 6.7) between prediction and ground data revealed high correlation (r^2=0.83, p= 0.000). Root mean square error between observed and predicted number of species was slightly less than one species (RMSE = 0.73) per pixel. χ^2 "goodness of fit" also showed that the prediction was consistent with observed data, as the null hypothesis was failed to be rejected (χ^2 = 0.554; df = 29, while critical $\chi^2_{\alpha = 0.005}$ = 42.56)

A plot by plot investigation (Table 6.2) showed that in 17 out of 30 plots the numbers of species were predicted correctly. All the five sample plots which did not possess any shrub or tree species were predicted correctly as having zero species. In ten plots species number were under-predicted, while in three plots there were over-prediction. Except in one plot (sample plot 10) prediction errors were always confined to one species.

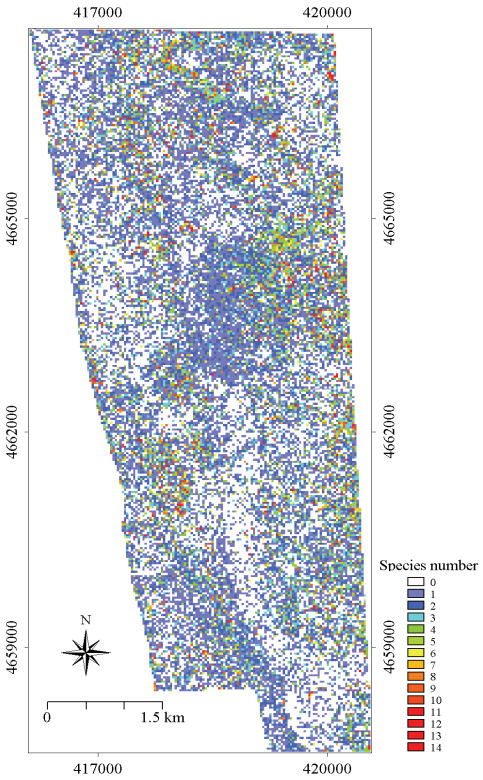

Figure 6.6 Composite species richness map, showing the number of species present per pixel.

Table 6.2 Plot by plot comparison of species number and composition between field data and prediction

Field samples	Sp. No. Field	Species found in field	Sp. No. Predicted	Species found from unmixing
1	3	*A. campestre, Q. pubescens, R. canina*	3	*A. campestre, Q. pubescens, R. canina*
2	2	*S. alba, Q. pubescens, R. canina*	2	*S. alba, R. canina*
3	0		0	
4	1	*R. canina*	1	*R. canina*
5	0		0	
6	5	*Q. pubescens, F. excelsior, A. campestre, T. cordata, R. canina*	4	*Q. pubescens, A. campestre, F. excelsior, R. canina*
7	5	*Q. pubescens, S. alba, F. excelsior, A. campestre, R. canina*	5	*A. campestre, Q. pubescens, S. alba, F. sylvatica, R. canina*
8	6	*A. campestre, J. regia, Q. pubescens, R. pseudoacacia, R. canina, C. monogyna*	7	*A. campestre, Q. pubescens, J. regia, R. pseudoacacia, S. alba, R. canina, C. monogyna*
9	5	*Q. pubescens, F. sylvatica, F. excelsior, R. canina*	5	*Q. pubescens, F. sylvatica, R. pseudoacacia, F. excelsior, R. canina*
10	1	*R. canina*	3	*R. canina, R. pseudoacacia, P. nigra*
11	0		0	
12	3	*A. campestre, R. canina, C. monogyna*	3	*A. campestre, R. canina, C. monogyna*
13	2	*A. campestre, C. avellana*	1	*A. campestre*
14	0		0	
15	1	*R. canina*	1	*R. canina*
16	0		0	
17	3	*Q. pubescens, F. excelsior, P. nigra*	3	*Q. pubescens, P. nigra, R. pseudoacacia*
18	1	*Q. pubescens*	1	*Q. pubescens*
19	3	*Q. pubescens, A. campestre, F. excelsior*	2	*Q. pubescens, A. campestre*
20	3	*Q. pubescens, F. excelsior, C. avellana*	2	*Q. pubescens, C. avellana*
21	4	*Q. pubescens, S. alba, F. excelsior, R. canina*	4	*Q. pubescens, S. alba, F. excelsior, R. canina*
22	2	*Q. pubescens, A. campestre, R. canina*	1	*Q. pubescens*
23	2	*Q. pubescens, R. canina*	1	*Q. pubescens*
24	3	*Q. pubescens, A. campestre, R. canina*	2	*Q. pubescens, A. campestre*
25	2	*Q. pubescens, C. avellana*	1	*Q. pubescens*
26	1	*F. sylvatica*	1	*F. sylvatica*
27	2	*F. sylvatica*	1	*F. sylvatica*
28	2	*F. sylvatica, J. communis*	1	*F. sylvatica*
29	1	*F. sylvatica*	1	*F. sylvatica*
30	2	*F. sylvatica, J. communis*	3	*F. sylvatica, Q. pubescens, J. communis*

Species by species comparison between field data and prediction (Table 6.3) revealed that 80% (52 out of 65) of the species were correctly spotted in the plots, i.e., observed in the field as well as predicted from the image. 20% (13 out of 65) of the species were under-predicted, i.e., observed in the field but not predicted from the image and 11% (7 out of 65) of the species were over-predicted, i.e., not observed in the field but predicted from the image. Hence, the total error was 20 species (combining both over and under prediction) out of 65 or 31% of the total. Predictability of different species varies, but it was inconclusive. Only two species (*R. canina* and *F. excelsior*) showed relatively high under-prediction, in contrast *R. pseudoacacia* show over-prediction.

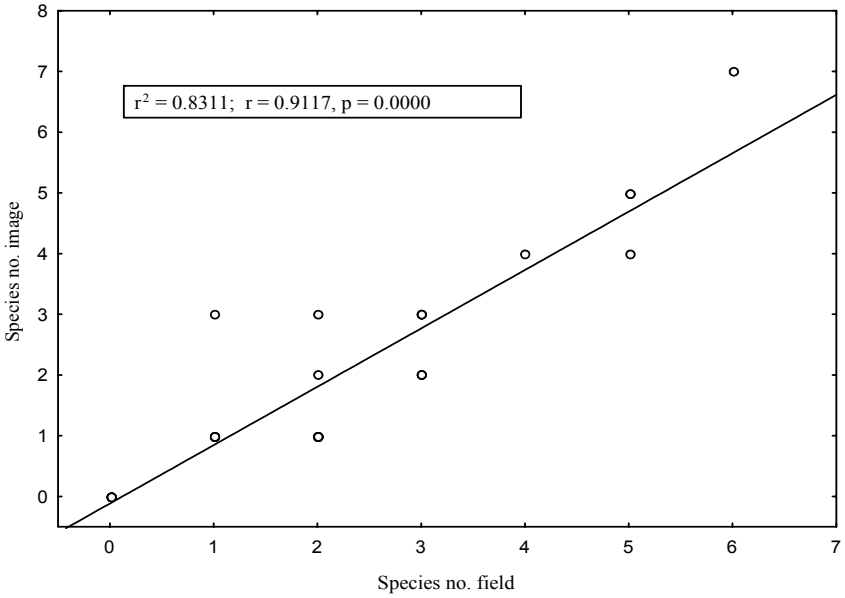

Figure 6.7 Scatter plot of species number from MF unmixing procedure versus field data. Best fit linear regression line is also shown.

6.4 Discussion and conclusion

Use of unmixing technique in not new in imaging spectroscopy (Adams, Smith and Johnson, 1985; Boardman, Kruse and Green, 1995), but its use in plant species mapping is still weakly developed, especially with complex vegetation pattern such as that found in the Mediterranean. The results of this study highlights the usefulness of techniques based on unmixing image processing of sub-pixels in the context of the spatial distribution of a particular plant species as well as the mapping of multi-species associations. Use of multi-species endmembers proved very encouraging as both intermediate fraction images (Figure 6.4) and final result (Figure 6.6) should have immense importance to the scientists as

well as managers. Spatial distribution map of each single endmember species (Figure 6.5), which is a derivative of fraction images can be used in the studies of population ecology of that species. Moreover, the final outcome of this process can be translated into a species richness map or a phyto-association map depending on the requirement.

Table 6.3 Species by species comparison between field observation and prediction.

Species	Field observation	Prediction from unmixing	Correct in both field & prediction	Under prediction	Over prediction
F. sylvatica	6	7	6	0	1
Q. pubescens	15	15	14	1	1
R. canina	14	11	11	3	0
A. campestre	9	8	8	1	0
F. excelsior	7	3	3	4	0
P. nigra	1	2	1	0	1
S. alba	3	4	3	0	1
J. regia	1	1	1	0	0
T. cordata	1	0	0	1	0
C. avellana	3	1	1	2	0
J. communis	2	1	1	1	0
R. pseudoacacia	1	4	1	0	3
C. monogyna	2	2	2	0	0
Total	65	59	52	13	7

Although Mundt et al., (2005) pointed out the importance of using multiple species endmembers in ecological studies, there have not been many endeavours on this regards, except for Aspinall, (2002) who discriminated three *Populus* sp. Most of the other studies have concentrated on discriminating single species, e.g. Mundt et al., (2005) mapped *Cardaria draba* and Parker Williams, and Hunt (2002) *Euphorbia esula* from other vegetation. Due to obvious limitations of spectral and spatial resolution, almost all multispectral unmixing endeavours have been limited to determining subpixel mixing of different community types (Caetano et al., 1997), habitat types (Novo and Shimabukuro, 1997) or landforms (Lewis, 2001; Ballantine et al., 2005). This study reveals the potential utility of using multiple endmembers unmixing to discriminate species at the sub-pixel level. As the technique is relatively less field intensive, using it to monitor changes of a complex and dynamic vegetation such as the Mediterranean ecosystem is promising. The process succeeds here because of the good quality of endmembers spectral data and the use of hyperspectral image. We limited our endmembers only to few common species which have larger canopy

cover. In addition, hyperspectral image provide spectral resolution which enable us to distinguish subtle variations between different plant spectra.

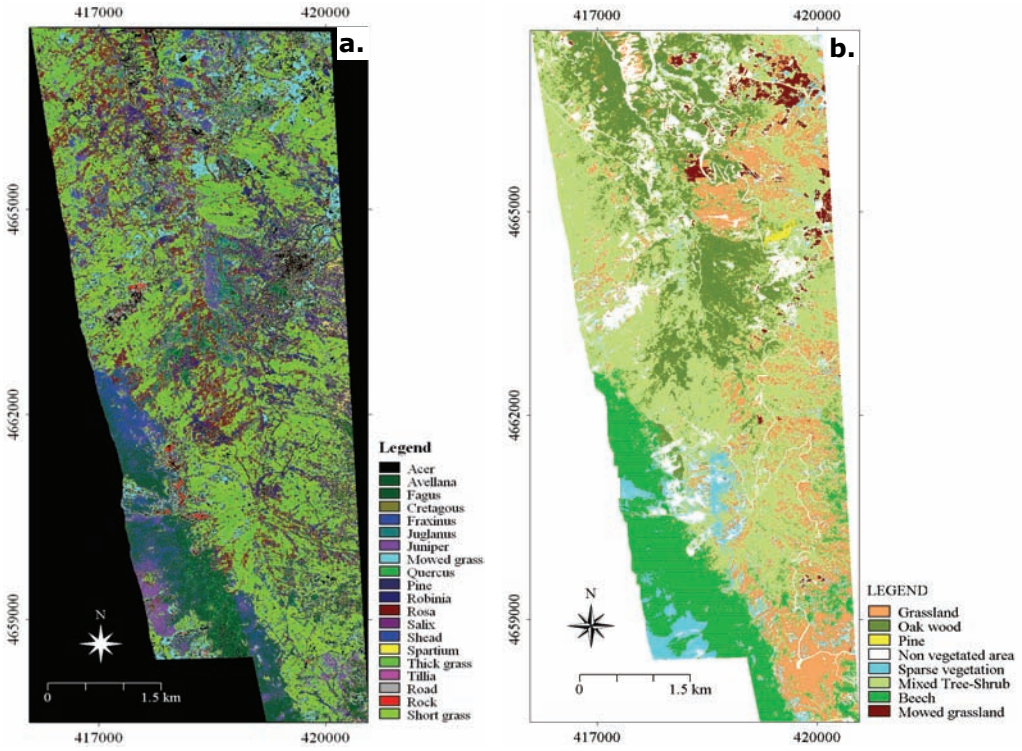

Figure 6.8 Figure shows the classification of the same study image done through spectral angle mapper (SAM), (a) using same endmembers used in sub-pixel classification and (b) using more generalized cover class endmembers.

Per-pixel classification can only bring out the species with highest cover percentage within that pixel, but for ecological studies this is not always enough. Particular species, especially shrubs which in most cases do not produce the largest cover class in a pixel, may give vital clues about the vegetation status. As shown in Figure 6.8 (a), the image we used can be classified with moderate accuracy (overall accuracy 58% ($\hat{K}$) 0.49) using the same endmembers we used in unmixing process. But comparing with the Figure 6.8 (b), which used more generalized land cover classes (overall accuracy 91%; ($\hat{K}$) 0.907), it was too well evident that increasing the number of endmembers increased the number of "unclassified" pixels. Murwira and Skidmore (2006) showed that landscape level spatial heterogeneity can be monitored by using intensity and dominant scale of NDVI data. However, understanding the heterogeneity or species richness within the pixel remains the main shortcoming of pixel based approaches compared to sub-pixel unmixing techniques.

In our study, problems with high "false positive" response for rare endmembers was not as overwhelming as reported by some other studies (Blackburn, 1998; Parker Williams, and Hunt, 2004). The results from species by species comparison of our study (Table 6.3) during accuracy assessment actually revealed more under prediction than over prediction. The only real over predicted rare species was *R. pseudoacacia*. Out of three important under predicted species, both *R. canina* and *F. excelsior* have a very open type of canopy, which may undermine their spectral strength in the pixel and hence cause their under prediction. However, the sample number for many species was not large enough to conclude the statistical significance of this finding. The selection of high threshold value (0.2) of degree of match for designating species presence was also taken to minimize the "false positive" response. But the negative side of this high threshold was omitting many legitimate presences of species. So actually many white pixels (no species) in Figure 6.5 may still have shrubs or small trees which failed to create enough spectral response to be recognised during the unmixing.

Traditionally, maps for vegetation dynamics are based on species association or phyto-sociological boundaries with added expert judgment,

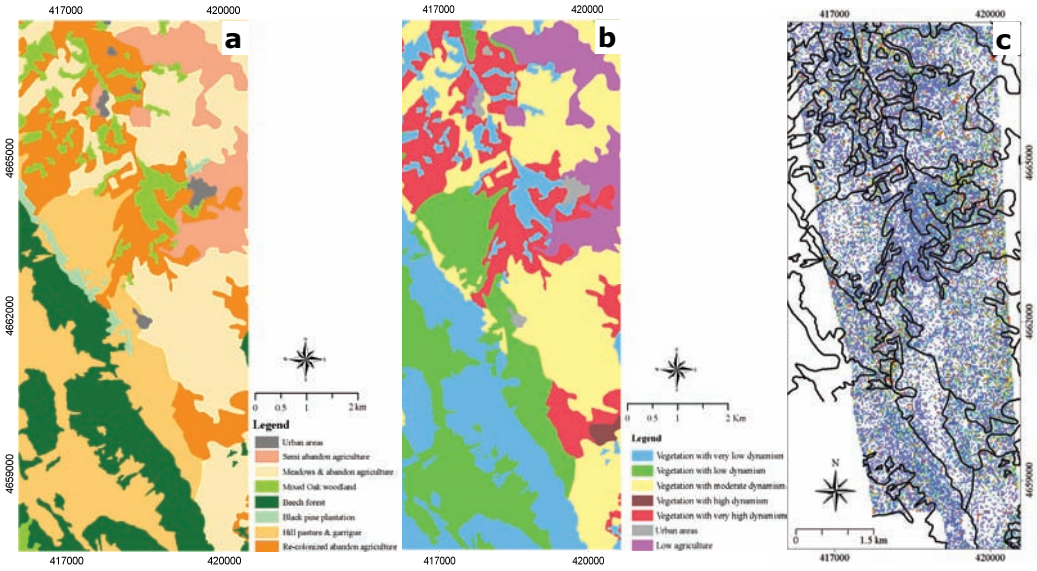

Figure 6.9 (a) Phyto-sociological map of the study area (b) Map for vegetation dynamism and (c) species richness map from unmixing process with overlaid polygon boundaries of vegetation dynamism map. Map (a) and (b) are produce by the Majella national park authority and published on February 1999.

as shown in Figure 6.9. To prepare a phyto-sociological map and consequently convert it into a vegetation dynamic map is a costly and time-consuming effort. In a fast changing landscape keeping pace with

the transformation is also essential. To get a quick and reliable species composition map, the method we used can be very useful. The pixel-based system can also reduce the subjective nature of polygon boundaries. Overlaying the polygon boundaries of dynamisms map on our species richness map (Figure 6.9 (c)) and the histogram of mean species number per pixel per dynamism class (Figure 6.10) highlighted the relationship between species assemblage and dynamisms status. It is evident from the histogram (Figure 6.10) that the polygons designated as lower dynamic status also contain less number of species. This is especially true for hill pasture and garrigue areas showed in Figure 6.9 (a), which still remained primarily as grassland and used for sheep grazing in the summer. Much of these grasslands are also mowed for winter fodder reserve for the cattle. The very low dynamic areas are mainly consists of pure beech (*F. sylvatica*) forest stands and hence the mean species number remained close to one (Figure 6.10). However, the differences of species number between moderate, high and very high dynamic areas were little. From an ecological point of view, it was also interesting to observe that relatively higher number of species assemblage was found along the polygon boundaries as evident in Figure 6.9 (c). Moreover, the higher heterogeneity in the landscape level (i.e., rapid change of vegetation associations) appeared to influence the species number positively.

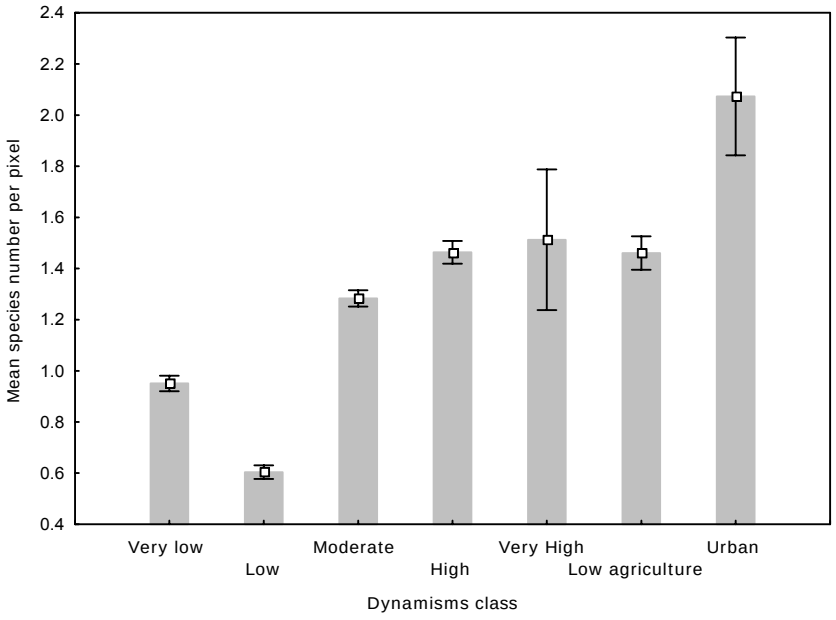

Figure 6.10 Mean shrub and tree species number per pixel in different dynamism classes as showed in Figure 6.9 (b).

One of the major limitations of unmixing techniques is to find endmember spectra which can truly represent that species. Spectral variations within a single endmember, especially in case of plant species are common due to various environmental factors. Even we had to limit our study area into a small subset of the national park as spectral signature from distance locations with different topography and micro-environment was giving unreliable endmember signature. Use of single mean spectrum per species was another notable weakness of this process as it fails to take care of the variability within each species.

Acknowledgments

The international Institute for Geo-Information Science and Earth Observation (ITC) and Nuffic provided financial support for this study. We also extend our gratitude to the management of Majella National Park, Italy, and particularly to Dr. Theodoro Andrisano.

Chapter 7

Plant species discrimination using hyperspectral remote sensing
The synthesis

7.1 Plant species discrimination

Sustainable ecosystem management requires the comprehensive understanding of species composition and distribution (Nagendra, 2002). Traditionally, species discrimination for floristic mapping has involved exhaustive and time-consuming fieldwork, including taxonomical information and the visual estimation of the percentage cover for each species (Kent and Coker, 1992). To understand species composition and distribution more accurately and also more efficiently, it is essential to use remotely sensed data for the species-level discrimination of plants.

The advent of hyperspectral sensors has raised new possibilities for spectrally discriminating species (Cochrane, 2000; Schmidt and Skidmore, 2003; Clark Roberts and Clark, 2005) and thus for improving the discrimination and mapping of vegetation communities or species. Researchers are able to discriminate and classify species based on their fresh leaf or field reflectance (Gong, Pu and Yu, 1997; Knapp and Carter, 1998; Kumar and Skidmore, 1998; Cochrane, 2000; Schmidt and Skidmore, 2001; Schmidt and Skidmore, 2003; Yamano et al., 2003). However, several concerns still exist regarding the usefulness of plant reflectance spectra for separating species. Price (1994) and Portigal et al. (1997) are sceptical about the possibility of utilizing plant spectra for species-level discrimination. Moreover, both intraspecies variations in spectra owing to various environmental factors (Gausman, 1985; Westman and Price, 1987; Carter, 1993; Carter, 1994; Portigal et al., 1997; Roberts et al., 1998; Gracia and Ustin, 2001; Smith et al., 2004) and high data dimensionality are other causes of concern in this regard.

Using hyperspectral remote sensing for the species-level discrimination or mapping of plants is a complex process, and it is therefore important to understand all the different aspects before coming to a conclusion.

The main objective of this study was to investigate the potential of hyperspectral remote sensing for plant species discrimination. To realize this main objective, we subdivided it into sub-objectives: (1) to identify the potential spectral regions containing information regarding species discrimination, (2) to investigate the usefulness of spectral matching algorithms for discriminating spectra of different plant species, (3) to examine whether phenological events can be used to enhance the separability between species, and (4) to examine whether sub-pixel unmixing techniques can be used to map the species distribution and richness in a landscape.

7.2 Reliability of laboratory measurement

Frequently, leaves are collected in the field and transported to the laboratory for spectral measurement because *in situ* spectroscopic measurements are often impractical owing to poor or highly variable lighting conditions, and inaccessibility for portable spectral equipment

(Foley et al., 2006). But how “safe” is it to collect spectral measurements in a laboratory yet still treat them as *in situ* measurements? Although the foliar spectral signature is controlled by foliar biochemical contents (e.g. chlorophyll and nitrogen concentrations (Asner, 1998)), all these biochemical contents are subject to change according to the leaf hydration state. The sudden disruption in energy, nutrient and hormone supplies subjects harvested leaves to considerable stress (Page et al., 2001). Stress is manifested by changes in leaf biochemical constituents such as water content and pigment concentration (Böttcher et al., 2001; Able et al., 2005). As the changes in leaf physiology affect its spectral properties (Horler et al., 1983; Hunt and Rock 1989; Carter, 1993, 1994; Peñuelas et al., 1994; Carter and Knapp, 2001), results based on laboratory measurements may not truly reflect *in situ* spectra.

The results of this study show that from the moment of harvest the spectral properties of fresh leaves change significantly over time. The safe period to perform spectral measurement, irrespective of species variations, was found to be six hours – although leaf samples must be stored in plastic bags and under cool dark conditions. However, the rate of change in spectral indices differs because of the varying leaf structure of different species. Although leaf dehydration influences reflectance across the whole spectrum, the effects are more noticeable in the NIR and SWIR than in the visible spectrum. Of the indices, the two water indices were the most sensitive, and for all species they defined the minimum “safe” period.

7.3 Dimensionality: Are all bands necessary?

The high dimensionality of hyperspectral data is a known phenomenon that can cause imprecise class estimation in the spectral feature space and can lower classification accuracy (Bellman, 1961). Moreover, this phenomenon requires more training samples in order to construct better estimates of class models, thereby increasing the field survey requirement. However, Roberts et al., 1993; Kokaly et al., 2003; and Clark et al., 2005 argue that the high spectral resolution of hyperspectral data is essential for capturing and discriminating the subtle differences in targets that help species-level discrimination, and that any band reduction procedure decreases the information content captured by the measurement.

Various data reduction techniques, including the search for the most informative bands and the linear transformation of reflectance spectra into lower-dimensional spectral space, have traditionally been applied to this problem. A number of feature extraction techniques have already been tested to reduce the number of dimensions in hyperspectral data. Linear and stepwise discriminant analysis (Duda and Hart, 1973), principal component analysis (Anderson, 1984), canonical analysis (Richards, 1986), decision boundary feature extraction (Lee and Landgrebe, 1993) and genetic algorithms (Vaiphasa, 2003) are among

the typical data extraction methods to reduce data dimensionality. In spite of the problems of information loss and data distribution, several studies have found that these techniques help to improve classification accuracies (Harsanyi and Chang, 1994; Du and Chang, 2001; Gong et al., 2002; Metternicht and Zinck, 2003). However, the recent development of various spectral matching algorithms has reduced dependency on dimension reduction techniques, as most of these techniques can handle high dimensional data quite easily. In fact, these algorithms treat the spectral signatures as vectors, and compare their geometrical shapes or probability distributions in order to separate them from each other. For example, spectral angle mapper (SAM) (Skidmore et al., 1987; Yuhas, 1992; Kruse et al., 1993) measures the similarity between two spectra by calculating the spectral angle between them, treating them as vectors in a space with dimensionality equal to the number of spectral bands used. On the other hand, spectral information divergence (SID) (Chang, 2000) calculates the probabilistic behaviours between spectral signatures. But these techniques too have their weaknesses when separating vegetation spectra. For example, SAM is relatively insensitive to illumination and albedo effects because the angle between two vectors is invariant with respect to the length of the vectors (Kruse, 1997), while Schmidt and Skidmore, 2003 point out that albedo contributes largely to the differences between vegetation types.

In this thesis, we have used both methods. In chapter 3, band selection techniques are applied to discriminate leaf spectra, while in chapter 4 spectral matching techniques are applied. Both types of technique perform well and manage to differentiate species from leaf spectra. However, comparing an “all bands” approach with a “selected band” approach is difficult, as they produce completely different units of measurement.

7.4 Which part of the spectrum is most important?

During the band selection process (chapter 3), it was evident that important spectral regions do exist in different parts of the spectral signature. Hence, close inspection reveals that, out of the seven information-rich regions described in chapter 3, three lie within the visible part of the spectra. The relatively high importance of the visible part is also supported by Everitt et al. (1992) and Hunt et al. (2004). Furthermore, this illustrates the relative importance of different parts of the spectrum for species discrimination. This result could lead us to hypothesize that the spectral responses of leaf pigment and other biochemical properties contain more spectral information regarding species discrimination than can be gained from leaf morphology. It is also evident that these selected spectral regions have important vegetation parameters (Table 3.7), as established by various authors (Curran et al., 1992; Johnson et al., 1994; Yoder and Pettigrew-Crosby, 1995; Blackburn, 1998; Blackburn, 1999; Datt, 1999). Chapters 4 and 5 highlight the importance of the visible portion of the electromagnetic spectrum, especially

when using phenological support to differentiate species. Even in the "without flower" condition as portrayed in Figure 5.3, the visible portion showed higher differences between species. We also observed that the visible portion, compared with the NIR or the SWIR, remains unaffected by dehydration much longer when spectral measurements are performed in the laboratory. However, this could be misleading as Schmidt and Skidmore (2001, 2003) show that the NIR portion also contains a high level of information regarding species separation. One of the major causes of this discrepancy may be the lack of canopy information in our experiment design, where layers of leaf were used to collect the spectra.

7.5 What is essential to optimize a sensor for species discrimination?

Designing a sensor is always complicated, as a balance between the data acquisition rate and the storage and handling facility is crucial (Goetz et al., 1985). An optimum sensor specialized for species discrimination should have bands of narrow bandwidth but not necessarily contiguous from the visible to the SWIR spectral range. High spatial resolution is essential, but exact pixel size is difficult to define. As discussed in chapter 3, information regarding species discrimination was found to be concentrated in seven spectral regions, as separability calculated between species (Bhattacharya distances) using bands within these

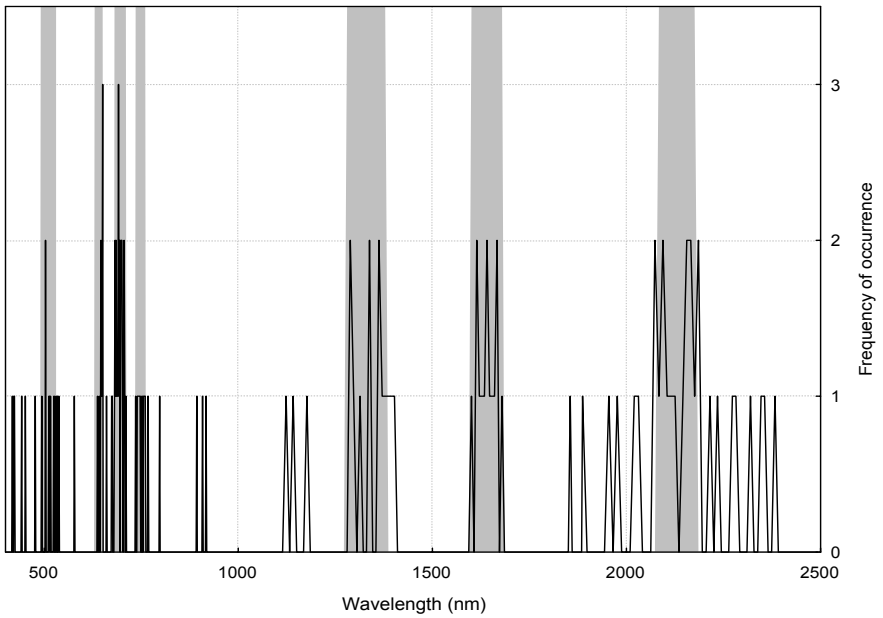

Figure 7.1 Selected regions (in gray) where discriminating wavebands occurred most frequently.

regions showed significantly higher distances compared with those shown using bands from outside these ranges. The result also revealed that bands within these regions share similar information between them. As a result, a sensor designed to be used for species discrimination should have bands within the selected regions (Figure 7.1). Selecting an optimal spatial resolution is more complicated. Ideal pixel size depends on the size of the canopy of the target species, which can vary widely from species to species as well as within species (Nagendra, 2002).

Most of the current airborne hyperspectral sensors (HyMap, HYDICE or AVIRIS) have a spectral resolution of 10 nm or more, with 100 to 250 spectral bands (Cocks et al., 1998). Because of the airborne platform, these sensors can vary their spatial resolution by changing the flight height – although most of them cannot reach below 2 m. The only available satellite-platform-based hyperspectral sensor is EO-1 Hyperion, with 220 spectral bands and 30 m ground resolution. So, even though most of these sensors have sufficient spectral resolution to capture spectral differences between species, their spatial resolution is not high enough to capture pure spectra, except large tree or shrub canopies.

When species discrimination is performed using unmixing techniques in a multispecies pixel condition (chapter 6), the spectral resolution is more important than the spatial resolution, as long as the pure endmember spectral measurements are available. Since these endmember spectral measurements can also be obtained by using a spectrometer in the field, the use of very high spatial resolution imagery is not obligatory.

7.6 When to measure?

Two species can have different discriminatory probability at different times of the year. This phenomenon is due largely to the change of phenological stages of plant species. Phenology has a well-defined temporal pattern, which can be used to characterize an individual species and discriminate it from others (Turner et al., 2003; Underwood, Ustin, and DiPietro, 2003). Although most authors mention using multitemporal images from two different phenological stages (Verbyla, 1995) and changes in the spectral characteristics of leaves during autumn senescence (Boyer et al., 1988; Miller et al., 1991; Rock, Lauten, and Moss, 1993; Gitelson, Merzlyak, and Lichtenthaler, 1996) to discriminate species, in this study (chapter 5) we concentrate on using the flowering period as a phenological stage and investigate the influence of flowering on species separability.

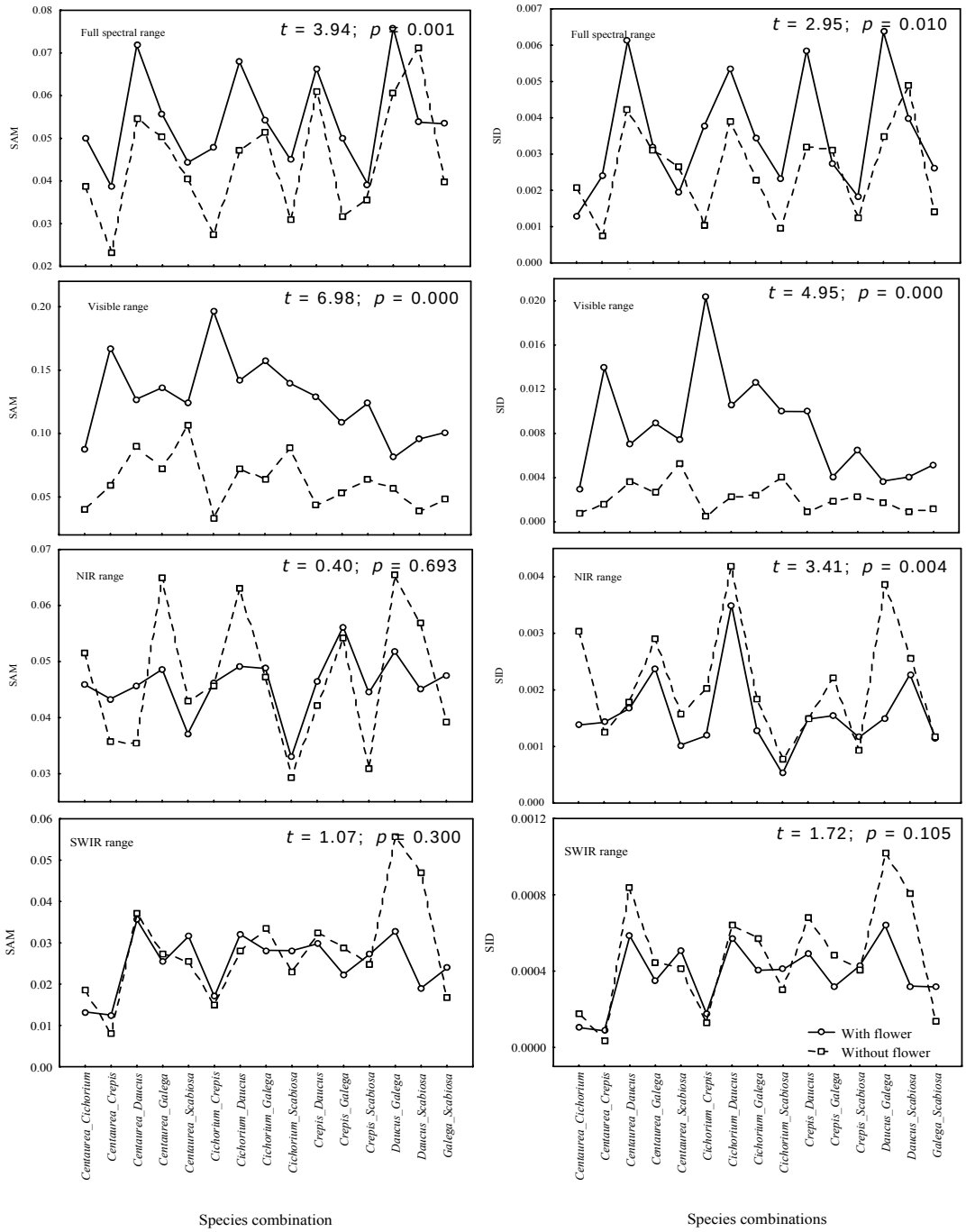

Figure 7.2 Comparisons of similarity measure values between with-flower and without-flower measurements in all four spectral configurations. *t*-test results showing the significance of their differences. Left column is for SAM and right column is for SID measurements.

In this thesis, we observe that flowers have a distinct influence on vegetation spectra and hence on their separability. The presence of flowers induces extra pigment absorption in the visible spectral regions, and during the flowering stage the visible portion demonstrates a very significant enhancement in separability, whereas the NIR and SWIR show little change. However, because of the big change in the visible portion, the full spectral configuration also shows significant enhancement (Figure 7.2). Furthermore, continuum-removed band depth measurements of two pigment absorption pits also reveal that most of the species pairs are more separable when flowering.

This study also uses phenological differences to investigate the change in classification accuracy between two shrub species. The result shows a significant increase in classification accuracy with flowers in the canopy (2005), as against the non-flowering state (2004) (Figure 7.3). Both overall accuracy and Kappa coefficient increased significantly (Table 5.3). However, a more detailed insight into the changes (Table 5.4) reveals that the increased accuracy of our target species *Spartium junceum* was very high. Both producer and user accuracies exceeded 90% in 2005, rising from 67% and 41% respectively in the previous year. This also pushed up the accuracies for its associate shrub (*Prunus spinosa*).

The results show that different species can have different discriminatory probability at different times of the year. Consequently, it is very important to know the phenological cycles of the species to be discriminated in order to schedule image acquisition. In fact, one should conclude that the species are “separable at the time of measurement”.

7.7 Discriminating species at a landscape scale

At a landscape level, species discrimination using airborne hyperspectral data encounters a completely different set of difficulties to those relating to laboratory measurement – although it is more ecologically relevant. Species grow together and share the spatial space and reflectance spectra of a pixel. In this thesis, a sub-pixel spectral unmixing technique (matched filtering) is applied to a HyMap hyperspectral image of Majella

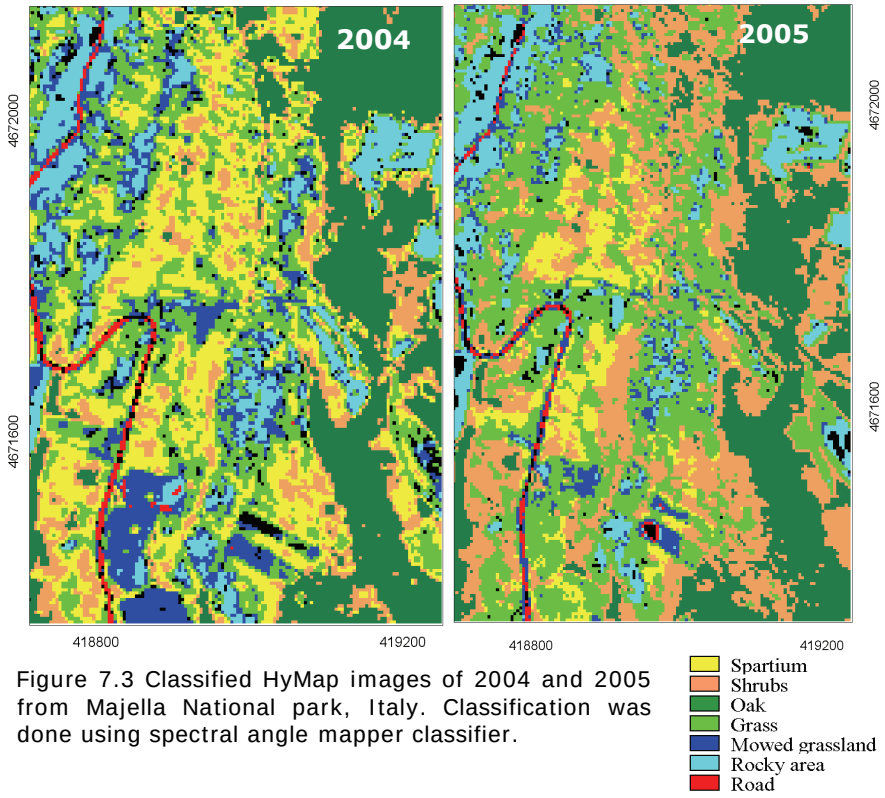

Figure 7.3 Classified HyMap images of 2004 and 2005 from Majella National park, Italy. Classification was done using spectral angle mapper classifier.

National Park, Italy, to spectrally separate species based on their abundance in the pixel.

Although the use of unmixing techniques in imaging spectroscopy is not new, it has been little explored in plant species discrimination and mapping. The results of this study (chapter 6) highlight the usefulness of sub-pixel-based unmixing image processing techniques in the context of the spatial distribution of a particular plant species as well as the mapping of multispecies associations. Use of multispecies endmembers proved very encouraging, as both the intermediate single species distribution map (Figure 7.4) and the final species composition or richness map (Figure 7.5) can enhance understanding of the spatial distribution of each single endmember species, as well as the overall vegetation composition. This technique also proved to be more useful than per-pixel classification. The per-pixel classifier can bring out only the species with the highest cover percentage, but this is not always enough for ecological studies. Species, especially shrubs and herbs that in most cases do not produce the largest cover class in a pixel may yet give vital clues about the vegetation status.

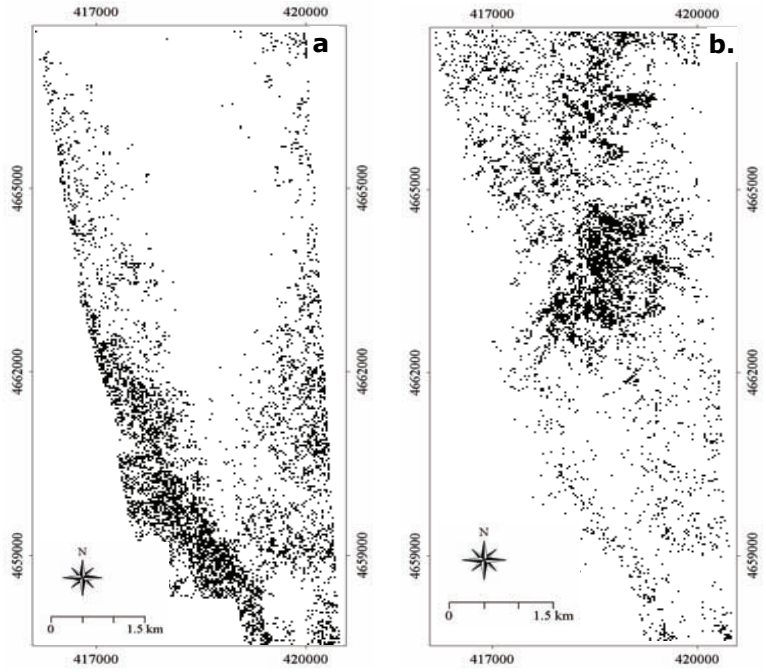

Figure 7.4 Present-absent binary images produced by slicing the fraction images shown in Figure 6.2 (a) beech (*F. sylvatica*) and (b) oak (*Q. pubescens*)

One of the main limitations of unmixing techniques is finding species endmember spectra that can truly represent that species, as this technique utilizes an average spectrum for each endmember. Owing to various environmental factors, spectral variations within a single endmember are common, particularly in the case of plant species, and because of this variation in spectral reflectance there is the risk of omitting valid endmember species from the result. Moreover, we had to limit our study to common shrub and tree species because of the difficulties associated with obtaining pure endmember spectra from the 4 m pixel we used. However, it may be possible to avoid this difficulty by using field-level spectrometer measurements of the endmembers.

7.8 Conclusion: Species discrimination – is it possible?

Among scientists today, there are two different schools of thought regarding the possibility of species discrimination by using hyperspectral data: the believers and the sceptics.

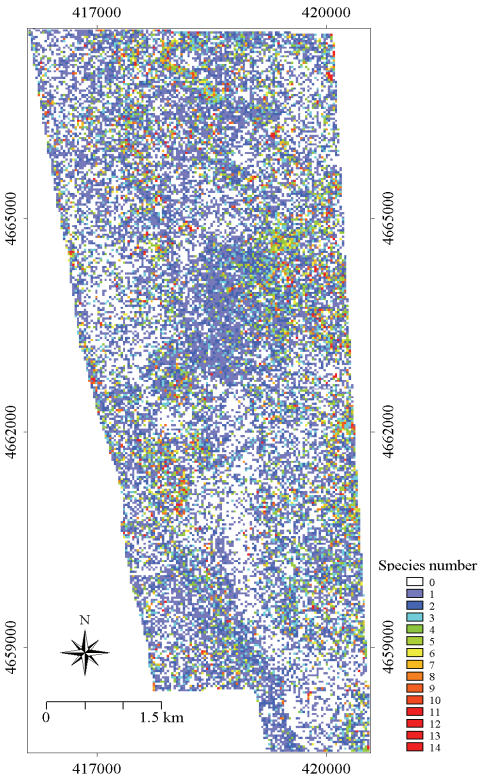

Figure 7.5 Composite species richness map, showing the number of species present per pixel.

Let's first look at the arguments put forward by the sceptics. Price (1994) questions the uniqueness of the vegetation spectra and hence the use of them to discriminate species. He suggests that several species may actually have quantitatively similar spectra, and that a spectrum is a mixture of physical and chemical properties that can change owing to various environmental factors. In an earlier article, Price (1992) argues that spectral reflectance is controlled by a small number of independent variables such as chlorophyll *a*, chlorophyll *b* and the carotenoids in visible regions (Tucker and Garrett, 1977) and the number and configuration of the air spaces that form the internal leaf structure in NIR (Danson 1995). Portigal et al. (1997) also argue that the reflectances of vegetation of different species are highly correlated because of their common chemical composition, and discrimination observed between species could be a result of the variation in biochemical compounds owing to environmental factors. Furthermore, interspecies spectral variability has to be lower than intraspecies spectral variability to successfully discriminate plant spectra.

However, the group of scientists who believe that spectral reflectance can be used to discriminate species has tried to counter these arguments. Cochrane (2000) argues that, despite some problems, the potential for separating different species based on foliar reflectance does exist. This group has further argued that although, because of the non-unique nature of the spectral response, species level may never be perfect or very robust, the spectral response still provides enough information to separate one species from another and can be a useful tool. Moreover, hyperspectral data have proved capable of quantifying all the independent variables mentioned by Price (1992), such as chlorophyll content of plants (Blackburn, 1999), biochemical variables such as nitrogen and lignin (Curran, 1994), crop moisture variations (Peñuelas et al., 1993; Peñuelas et al., 1995), and leaf pigment concentrations (Blackburn and Steele, 1999). In natural environment conditions, environmental variables generally follow a slow continuous gradient (Schmidtlein and Sassin, 2004). Under such conditions, the variability of biochemical compounds and canopy/leaf structure, two major drivers of vegetation reflectance spectra, should be controlled by the genetic variability of different species.

So let's return to the main question of this study: Is it possible to differentiate plant species by using hyperspectral remote sensing? The answer is: Yes, it is possible. Various aspects of species discrimination were explored to determine the answer, and some of the major conclusions of this dissertation are summarized below.

- Species can be discriminated spectrally with or without reducing the data dimension.

- Seven spectral regions shown to contain the highest species discriminatory properties were detected. Moreover, the bands within these regions share similar information between them.

- Phenological changes such as the emergence of flowers can be used to enhance species-level discrimination.

- The sub-pixel unmixing classification technique successfully revealed its usefulness in the context of mapping the spatial distribution of both individual plant species and multispecies associations.

Bibliography

Able, A. J., Wong, L. S., Prasad, A. and O'Hare, T. J. (2005). The physiology of senescence in detached pak choy leaves (*Brassica rapa* var. *chinensis*) during storage at different temperatures. *Postharvest Biology and Technology*, *35*(3): 271-278.

Adams, J. B., Smith, M. O. and Gillespie, A. R. (1993). Imaging spectroscopy: Interpretation based on spectral mixture analysis. In C. M. Pieters and P. A. J. Englert (Ed.), *Remote geochemical analysis: Elemental and mineralogical composition* (pp. 145 - 166) Cambridge, England: Press Syndicate of Univ. of Cambridge.

Adams, J. B., Smith, M. O. and Johnson, P. E. (1985). Spectral mixture modeling: a new analysis of rock and soil types at the Viking Lander I site. *Journal of Geophysical Research*, *91*: 8098–8112.

Aldakheel, Y. Y. and Danson, F. M. (1997). Spectral reflectance of dehydrating leaves: measurements and modelling. *International Journal of Remote Sensing*, *18*(17): 3683-3690.

Ales, R. F., Martin, A., Ortega, F. and Ales, E. E. (1992). Recent changes in landscape structure and function in a Mediterranean region of SW Spain (1950-1984). *Landscape Ecology*, *7* (1): 3-18.

Anderson, J. R., Hardy, E. E., Roach, J. T. and Witmer, R. E. (1976). A land use and land cover classification system for use with remote sensor data. *U.S. Geological Service Professional Paper*, *964*.

Armesto, J. J. and Pickett, S. T. A. (1985). Experiments on disturbance in old-field plant communities: impact on species richness and abundance. *Ecology*, *66*(1): 230-240.

Asner, G. P. (1998). Biophysical and biochemical sources of variability in canopy reflectance. *Remote Sensing of Environment*, *64*(3): 234-253.

Asner, G. P., Wessman, C. A., Schimel, D. S. and Archer, S. (1998). Variability in Leaf and Litter Optical Properties: Implications for BRDF Model Inversions Using AVHRR, MODIS, and MISR. *Remote Sensing of Environment*, *63*(3): 243-257.

Asner, G. P., Wessman, C. A., Bateson, C. A. and Privette, J. L. (2000). Impact of Tissue, Canopy, and Landscape Factors on the Hyperspectral Reflectance Variability of Arid Ecosystems. *Remote Sensing of Environment*, *74*(1): 69-84.

Aspinall, R. J. (2002). Use of logistic regression for validation of maps of the spatial distribution of vegetation species derived from high spatial resolution hyperspectral remotely sensed data. *Ecological Modelling*, *157*(2-3): 301-312.

Atkinson, M. D., Jervis, A. P. and Sangha, R. S. (1997). Discrimination between *Betula pendula*, *Betula pubescens* and their hybrids using near-infrared reflectance spectroscopy. *Canadian Journal of Forest Resources*, *27*: 1896-1900.

Bajjouk, T., Guillaumont, B. and Populus, J. (1996). Application of airborne imaging spectrometry system data to intertidal seaweed classification and mapping. *Hydrobiologia*, *326/327*: 463-471.

Bajwa, S. G., Bajcsy, P., Groves, P. and Tian, L. F. (2004). Hyperspectral image data mining for band selection in agricultural application. *Transactions of the ASAE*, *43*(3): 895-907.

Bakker, W. H. and Schmidt, K. S. (2002). Hyperspectral edge filtering for measuring homogeneity of surface cover types. *ISPRS Journal of Photogrammetry and Remote Sensing*, *56*(4): 246-256.

Ballantine, J.-A. C., Okin, G. S., Prentiss, D. E. and Roberts, D. A. (2005). Mapping North African landforms using continental scale unmixing of MODIS imagery. *Remote Sensing of Environment*, *97*(4): 470-483.

Barbero, M., Bonin, G. and Quezel, P. (1990). Changes and disturbances of forest ecosystems caused by human activities in the western part of the Mediterranean basin. *Vegetatio*, *97*: 151–173.

Ben-Dor, E. and Levin, N. (2000). Determination of surface reflectance from raw hyperspectral data without simultaneous ground data measurements: a case study of the GER 63-channel sensor data acquired over Naan, Israel. *International Journal of Remote Sensing*, *21*: 2053-2074.

Bhattacharya, A. (1943). On a measure of divergence between two statistical populations defined by their probability distributions. *Bulletin of Calcutta Maths Society*, *35*: 99-110.

Blackburn, G. A. (1998). Spectral indices for estimating photosynthetic pigment concentrations: in a test using senescent tree leaves. *International Journal of Remote Sensing*, *19*(4): 657-675.

Blackburn, G. A. (1998a). Quantifying Chlorophylls and Caroteniods at Leaf and Canopy Scales: An Evaluation of Some Hyperspectral Approaches. *Remote Sensing of Environment*, *66*(3): 273-285.

Blackburn, G. A. (1998b). Spectral indices for estimating photosynthetic pigment concentrations: in a test using senescent tree leaves. *International Journal of Remote Sensing*, *19*(4): 657-675.

Blackburn, G. A. (1999). Relationships between Spectral Reflectance and Pigment Concentrations in Stacks of Deciduous Broadleaves. *Remote Sensing of Environment*, *70*(2): 224-237.

Boardman, J. W. (1998). Leveraging the high dimensionality of AVIRIS data for improved sub-pixel target unmixing and rejection of false positives: Mixture Tuned Matched Filtering. *Proceedings of the AVIRIS 1998 Proceedings.* (pp. JPL, California.

Boardman, J. W., Kruse, F. A. and Green, R. O. (1995). Mapping target signatures via partial unmixing of AVIRIS data, BEACON eSpace at Jet Propulsion Laboratory

Bonet, A. (2004). Secondary succession of semi-arid Mediterranean old-fields in south-eastern Spain: insights for conservation and restoration of degraded lands. *Journal of Arid Environments*, *56*(2): 213-233.

Boochs, F., Kupfer, G., Dockter, K. and Kuhbauch, W. (1990). Shape of the red-edge as vitality indicator for plants. *International Journal of Remote Sensing*, *11*(10): 1741-1753.

Böttcher, H., Gunther, I., Franke, R. and Warnstorff, K. (2001). Physiological postharvest responses of Matricaria (*Matricaria recutita* L.) flowers. *Postharvest Biology and Technology*, *22*(1): 39-51.

Boyer, M., Miller, J., Belanger, M., Hare, E. and Wu, J. (1988). Senescence and spectral reflectance in leaves of northern pin oak (*Quercus palustris* Muenchh.). *Remote Sensing of Environment*, *25*(1): 71-87.

Brisco, B., Brown, R., J and Manore, M. J. (1989). Early season crop discrimination with combined SAR and TM data. *Canadian Journal of Remote Sensing*, *15*(44-54).

Caetano, M. R., Oliveira, T., Paul, J., Vasconcelos, M. J. and Pereira, J. M. (1997). Mapping shrublands and forests with multispectral satellite images based on spectral unmixing of scene components. *Proceedings of the SPIE. 3222,* (pp. 4-14) London, UK. The International Society for Optical Engineering

Cao, K. F. (2000). Leaf anatomy and chlorophyll content of 12 woody species in contrasting light conditions in a Bornean heath forest. *Canadian Journal of Botany*, *78*(10): 1245-1253.

Carson, W. P. and Barrett, G. W. (1988). Succession in old-field plant communities: effects of contrasting types of nutrient enrichment. *Ecology*, *69*(4): 984-994.

Carter, G. A. (1991). Primary and secondary effects of water content on the spectral reflectance of leaves. *American Journal of Botany*, *78*: 916-924.

Carter, G. A. (1993). Responses of leaf spectral reflectance to plant stress. *American Journal of Botany*, *80*(3): 239-243.

Carter, G. A. (1994). Ratios of leaf reflectances in narrow wavebands as indicators of plant stress. *International Journal of Remote Sensing*, *15*: 697-703.

Carter, G. A. and Knapp, A. K. (2001). Leaf optical properties in higher plants: linking spectral characteristics to stress and chlorophyll concentration. *American Journal of Botany*, *88*(4): 677-684.

Chang, C. I. (2000). An information- theoretic approach to spectral variability similarity and discrimination for hyperspectral image analysis. *IEEE Transactions on Information Theory*, *46*(5): 1927-1932.

Chang, C. I. (2003). *Hyperspectral Imaging: Techniques for spectral detection and classification*. Dordrecht, Kluwer Academic Publishers,.

Chang, S. H. and Collins, W. (1983). Confirmation of the airborne biogeophysical mineral exploration technique using laboratory methods. *Economic Geology and the Bulletin of the Society of Economic Geologists*, *78*: 723-736.

Cho, M. A. and Skidmore, A. K. (2006). A new technique for extracting the red edge position from hyperspectral data: The linear extrapolation method. *Remote Sensing of Environment*, *101*(2): 181-193.

Clark, A. F. (1999). Spectroscopy of rocks and minerals and principles of spectroscopy. In A. N. Rencz (Ed.), *Manual of Remote Sensing: Remote Sensing for the Earth Sciences.* (pp. 3-58) New York: John Wiley and Sons.

Clark, M. L., Roberts, D. A. and Clark, D. B. (2005). Hyperspectral discrimination of tropical rain forest tree species at leaf to crown scales. *Remote Sensing of Environment*, *96*(3-4): 375-398.

Clark, R. N., King, T. V. V., Kleijwa, M., Swayze, G. A. and Vergo, N. (1990). High spectral resolution reflectance spectroscopy of minerals. *Journal of Geophysical Research*, *95*: 12653-12680.

Clevers, J. G. P. W., Jong, S. M. D., Epema, G. F., Meer, F. D. V. D., Bakker, W. H., Skidmore, A. K. and Scholte, K. H. (2002). Derivation of the red edge index using the MERIS standard band setting. *International Journal of Remote Sensing*, *23*(16): 3169-3184.

Cochrane, M. A. (2000). Using vegetation reflectance variability for species level classification of hyperspectral data. *International Journal of Remote Sensing*, *21*(10): 2075-2087.

Collins, W. (1978). Remote sensing of crop type and maturity. *Photogrammetric Engineering and Remote Sensing*, *44*: 43-55.

Conti, F. (1998). *Flora D'Abruzzo: An annotated check-list of the flora of the Abruzzo*. Palermo, Herbarium Mediterraneum Panormitanum.

Curran, P. J. (1989). Remote sensing of foliar chemistry. *Remote Sensing of Environment*, *30*: 271-278.

Curran, P. J., Dungan, J. L. and Gholz, H. L. (1990). Exploring the relationship between reflectance red edge and chlorophyll content in slash pine. *Tree Physiology*, *7*: 33-48.

Curran, P. J., Dungan, J. L., Macler, B. A. and Plummer, S. E. (1991). The effect of a Red leaf pigment on the relationship between red edge and chlorophyll concentration. *Remote Sensing of Environment*, *35*: 69-76.

Curran, P. J., Dungan, J. L., Macler, B. A., Plummer, S. E. and Peterson, D. L. (1992). Reflectance spectroscopy of fresh whole leaves for the estimation of chemical concentration. *Remote Sensing of Environment*, *39*(2): 153-166.

Curran, P. J., Windham, W. R. and Gholz, H. L. (1995). Exploring the relationship between reflectance red edge and chlorophyll concentration in slash pine leaves. *Tree Physiology*, *15*: 203-206.

Danson, F. M. and Plummer, S. E. (1995). Red edge response to forest leaf area index. *International Journal of Remote sensing*, *16*(1): 183-188.

Datt, B. (1999). Visible/near infrared reflectance and chlorophyll content in eucalyptus leaves. *International Journal of Remote Sensing*, *20*(14): 2741-2759.

Daughtry, C. S. T., Gallo, K. P., Goward, S. N., Prince, S. D. and Kustas, W. P. (1992). Spectral estimates of absorbed radiation and phytomass production in corn and soybean canopies. *Remote Sensing of Environment*, *39*(2): 141-152.

Dawson, T. P. and Curran, P. J. (1998). A new technique for interpolating the reflectance red edge position. *International Journal of Remote Sensing*, *19*(11): 2133-2139.

Debussche, M. and Lepart, J. (1992). Establishment of woody plants in Mediterranean old fields: opportunity in space and time. *Landscape Ecology*, *6*: 133–145.

Debussche, M., Escarr!e, J., Lepart, J., Houssard, C. and Lavorel, S. (1996). Changes in Mediterranean plant succession: old-fields revisited. *Journal of Vegetation Science*, *7*: 519–526.

Du, Y., Chang, C.-I., Ren, H., Chang, C.-C., Jensen, J. O. and D'Amico, F. M. (2004). New hyperspectral discrimination measure for spectral characterization. *Optical Engineering*, *43*(8): 1777–1786.

Du, Y., Chang, C.-I., Ren, H., D'Amico, F. and Jensen, J. O. (2003). A New hyperspectral discrimination measures for spectral similarity. *Proceedings of the International Society for Optical Engineering (SPIE) Conference. Vol-5093 - Algorithms and Technologies for Multispectral, Hyperspectral, and Ultraspectral Imagery IX,* (pp. 430-439) Orlando, FL, USA. SPIE

Elvidge, D. E. (1990). Visible and near infrared reflectance characteristice of dry plant materials. *International Journal of Remote Sensing*, *11*(10): 1775-1795.

Everitt, J. H., Alaniz, M. A., Escobar, D. E. and Davis, M. R. (1992). Using remote sensing to distinguish common (*Isocoma coronopifolia*) and

Drummond goldenweed (*Isocoma drummondii*). *Weed Science 40*(4): 621-628.

Everitt, J. H., Anderson, G. L., Escobar, D. E., Davis, M. R., Spencer, N. R. and Andrascik, R. J. (1995). Use of remote sensing for detecting and mapping leafy spurge (*Euphorbia esula*). *Weed Science*, *9*(3): 599-609.

Fernández, J. B. G., Mora, M. R. G. and Novo, F. G. (2004). Vegetation dynamics of Mediterranean shrublands in former cultural landscape at Grazalema Mountains, South Spain. *Plant Ecology*, *172*: 83-94.

Ferrier, G. (1999). Application of Imaging Spectrometer Data in Identifying Environmental Pollution Caused by Mining at Rodaquilar, Spain. *Remote Sensing of Environment*, *68*(2): 125-137.

Ferwerda , J. G., Skidmore , A. K. and Mutanga, O. (2005). Nitrogen detection with hyperspectral normalized ratio indices across multiple plant species. *International Journal of Remote Sensing*, *26*(18): 4083-4095.

Ferwerda, J. G., Skidmore, A. K. and Stein, A. (2006). A bootstrap procedure to select hyperspectral wavebands related to tannin content. *International Journal of Remote Sensing*, *27*(7): 1413-1424.

Filella, I. and Peñuelas, J. (1994). The red edge position and shape as indicators of plant chlorophyll content, biomass and hydric status. *International Journal of Remote Sensing*, *15*(7): 1459-1470.

Foley, B., Mcllwee, A., Lawler, I., Agragones, l., woolnough, A. P. and Berding, N. (1998). Ecological applications of near infrared spectroscopy - a tool for rapid, cost effective prediction of the composition of plant and animal tissues and aspect of animal performance. *Oecologia*, *116*(293-305).

Foley, S., Rivard, B., Sanchez-Azofeifa, G. A. and Calvo, J. (2006). Foliar spectral properties following leaf clipping and implications for handling techniques. *Remote Sensing of Environment*, *103*(3): 265-275.

Gamon, J. A., Peñuelas, J. and Field, C. B. (1992). A narrow-waveband spectral index that tracks diurnal changes in photosynthetic efficiency. *Remote Sensing of Environment*, *41*: 35-44.

Gamon, J. A., Serrano, L. and Surfus, J. S. (1997). The photochemical reflectance index: An optical indicator of photosynthetic radiation use efficiency across species, functional types and nutrient levels. *Oecologia*, *112*: 492-501.

Gamon, J. A. and Surfus, J. S. (1999). Assessing leaf pigment content and activity with a reflectometer. *New Phytologist*, *143*(1): 105-117.

Gao, B. C. (1996). NDWI - a normalized difference water index for remote sensing of vegetation liquid water from space. *Remote Sensing of Environment*, *58*: 257-266.

Gao, X., Huete, A. R., Ni, W. and Miura, T. (2000). Optical-Biophysical Relationships of Vegetation Spectra without Background Contamination. *Remote Sensing of Environment*, *74*(3): 609-620.

Gates, D. M., Keegan, H. J., Schleter, J. C. and Weidner, V. R. (1965). Spectral properties of plants. *Applied Optics*, *4*(1): 11−20.

Gausman, H. W. (1985). *Plant leaf optical properties in visible and near infrared light*. Lubbock, Texas, Texas Technical Press.

Gausman, H. W., Allen, W. A., Cardenas, R. and Richardson, A. J. (1970). Relationship of light reflectance to histological and physical evaluation of cotton leaf maturity. *Applied Optics*, *9*(3): 545-552.

Gausman, H. W. and Allen, W. A. (1973). Optical parameters of leaves of 30 plant species. *Plant Physiology*, *52*: 57-62.

Ge, S., Everitt, J., Carruthers, R., Gong, P. and Anderson, G. (2006). Hyperspectral Characteristics of Canopy Components and Structure for Phenological Assessment of an Invasive Weed. *Environmental Monitoring and Assessment*, *120*(1): 109-126.

Gillespie, A. R., Smith, M. O., Adams, J. B., Willis, S. C., Fischer, A. F. and Sabol, D. E. (1990). Interpretation of residual images: spectral mixture analysis of AVIRIS images, Owens Valley, California. *Proceedings of the Second Airborne Imaging Spectrometer Data Analysis Conference.* (pp. 243- 270) Pasadena, CA. Jet Propulsion Laboratory

Gitelson, A. A., Merzlyak, M. N. and Lichtenthaler, H. K. (1996). Detection of red-edge position and chlorophyll content by reflectance measurements near 700 nm. *Journal of plant physiology*, *148*: 494-500.

Gitelson, A. A., Zur, Y., Chivkunova, O. B. and Merzlyak, M. N. (2002). Assessing carotenoid content in plant leaves with reflectance spectroscopy. *Photochemistry and Photobiology*, *75*(3): 272-281.

Gong, P., Pu, R. and Yu, B. (1997). Conifer species recognition: An exploratory analysis of in situ hyperspectral data. *Remote Sensing of Environment*, *62*(2): 189-200.

Gong, P., Pu, R. and Heald, R. C. (2002). Analysis of in situ hyperspectral data for nutrient estimation of giant sequoia. *International Journal of Remote Sensing*, *23*(9): 1827-1850.

Goward, S. N., Tucker, C. J. and Dye, D. G. (1985). North American vegetation patterns observed with the NOAA-7 advanced very high resolution radiometer. *Plant Ecology*, *64*(1): 3-14.

Goward, S. N., Huemmrich, K. F. and Waring, R. H. (1994). Visible-near infrared spectral reflectance of landscape components in western Oregon. *Remote Sensing of Environment*, *47*(2): 190-203.

Gower, S. T., Kucharik, C. J. and Norman, J. M. (1999). Direct and Indirect Estimation of Leaf Area Index, fAPAR, and Net Primary Production of Terrestrial Ecosystems. *Remote Sensing of Environment*, *70*(1): 29-51.

Gracia, M. and Ustin, S. L. (2001). Detection of interannual vegetation responses to climatic variability using AVIRIS data in a coastal savanna in California. *IEEE Transactions on Geoscience and Remote Sensing*, *39*: 1480-1490.

Green, R. O., Eastwood, M. L., Sarture, C. M., Chrien, T. G., Aronsson, M., Chippendale, B. J., Faust, J. A., Pavri, B. E., Chovit, C. J., Solis, M., Olah, M. R. and Williams, O. (1998). Imaging Spectroscopy and the Airborne Visible/Infrared Imaging Spectrometer (AVIRIS). *Remote Sensing of Environment*, *65*(3): 227-248.

Grime, J. P. (1979). *Plant strategies and vegetation processes*. New York, John Wiley and Sons.

Guyot, G. and Baret, F. (1988). Utilisation de la haute résolution spectrale pour suivre l'état des couverts végétaux. *Proceedings of the 4th International colloquium on spectral signatures of objects in remote sensing. SP-287,* (pp. 279-287) Assois, France. ESA

Harsanyi, J. C. and Chang, C. I. (1994). Hyperspectral image classification and dimensionality reduction: an orthogonal subspace projection approach. *IEEE Transactions on Geoscience and Remote Sensing*, *32*: 779-785.

Horler, D. N. H., Barber, J. and Barringer, A. R. (1980). Effects of heavy metals on the absorbance and reflectance spectra of plants. *International Journal of Remote Sensing*, *1*: 121.

Horler, D. N. H., Dockray, M. and Barber, J. (1983). The red edge of plant leaf reflectance. *International Journal of Remote Sensing*, *4*(2): 273-288.

Huete, A. R. and Jackson, R. D. (1988). Soil and atmosphere influences on the spectra of partial canopies. *Remote Sensing of Environment*, *25*(1): 89-105.

Hunt, E. R. J., Everitt, J. H., Ritchie, J. C., Moran, S. M., Booth, D. T., Anderson, G. L., Clark, P. E. and Seyfried, M. S. (2003). Applications and Research Using Remote Sensing for Rangeland Management. *Photogrammetric Engineering and Remote Sensing*, *69*(6): 675-693

Hunt, E. R., McMurtrey, J. E., Parker Williams, A. E. and Corp, L. A. (2004). Spectral characteristics of leafy spurge (*Euphorbia esula*) leaves and flower bracts. *Weed Science*, *52*(4): 492-497.

Hunt, R. E. J. and Rock , B. N. (1989). Detection of changes in leaf water content using near- and middle-infrared reflectance. *Remote Sensing of Environment*, *30*: 43-54.

Hunt, R. E. J., Rock , B. N. and Nobel, P. S. (1987). Measurement of leaf relative water content by infrared reflectance. *Remote Sensing of Environment*, *22*: 429-435.

Hunt, G. R. (1977). Spectral signatures of particulate minerals in the visible and near-infrared. *Geophysics*, *42*: 501-513.

Jacobsen, A., Heidebrecht, K. B. and Nielsen, A. A. (1998). Monitoring grasslands using convex geometry and partial unmixing - A case study. In M. Shaepman, D. Schläpfer and K. Itten (Ed.), *1st EARSel Workshop on Imaging Spectroscopy*. (pp. 309-316) Remote Sensing Laboratories, University of Zürich, Switzerland.

Jacquemond, S. and Baret, F. (1990). PROSPECT: A model of leaf optical properties spectra. *Remote Sensing of Environment*, *34*(2): 75-91.

John, G. A., Kohavi, R. and Pfleger, K. (1994). Irrelevant features and the subset selection problem. In W. W. Cohen and H. Hirsh (eds.), *Machine Learning*. (pp. 121-129). San Francisco: Morgan Kaufmann.

Johnson, L. F., Hlavka, C. A. and Peterson, D. L. (1994). Multivariate analysis of AVIRIS data for canopy biochemical estimation along the oregon transect. *Remote Sensing of Environment*, *47*: 216-230.

Justice, C. O., Townshend, J. R. G., Holben, B. N. and Tucker, C. J. (1985). Analysis of the phenology of global vegetation using meteorological satellite data. *International Journal of Remote Sensing*(6): 8.

Kavzoglu, T. and Mather, P. M. (2002). The role of feature selection in artificial neural network applications. *International Journal of Remote Sensing*, *23*: 2919-2937.

Keegan, H. J., Schleter, J. C., Hall, W. A. and Hass, G. M. (1955). Spectrophotometric and colorimetric study of foliage stored in covered metal containers. *U.S. Bureau of Standards*.

Kent, M. and Coker, P. (1992). *Vegetation description and analysis, A practical approach*. London, John Wiley & Sons.

Kerr, J., T. and Ostrovsky, M. (2003). From space to species: ecological applications for remote sensing. *Trends in Ecology and Evolution*, *18*(6): 299-305.

Klecka, W. R. (1980). *Discriminant Analysis, Quantitative Applications in the Social Sciences, 19*. Thousand Oaks, CA, Sage Publications.

Knapp, A. K. and Carter, G. A. (1998). Variability in leaf optical properties among 26 species from a broad range of habitat. *American Journal of Botany*, *85*(7): 940-946.

Knipling, E. B. (1970). Physical and physiological basis for the reflectance of visible and near-infrared radiation from vegetation. *Remote Sensing of Environment*, *1*: 155-159.

Kohavi, R. and John, G. H. (1997). Wrappers for feature subset selection. *Artificial Intelligence*, *97*: 273-324.

Kokaly, R. F. and Clark, R. N. (1999). Spectroscopic determination of leaf biochemistry using band-depth analysis of absorption features and stepwise multiple linear regression. *Remote Sensing of Environment*, *67*: 267-287.

Kokaly, R. F., Despain, D. G., Clark, R. N. and Livo, K. E. (2003). Mapping vegetation in Yellowstone National Park using spectral feature analysis of AVIRIS data. *Remote Sensing of Environment*, *84*(3): 437-456.

Kraft, M., Weigel, H., Mejer, G. and Brandes, F. (1996). Reflectance measurements of leaves for detecting visible and non-visible ozone damage to crops. *Journal of plant physiology*, *148*(148-154).

Kruse, F. A., Lefkoff, A. B., Boardman, J. W., Heidebrecht, K. B., Shapiro, A. T., Barloon, P. J. and Goetz, A. F. H. (1993). The spectral image processing system (SIPS)--interactive visualization and analysis of imaging spectrometer data. *Remote Sensing of Environment*, *44*(2-3): 145-163.

Kruse, F. A., Richardson, L. L., and Ambrosia, V. G., (1997). Techniques developed for geologic analysis of hyperspectral data applied to near-shore hyperspectral ocean data. *Proceedings of the Fourth International Conference on Remote Sensing for Marine and Coastal Environments. 1,* (pp. 233-246) Orlando, Florida.

Kullback, S. (1959). *Information theory and Statistics*. N.Y., John Wiley and Sons.

Kumar, L. and Skidmore, A. K. (1998). Use of derivative spectroscopy to identify regions of difference between some Australian eucalypt species. *Proceedings of the 9th Australasian Remote Sensing and Photogrammetry Conference.* (pp. Sydney, Australia.

Lacaze, B. and Joffre, R. (1994). Extracting biochemical information from visible and near infrared reflectance spectroscopy of fresh and dried leaves. *Journal of plant physiology*, *144*(3): 277-281.

Lass, L. W., Thill, D. C., Shafii, B. and Prather, T. S. (2002). Detecting Spotted Knapweed (*Centaurea maculosa*) with Hyperspectral Remote Sensing Technology. *Weed Technology*, *16*(2): 426-432.

Lehmann, E. L. (1998). *Nonparametrics: statistical methods based on ranks*, Upper Saddle River, Prentice Hall

Lepart, J. & Debussche, M. (1992). Human impact on landscape patterning: Mediterranean examples. In A. J. Handsen & F. di Castri (Ed.), *Landscape Boundaries, Consequences for Biotic Diversity and Ecological Flows.* (pp. 76–106) New York, NY: Springer.

Lepš, J., Osbornová-Kosinová, J. and Rejmánek, M. (1982). Community stability, complexity and species life history strategies. *Vegetatio*, *50*: 53–63.

Lewis, M. M. (1998). Numerical classification as an aid to spectral mapping of vegetation communities. *Plant Ecology*, *136*: 133-149.

Lewis, M. M. (2001). Mapping arid landscapes with multispectral and hyperspectral imagery. *Proceedings of the Geoscience and Remote Sensing Symposium. 6,* (pp. 2902-2904) Sydney, NSW, Australia. IGARSS '01, IEEE 2001 International

Martin, M. E., Newman, S. D., Aber, J. D. and Congalton, J. C. (1998). Determining forest species composition using high spectral resolution remote sensing data. *Remote Sensing of Environment*, *65*: 249–254.

Martin, M. E., Newman, S. D., Aber, J. D. and Congalton, J. C. (1998). Determining forest species composition using high spectral resolution remote sensing data. *Remote Sensing of Environment*, *65*: 249–254.

McGwire, K., Minor, T. and Fenstermaker, L. (2000). Hyperspectral mixture modeling for quantifying sparse vegetation cover in arid environments. *Remote Sensing of Environment*, *72*: 360–374.

Merzlyak, M. N., Gitelson, A. A., Chivkunova, O. B. and Rakitin, V. Y. (1999). Non-destructive optical changes during leaf senescence and fruit ripening. *Physiologia Plantarum*, *106*: 135-141.

Miller, J. R., Wu, J., Boyer, M. G., Belanger, M. and Hare, E. W. (1991). Seasonal patterns in leaf reflectance red-edge characteristics. *International Journal of Remote Sensing*, *12*(7): 1509-1523.

Minekawa, Y., Uto, K., Kosaka, N., Kosugi, Y., Ho, A., Sasaki, Y., Oda, K., Mori, S. and Saito, G. (2005). Salt-damaged paddy fields analyses using high-spatial-resolution hyperspectral imaging system. *Proceedings of the Geoscience and Remote Sensing Symposium, 2005. IGARSS '05. Proceedings. 2005 IEEE International. 3,* (pp. 2153-2156) Seoul, Korea.

Moore, D. S. and McCabe, G. P. (2003). *Introduction to the practice of statistics*. New York, W. H. Freeman and Company.

Moulin, S., Kergoat, L., Viovy, N. and Dedieu, G. G. (1997). Global-scale assessment of vegetation phenology using NOAA/AVHRR satellite measurements. *Journal of Climate*, *10*: 1154-1170.

Mundt, J. T., Glenn, N. F., Weber, K. T., Prather, T. S., Lass, L. W. and Pettingill, J. (2005). Discrimination of hoary cress and determination of its detection limits via hyperspectral image processing and accuracy assessment techniques. *Remote Sensing of Environment*, *96*(3-4): 509-517.

Murwira, A. and Skidmore, K. A. (2006). Monitoring change in the spatial heterogeneity of vegetation cover in an African savanna. *International Journal of Remote Sensing*, *27*(11): 2255-2269.

Mutanga, O. and Skidmore, A. (2004). Narrow band vegetation indices overcome the saturation problem in biomass estimation. *International Journal of Remote Sensing*, *25*: 1-16.

Mutanga, O. and Skidmore, A. K. (2004). Integrating imaging spectroscopy and neural networks to map grass quality in the Kruger National Park, South Africa. *Remote Sensing of Environment*, *90*(1): 104-115.

Mutanga, O., Skidmore, A. K. and van Wieren, S. (2003). Discriminating tropical grass (Cenchrus ciliaris) canopies grown under different nitrogen treatments using spectroradiometry. *ISPRS Journal of Photogrammetry and Remote Sensing*, *57*(4): 263-272.

Mutanga, O., Skidmore, A. K. and Prins, H. H. T. (2004). Predicting in situ pasture quality in the Kruger National Park, South Africa, using continuum-removed absorption features. *Remote Sensing of Environment*, *89*(3): 393-408.

Nagendra, H. (2002). Using remote sensing to assess biodiversity. *International Journal of Remote Sensing*, *22*(12): 2377–2400.

Naveh, Z. (1991). Mediterranean uplands as anthropogenic perturbation-dependent system and their dynamic conservation management. Terrestrial and aquatic ecosystems: perturbation and recovery. O. Ravera. New York, Ellis Horwood**:** 544-556.

Naveh, Z. and Lieberman, A. (1994). *Landscape ecology: Theory and application*. New York, Springer-Verlag.

Ne'eman, G. and Izhaki, I. (1996). Colonization in abandoned east Mediterranean vineyard. *Journal of Vegetation Science*, *7*: 465-472.

Noomen, M. F., Skidmore, A. K., van der Meer, F. D. and Prins, H. H. T. (2006). Continuum removed band depth analysis for detecting the effects of natural gas, methane and ethane on maize reflectance. *Remote Sensing of Environment*, *105*(3): 262-270.

Novo, M. E. and Shimabukuro, E. Y. (1997). Identification and mapping of the Amazon habitats using a mixing model. *International Journal of Remote Sensing*, *18*(3): 663-670.

Page, T., Griffiths, G. and Buchanan-Wollaston, V. (2001). Molecular and Biochemical Characterization of Postharvest Senescence in Broccoli. *Plant Physiology*, *125*: 718-727.

Parker Williams, A. and Hunt, E. R. (2002). Estimation of leafy spurge cover from hyperspectral imagery using mixture tuned matched filtering. *Remote Sensing of Environment*, *82*(2-3): 446-456.

Parker Williams, A. and Hunt, E. R. (2004). Accuracy assessment for detection of leafy spurge with hyperspectral imagery. *Rangeland Ecology and Management*, *57*(1): 106-112.

Peñuelas, J., Baret, F. and Filella, I. (1995). Semi-empirical indices to assess carotenoid/chlorophyll a ratio from leaf spectral reflectance. *Photosynthetica*, *31*(2): 221-230.

Peñuelas, J., Field, C. B., Griffin, K. and Gamon, J. A. (1993). Assessing community type, plant biomass, pigment composition and photosynthetic efficiency of aquatic vegetation from spectral reflectance. *Remote Sensing of Environment*, *46*: 110-118.

Peñuelas, J., Filella, I., Lioret, P., Muñoz, F. and Vilajeliu, M. (1995). Reflectance assessment of mite effects on apple trees. *International Journal of Remote Sensing*, *16*: 2727-2733.

Peñuelas, J., Gamon, J. A., Fredeen, A. L., Merino, J. and Field, C. B. (1994). Reflectance indices associated with physiological changes in nitrogen- and water-limited sunflower leaves. *Remote Sensing of Environment*, *48*: 135-146.

Peñuelas, J., Pinol, J., Ogaya, R. and Filella, I. (1997). Estimation of plant water concentration by the reflectance Water Index WI (R900/R970). *International Journal of Remote Sensing*, *18*(13): 2869-2875.

Petzold, D. E. and Goward, S. N. (1988). Reflectance spectra of subarctic lichens. *Remote Sensing of Environment*, *24*(3): 481-492.

Pickett, S. T. A. (1976). Succession: an evolutionary interpretation. *American Naturalist*, *110*: 107-119.

Portigal, F., Holasek, R., Mooradian, G., Owensby, P., Dicksion, M., Fene, M., Elliot, M., Hall, E. and Driggett, D. (1997). Vegetation classification using red-edge first derivative and green peak statistical moment indices with the Advanced Airborne Hyperspectral Imaging System (AAHIS). *Proceedings of the Third International Airborne Remote Sensing Conference and Exhibition*, *Copenhagen, Denmark, 7-10 July 1997.vol. II (Ann Arbor, MI: ERIM)*, (pp. 789-797)

Prévosto, B. and Curt, T. (2004). Dimensional relationships of naturally established European beech trees beneath Scots pine and Silver birch canopy. *Forest Ecology and Management*, *194*: 335-348.

Price, J. C. (1994). How unique are spectral signatures? *Remote Sensing of Environment*, *49*: 181-186.

Prins, H. H. T. and Gordon, I. (2007). Grazers and browsers in a changing world. In I. Gordon and H. H. T. Prins (Ed.), *Ecology of Grazers and Browsers.* Ecological Studies -195. New York: Springer.

Prins, H. H. T. and Loth, P. E. (1988). Rainfall Patterns as Background to Plant Phenology in Northern Tanzania. *Journal of Biogeography*, *15*(3): 451-463.

Qi, J., Moran, M. S., Cabot, F. and Dedieu, G. (1995). Normalization of sun/view angle effects using spectral albedo-based vegetation indices. *Remote Sensing of Environment*, *52*(3): 207-217.

Quattrochi, D. A. and Pelletier, R. E. (1991). Remote sensing for analysis of landscapes: an introduction. In M. G. Turner and R. H. Gardner (Ed.), *Quentitative methods in landscape ecology*. (pp. 51-76) New York: Springer-Verlag.

Ramsey III, E. W. and Jensen, J. R. (1996). Remote sensing of Mangrove wetlands: relating canopy spectra to site-specific data. *Photogrammetric Engineering and Remote Sensing*, *62*(8): 939-948.

Ramsey III, E. W., Rangoonwala, A., Nelson, G., Ehrlich, R. and Martella, K. (2005). Generation and validation of characteristic spectra from EO1 Hyperion image data for detecting the occurrence of the invasive species, Chinese tallow. *International Journal of Remote Sensing*, *26*: 1611-1636.

Reed, B. C., Brown, J. F., VanderZee, D., Loveland, T. R., Merchant, J. W. and Ohlen, D. O. (1994). Measuring Phenological Variability from Satellite Imagery *Journal of Vegetation Science*, *5*(5): 703-714.

Reidsma, P., Tekelenburg, T., van den Berg, M. and Alkemade, R. (2006). Impacts of the land-use change on biodiversity: An assessment of agricultural biodiversity in the European Union. *Agriculture, Ecosystems and Environment*, *114*: 86-102.

Resmini, R. G., Kappus, M. E., Aldrich, W. S., Harsanyi, J. C. and Anderson, M. (1997). Mineral mapping with HYperspectral Digital Imagery Collection Experiment (HYDICE) sensor data at Cuprite, Nevada, U.S.A. *International Journal of Remote Sensing*, *18*(7): 1553-1570.

Richardson, A. D. and Berlyn, G. P. (2002). Changes in foliar spectral reflectance and chlorophyll fluorescence of four temperate species following branch cutting. *Tree Physiology*, *22*: 499-506.

Roberts, D. A., Gardner, M., Church, R., Ustin, S., Scheer, G. and Green, R. O. (1998). Mapping chaparral in the Santa Monica mountains using multiple endmember spectral mixture models. *Remote Sensing of Environment*, *65*(267– 279).

Roberts, D. A., Nelson, B. W., Adams, J. B. and Palmer, F. (1998). Spectral changes with leaf aging in Amazon caatinga. *Trees*, *12*: 315-325.

Roberts, D. A., Smith, M. O. and Adams, J. B. (1993). Green vegetation, nonphotosynthetic vegetation and soils in AVIRIS data. *Remote Sensing of Environment 44*: 255–269.

Robichaud, P. R., Lewis, S. A., Laes, D. Y. M., Hudak, A. T., Kokaly, R. F. and Zamudio, J. A. (2007). Postfire soil burn severity mapping with hyperspectral image unmixing. *Remote Sensing of Environment*, *108*(4): 467-480.

Rock, B. N., Lauten, G. N. and Moss, D. N. (1993). High-spectral resolution reflectance measurements of red spruce and eastern hemlock foliage over a growing season. *Ground Sensing SPIE*, *vol. 1941*: 1-12.

Rock, B. N., Vogelmann, J. E., Williams, D. L., Vogelmann, A. F. and Hoshizaki, T. (1986). Remote Detection of Forest Damage. *BioScience*, *36*(7): 439-445.

Rouse, J. W., Haas, R. H., Schell, J. A. and Deering, D. W. (1973). Monitoring vegetation systems in the Great Plains with ERTS. *Proceedings of the Third ERTS Symposium. 1,* (pp. 309-317) Washington DC. NASA SP-351,

Sabol, D. E., Adams, J. B. and Smith, M. O. (1992). Quantitative sub-pixel spectral detection of targets in multispectral images. *Journal of Geophysical Research*, *97*: 2659-2672.

Saïd, S. (2001). Floristic and life form diversity in post-pasture successions on a Mediterranean island (Corsica). *Plant Ecology*, *162*(1): 67-76.

Salvador, R. (2000). An assessment of the spatial variability of basal area in a terrain covered by Mediterranean woodlands. *Agriculture, Ecosystems and Environment*, *81*(1): 17-28.

Satterwhite, M. B. and Ponder Henley, J. (1987). Spectral characteristics of selected soils and vegetation in Northern Nevada and their discrimination using band ratio techniques. *Remote Sensing of Environment*, *23*(2): 155-175.

Savitzky, A. and Golay, M. J. E. (1964). Smoothing and differentiation of data by simplified least-squares procedures. *Analytical Chemistry*, *36*(8): 1627-1639.

Schmidt, K. S. and Skidmore, A. K. (2001). Exploring spectral discrimination of grass species in African rangelands. *International Journal of Remote Sensing*, *22*(17): 3421 - 3434.

Schmidt, K. S. and Skidmore, A. K. (2003). Spectral discrimination of vegetation types in a coastal wetland. *Remote Sensing of Environment*, *85*(1): 92-108.

Schmidt, K. S. and Skidmore, A. K. (2004). Smoothing vegetation spectra with wavelets. *International Journal of Remote Sensing*, *25*(6): 1167-1184.

Schmidt, K. S., Skidmore, A. K., Kloosterman, E. H., Van Oosten, H., Kumar, L. and Janssen, J. A. M. (2004). Mapping Coastal Vegetation Using an Expert System and Hyperspectral Imagery. *Photogrammetric Engineering and Remote Sensing*, *70*(6): 703-715.

Scurlock, J. M. O. & Prince, S. D. (1993). Remote sensing of biomass and productivity. In D. O. Hall, J. M. O. Scurlock & H. R. Bolhar-Nordenkampf (Ed.), *Photosynthesis and production in a changing*

environment: A field and laboratory manual. (pp. 23-46) London: Chapman & Hall.

Seixas, J. (2000). Assessing heterogeneity from remote sensing images: the case of desertification in southern Portugal. *International Journal of Remote Sensing*, *21*: 2645–2663.

Seller, P. J. (1985). Canopy reflectance, photosynthesis and transpiration. *International Journal of Remote Sensing*, *6*(8): 1335-1372.

Siedlecki, W. and Sklansky, J. (1989). A note on genetic algorithms for largesale feature selection. *Pattern Recognition Letters*, *10*: 335-347.

Silvestri, S., Marani, M. and Marani, A. (2003). Hyperspectral remote sensing of salt marsh vegetation, morphology and soil topography. *Physics and Chemistry of the Earth, Parts A/B/C*, *28*(1-3): 15-25.

Sims, D. A. and Gamon, J. A. (2002). Relationships between leaf pigment content and spectral reflectance across a wide range of species, leaf structures and developmental stages. *Remote Sensing of Environment*, *81*(2-3): 337-354.

Skidmore, A.K., Wood, G.B. and K.R. Shepherd. (1987). Remotely sensed digital data in forestry: A Review. *Australian Forestry* 50:40-53.

Skidmore, A.K., and Knowles, E. (1996). Neural networks for image processing*. Proceedings of the 8th Australasian remote sensing conference ARSC* (Vol. 2, pp. 169 - 174). Canberra, Australia.

Smith, K. L., Steven, M. D. and Colls, J. J. (2004). Use of hyperspectral derivative ratios in the red-edge region to identify plant stress responses to gas leaks. *Remote Sensing of Environment*, *92*(2): 207-217.

Smith, M. O., Ustin, S. L., Adams, J. B. and Gillespie, A. R. (1990). Vegetation in deserts: I. A regional measure of abundance from multispectral images. *Remote Sensing of Environment*, *31*: 1–26.

Soukupová, J., Rock , B. N. and Albrechtova, J. (2002). Spectral characteristics of lignin and soluble phenolics in the near infrared- a comparative study. *International Journal of Remote Sensing*, *23*(15): 3039-3055.

Suits, G. H. (1983). The nature of electromagnetic radiation. In R. N. Colwell (Ed.), *Manual of Remote Sensing, Volume 1.* (pp. Falls Church, Virginia: ASPRS.

Swain, P. H. and Davis, S. M. (1978). *Remote sensing: the quantitative approach*. New York, McGraw-Hill.

Tatoni, T. and Roche, P. (1994). Comparison of old-field and forest revegetation dynamics in provence. *Journal of Vegetation Science*, *5*: 295–302.

Tatoni, T., Magnin, F., Bonin, G. and Vaudour, J. (1994). Secondary successions on abandoned cultivation terraces in calcareous provence. I—vegetation and soil. *Acta Oecologica*, *15*(4): 431–447.

Thenkabail, P. S., Enclona, E. A., Ashton, M. S. and Van Der Meer, B. (2004). Accuracy assessments of hyperspectral waveband performance for vegetation analysis applications. *Remote Sensing of Environment*, *91*(3-4): 354-376.

Thenkabail, P. S., Smith, R. B. and De Pauw, E. (2000). Hyperspectral vegetation indices and their relationship with agricultural crop characteristics. *Remote Sensing of Environment*, *71*: 158-182.

Thenkabail, P. S., Smith, R. B. and De Pauw, E. (2002). Evaluation of narrowband and broadband vegetation indices for determining optimal hyperspectral wavebands for agricultural crop characterization. *Photogrammetric Engineering and Remote Sensing*, *68*(6): 607-621.

Thomas, J. R. and Gaussman, H. W. (1987). Leaf reflectance vs leaf chlorophyll and carotenoid concentration for eight crops. *Journal of Agronomy*, *69*(799-802).

Tilman, D. (1985). The resource-ratio hypothesis of plant succession. *American Naturalist*, *125*: 827-852.

Todd, W. S., Hoffer, M. R. and Milchunas, G. D. (1998). Biomass estimation on grazed and ungrazed rangelands using spectral indices. *International Journal of Remote Sensing*, *19*(3): 427-438.

Tucker, C. J. (1979). Red and photographic infrared linear combinations for monitoring vegetation. *Remote Sensing of Environment*, *8*(2): 127-150.

Turner, M. G. (1989). Landscape ecology: The effect of pattern on process. *Annual Review of Ecology and Systematics*, *20*: 171-197.

Turner, W., Spector, S., Gardiner, N., Fladeland, M., Sterling, E. and Steininger, M. (2003). Remote sensing for biodiversity science and conservation. *TRENDS in Ecology and Evolution*, *18*(6): 306-314.

Underwood, E., Ustin, S. and DiPietro, D. (2003). Mapping non-native plants using hyperspectral imagery. *Remote Sensing of Environment*, *86*(2): 150-161.

Vaiphasa, C. (2003). Innovative genetic algorithm for hyperspectral image classification. *Proceedings of the International Conference Map Asia, Map Asia. vol. 20*.

Vaiphasa, C., Ongsomwangc, S., Vaiphasa, T. and Skidmore, A. K. (2005). Tropical mangrove species discrimination using hyperspectral data: a laboratory study. *Estuarine, Costal and Shelf Science*, *65*: 371-379.

van der Maarel, E. (1993). Some remarks on disturbance and its relations to diversity and stability. *Journal of Vegetation Science*, *4*: 733–736.

van der Meer, F. and Bakker, W. (1997). Cross correlogram spectral matching: Application to surface mineralogical mapping by using AVIRIS data from Cuprite, Nevada. *Remote Sensing of Environment*, *61*(3): 371-382.

van der Meer, F. (2006). The effectiveness of spectral similarity measures for the analysis of hyperspectral imagery. *International Journal of Applied Earth Observation and Geoinformation*, *8*(1): 3-17.

van der Putten, W. H., Mortimer, S. R., Hedlund, K., van Dijk, C., Brown, V. K., Lepä, J., Rodriguez-Barrueco, C., Roy, J., Diaz Len, T. A., Gormsen, D., Korthals, G. W., Lavorel, S., Santa Regina, I. and Smilauer, P. (2000). Plant species diversity as a driver of early succession in abandoned fields: a multi-site approach. *Oecologia*, *124*: 91-99.

Verbyla, D. L. (1995). *Satellite Remote Sensing of Natural Resources*. New York, Lewis Publishers.

Verdebout, J., Jacquemoud, S. and Schmuck, G. (1994). Optical properties of leaves: modelling and experimental studies. In J. L. Hill and J. Megier (eds.), *Imaging Spectrometry - a Tool for Environmental Observations*. (pp. 169-191). Brussels and Luxembourg, Printed in the Netherlands: ECSC, EEC, EAEC.

Verdú, J. R., Crespo, M. B. and Galante, E. (2000). Conservation strategy of a nature reserve in Mediterranean ecosystems: the effects of protection

from grazing on biodiversity. *Biodiversity and Conservation*, *9*(12): 1707-1721.

Vinogradov, B. V. (1977). Remote sensing in ecological botany. *Remote Sensing of Environment*, *6*(2): 83-94.

Westman, W. E. and Price, C. V. (1987). Remote detection of air pollution stress to vegetation: laboratory level studies. *Proceedings of the International Geoscience and Remote Sensing Symposium*, *MI, 18-21 May 1987.vol.* (pp. 451-456)

Wikipedia, (2007). http://en.wikipedia.org/wiki/Phenology, accessed on March 2007.

Yamano, H., Chen, J. and Tamura, M. (2003). Hyperspectral identification of grassland vegetation in Xilinhot, Inner Mongolia, China. *International Journal of Remote Sensing*, *24*(15): 3171-3178.

Yoder, B. J. and Pettigrew-Crosby, R. E. (1995). Predicting nitrogen and chlorophyll content and concentrations from reflectance spectra (400–2500 nm) at leaf and canopy scales. *Remote Sensing of Environment*, *53*: 199-211.

Yu, S., de Backer, S. and Scheunders, P. (2002). Genetic feature selection combined with composite fuzzy nearest neighbour classifiers for hyperspectral satellite imagery. *Pattern Recognition Letters*, *23*: 183-190.

Yuhas, R. H., Goetz, F. H. A., and Boardmann, J. W., Ed. (1992). Discrimination among semiarid landscape endmembers using the Spectral Angle Mapper (SAM) algorithm. *In Summaries of the Third Annual JPL Airborne Geoscience Workshop*. Pasadena, CA, JPL publication.

Zarco-Tejada, P. J., Berjon, A., Lopez-Lozano, R., Miller, J. R., Martin, P., Cachorro, V., Gonzalez, M. R. and de Frutos, A. (2005). Assessing vineyard condition with hyperspectral indices: Leaf and canopy reflectance simulation in a row-structured discontinuous canopy. *Remote Sensing of Environment*, *99*(3): 271-287.

Zarco-Tejada, P. J., Pushnik, J. C., Dobrowski, S. and Ustin, S. L. (2003). Steady state chlorophyll a fluorescence detection from canopy derivative reflectance and double-peak red-edge effects. *Remote Sensing of Environment*, *84*(2): 283-294.

Zhang, X., Friedl, M. A., Schaaf, C. B., Strahler, A. H., Hodges, J. C. F., Gao, F., Reed, B. C. and Huete, A. (2003). Monitoring vegetation phenology using MODIS. *Remote Sensing of Environment*, *84*(3): 471-475.

Zonneveld, I. S. (1974). Aerial photography, remote sensing and ecology. *ITC Journal*, *4*: 553-560.

Author's Biography

Md. Istiak Sobhan was born on the 3rd of December 1964 in Barisal, Bangladesh. In 1985 he obtained Bachelor degree with honours in Botany and in 1986 he acquired Master's degree on plant genetics from University of Dhaka. He worked as research assistant in biotechnology research centre in the University of Dhaka from 1987 to 1989. In 1989 he joined NACOM (Nature Conservation Movement), a national NGO dedicated to nature conservation. From 1992 he started working as a consultant ecologist in Flood Action Plan. In 1997 he joined IUCN as wetland officer. But in the same year he obtained NFP scholarship to pursue another Master's degree in Environmental System Analysis and Monitoring at ITC. In 1999 he obtained his MSc degree (with distinction). His MSc thesis was entitled "Spatial Distribution of Southern African Woodland Species Using GIS Models". He went back to join Center for Environmental and Geographic Information Services (CEGIS), a public trust under ministry of water resources as Senior Ecologist. In April 2003, he was awarded a scholarship by Nuffic to pursue a PhD degree at ITC and Wageningen University in The Netherlands.

ITC Dissertation list

1. **Akinyede** (1990), Highway cost modelling and route selection using a geotechnical information system
2. **Pan He Ping** (1990), 90-9003-757-8, Spatial structure theory in machine vision and applications to structural and textural analysis of remotely sensed images
3. **Bocco Verdinelli, G.** (1990), Gully erosion analysis using remote sensing and geographic information systems: a case study in Central Mexico
4. **Sharif, M**. (1991), Composite sampling optimization for DTM in the context of GIS
5. **Drummond, J.** (1991), Determining and processing quality parameters in geographic information systems
6. **Groten, S.** (1991), Satellite monitoring of agro-ecosystems in the Sahel
7. **Sharifi, A.** (1991), 90-6164-074-1, Development of an appropriate resource information system to support agricultural management at farm enterprise level
8. **Zee, D. van der** (1991), 90-6164-075-X, Recreation studied from above: Air photo interpretation as input into land evaluation for recreation
9. **Mannaerts, C.** (1991), 90-6164-085-7, Assessment of the transferability of laboratory rainfall-runoff and rainfall - soil loss relationships to field and catchment scales: a study in the Cape Verde Islands
10. **Ze Shen Wang** (1991), 90-393-0333-9, An expert system for cartographic symbol design
11. **Zhou Yunxian** (1991), 90-6164-081-4, Application of Radon transforms to the processing of airborne geophysical data
12. **Zuviria, M. de** (1992), 90-6164-077-6, Mapping agro-topoclimates by integrating topographic, meteorological and land ecological data in a geographic information system: a case study of the Lom Sak area, North Central Thailand
13. **Westen, C. van** (1993), 90-6164-078-4, Application of Geographic Information Systems to landslide hazard zonation
14. **Shi Wenzhong** (1994), 90-6164-099-7, Modelling positional and thematic uncertainties in integration of remote sensing and geographic information systems
15. **Javelosa, R.** (1994), 90-6164-086-5, Active Quaternary environments in the Philippine mobile belt
16. **Lo King-Chang** (1994), 90-9006526-1, High Quality Automatic DEM, Digital Elevation Model Generation from Multiple Imagery
17. **Wokabi, S.** (1994), 90-6164-102-0, Quantified land evaluation for maize yield gap analysis at three sites on the eastern slope of Mt. Kenya
18. **Rodriguez, O.** (1995), Land Use conflicts and planning strategies in urban fringes: a case study of Western Caracas, Venezuela
19. **Meer, F. van der** (1995), 90-5485-385-9, Imaging spectrometry & the Ronda peridotites

20. **Kufoniyi, O.** (1995), 90-6164-105-5, Spatial coincidence: automated database updating and data consistency in vector GIS
21. **Zambezi, P.** (1995), Geochemistry of the Nkombwa Hill carbonatite complex of Isoka District, north-east Zambia, with special emphasis on economic minerals
22. **Woldai, T.** (1995), The application of remote sensing to the study of the geology and structure of the Carboniferous in the Calañas area, pyrite belt, SW Spain
23. **Verweij, P.** (1995), 90-6164-109-8, Spatial and temporal modelling of vegetation patterns: burning and grazing in the Paramo of Los Nevados National Park, Colombia
24. **Pohl, C.** (1996), 90-6164-121-7, Geometric Aspects of Multisensor Image Fusion for Topographic Map Updating in the Humid Tropics
25. **Jiang Bin** (1996), 90-6266-128-9, Fuzzy overlay analysis and visualization in GIS
26. **Metternicht, G.** (1996), 90-6164-118-7, Detecting and monitoring land degradation features and processes in the Cochabamba Valleys, Bolivia. A synergistic approach
27. **Hoanh Chu Thai** (1996), 90-6164-120-9, Development of a Computerized Aid to Integrated Land Use Planning (CAILUP) at regional level in irrigated areas: a case study for the Quan Lo Phung Hiep region in the Mekong Delta, Vietnam
28. **Roshannejad, A.** (1996), 90-9009-284-6, The management of spatio-temporal data in a national geographic information system
29. **Terlien, M.** (1996), 90-6164-115-2, Modelling Spatial and Temporal Variations in Rainfall-Triggered Landslides: the integration of hydrologic models, slope stability models and GIS for the hazard zonation of rainfall-triggered landslides with examples from Manizales, Colombia
30. **Mahavir, J.** (1996), 90-6164-117-9, Modelling settlement patterns for metropolitan regions: inputs from remote sensing
31. **Al-Amir, S.** (1996), 90-6164-116-0, Modern spatial planning practice as supported by the multi-applicable tools of remote sensing and GIS: the Syrian case
32. **Pilouk, M.** (1996), 90-6164-122-5, Integrated modelling for 3D GIS
33. **Duan Zengshan** (1996), 90-6164-123-3, Optimization modelling of a river-aquifer system with technical interventions: a case study for the Huangshui river and the coastal aquifer, Shandong, China
34. **Man, W.H. de** (1996), 90-9009-775-9, Surveys: informatie als norm: een verkenning van de institutionalisering van dorp - surveys in Thailand en op de Filippijnen
35. **Vekerdy, Z.** (1996), 90-6164-119-5, GIS-based hydrological modelling of alluvial regions: using the example of the Kisaföld, Hungary
36. **Pereira, Luisa** (1996), 90-407-1385-5, A Robust and Adaptive Matching Procedure for Automatic Modelling of Terrain Relief
37. **Fandino Lozano, M.** (1996), 90-6164-129-2, A Framework of Ecological Evaluation oriented at the Establishment and Management of Protected Areas: a case study of the Santuario de Iguaque, Colombia
38. **Toxopeus, B.** (1996), 90-6164-126-8, ISM: an Interactive Spatial and temporal Modelling system as a tool in ecosystem management: with two case studies: Cibodas biosphere reserve, West Java Indonesia: Amboseli biosphere reserve, Kajiado district, Central Southern Kenya

39. **Wang Yiman** (1997), 90-6164-131-4, Satellite SAR imagery for topographic mapping of tidal flat areas in the Dutch Wadden Sea
40. **Saldana-Lopez, Asunción** (1997), 90-6164-133-0, Complexity of soils and Soilscape patterns on the southern slopes of the Ayllon Range, central Spain: a GIS assisted modelling approach
41. **Ceccarelli, T.** (1997), 90-6164-135-7, Towards a planning support system for communal areas in the Zambezi valley, Zimbabwe; a multi-criteria evaluation linking farm household analysis, land evaluation and geographic information systems
42. **Peng Wanning** (1997), 90-6164-134-9, Automated generalization in GIS
43. **Lawas, C.** (1997), 90-6164-137-3, The Resource Users' Knowledge, the neglected input in Land resource management: the case of the Kankanaey farmers in Benguet, Philippines
44. **Bijker, W.** (1997), 90-6164-139-X, Radar for rain forest: A monitoring system for land cover Change in the Colombian Amazon
45. **Farshad, A.** (1997), 90-6164-142-X, Analysis of integrated land and water management practices within different agricultural systems under semi-arid conditions of Iran and evaluation of their sustainability
46. **Orlic, B.** (1997), 90-6164-140-3, Predicting subsurface conditions for geotechnical modelling
47. **Bishr, Y.** (1997), 90-6164-141-1, Semantic Aspects of Interoperable GIS
48. **Zhang Xiangmin** (1998), 90-6164-144-6, Coal fires in Northwest China: detection, monitoring and prediction using remote sensing data
49. **Gens, R.** (1998), 90-6164-155-1, Quality assessment of SAR interferometric data
50. **Turkstra, J.** (1998), 90-6164-147-0, Urban development and geographical information: spatial and temporal patterns of urban development and land values using integrated geo-data, Villaviciencia, Colombia
51. **Cassells, C.** (1998), 90-6164-234-5, Thermal modelling of underground coal fires in northern China
52. **Naseri, M.** (1998), 90-6164-195-0, Characterization of Salt-affected Soils for Modelling Sustainable Land Management in Semi-arid Environment: a case study in the Gorgan Region, Northeast, Iran
53. **Gorte B.G.H.** (1998), 90-6164-157-8, Probabilistic Segmentation of Remotely Sensed Images
54. **Tegaye, Tenalem Ayenew** (1998), 90-6164-158-6, The hydrological system of the lake district basin, central main Ethiopian rift
55. **Wang Donggen** (1998), 90-6864-551-7, Conjoint approaches to developing activity-based models
56. **Bastidas de Calderon, M.** (1998), 90-6164-193-4, Environmental fragility and vulnerability of Amazonian landscapes and ecosystems in the middle Orinoco river basin, Venezuela
57. **Moameni, A.** (1999), Soil quality changes under long-term wheat cultivation in the Marvdasht plain, South-Central Iran
58. **Groenigen, J.W. van** (1999), 90-6164-156-X, Constrained optimisation of spatial sampling: a geostatistical approach
59. **Cheng Tao** (1999), 90-6164-164-0, A process-oriented data model for fuzzy spatial objects

60. **Wolski, Piotr** (1999), 90-6164-165-9, Application of reservoir modelling to hydrotopes identified by remote sensing
61. **Acharya, B.** (1999), 90-6164-168-3, Forest biodiversity assessment: A spatial analysis of tree species diversity in Nepal
62. **Akbar Abkar, Ali** (1999), 90-6164-169-1, Likelihood-based segmentation and classification of remotely sensed images
63. **Yanuariadi, T.** (1999), 90-5808-082-X, Sustainable Land Allocation: GIS-based decision support for industrial forest plantation development in Indonesia
64. **Abu Bakr**, **Mohamed** (1999), 90-6164-170-5, An Integrated Agro-Economic and Agro-Ecological Framework for Land Use Planning and Policy Analysis
65. **Eleveld, M.** (1999), 90-6461-166-7, Exploring coastal morphodynamics of Ameland (The Netherlands) with remote sensing monitoring techniques and dynamic modelling in GIS
66. **Yang Hong** (1999), 90-6164-172-1, Imaging Spectrometry for Hydrocarbon Microseepage
67. **Mainam, Félix** (1999), 90-6164-179-9, Modelling soil erodibility in the semiarid zone of Cameroon
68. **Bakr, Mahmoud** (2000), 90-6164-176-4, A Stochastic Inverse-Management Approach to Groundwater Quality
69. **Zlatanova, Z.** (2000), 90-6164-178-0, 3D GIS for Urban Development
70. **Ottichilo, Wilber K.** (2000), 90-5808-197-4, Wildlife Dynamics: An Analysis of Change in the Masai Mara Ecosystem
71. **Kaymakci, Nuri** (2000), 90-6164-181-0, Tectono-stratigraphical Evolution of the Cankori Basin (Central Anatolia, Turkey)
72. **Gonzalez, Rhodora** (2000), 90-5808-246-6, Platforms and Terraces: Bridging participation and GIS in joint-learning for watershed management with the Ifugaos of the Philippines
73. **Schetselaar, Ernst** (2000), 90-6164-180-2, Integrated analyses of granite-gneiss terrain from field and multisource remotely sensed data. A case study from the Canadian Shield
74. **Mesgari, Saadi** (2000), 90-3651-511-4, Topological Cell-Tuple Structure for Three-Dimensional Spatial Data
75. **Bie, Cees A.J.M. de** (2000), 90-5808-253-9, Comparative Performance Analysis of Agro-Ecosystems
76. **Khaemba, Wilson M**. (2000), 90-5808-280-6, Spatial Statistics for Natural Resource Management
77. **Shrestha, Dhruba** (2000), 90-6164-189-6, Aspects of erosion and sedimentation in the Nepalese Himalaya: highland-lowland relations
78. **Asadi Haroni, Hooshang** (2000), 90-6164-185-3, The Zarshuran Gold Deposit Model Applied in a Mineral Exploration GIS in Iran
79. **Raza, Ale** (2001), 90-3651-540-8, Object-oriented Temporal GIS for Urban Applications
80. **Farah, Hussein** (2001), 90-5808-331-4, Estimation of regional evaporation under different weather conditions from satellite and meteorological data. A case study in the Naivasha Basin, Kenya
81. **Zheng**, **Ding** (2001), 90-6164-190-X, A Neural - Fuzzy Approach to Linguistic Knowledge Acquisition and Assessment in Spatial Decision Making

82. **Sahu, B.K.** (2001), Aeromagnetics of continental areas flanking the Indian Ocean; with implications for geological correlation and reassembly of Central Gondwana
83. **Alfestawi, Y.** (2001), 90-6164-198-5, The structural, paleogeographical and hydrocarbon systems analysis of the Ghadamis and Murzuq Basins, West Libya, with emphasis on their relation to the intervening Al Qarqaf Arch
84. **Liu, Xuehua** (2001), 90-5808-496-5, Mapping and Modelling the Habitat of Giant Pandas in Foping Nature Reserve, China
85. **Oindo, Boniface Oluoch** (2001), 90-5808-495-7, Spatial Patterns of Species Diversity in Kenya
86. **Carranza, Emmanuel John** (2002), 90-6164-203-5, Geologically-constrained Mineral Potential Mapping
87. **Rugege, Denis** (2002), 90-5808-584-8, Regional Analysis of Maize-Based Land Use Systems for Early Warning Applications
88. **Liu, Yaolin** (2002), 90-5808-648-8, Categorical Database Generalization in GIS
89. **Ogao, Patrick** (2002), 90-6164-206-X, Exploratory Visualization of Temporal Geospatial Data using Animation
90. **Abadi, Abdulbaset M.** (2002), 90-6164-205-1, Tectonics of the Sirt Basin – Inferences from tectonic subsidence analysis, stress inversion and gravity modelling
91. **Geneletti, Davide** (2002), 90-5383-831-7, Ecological Evaluation for Environmental Impact Assessment
92. **Sedogo, Laurent G.** (2002), 90-5808-751-4, Integration of Participatory Local and Regional Planning for Resources Management using Remote Sensing and GIS
93. **Montoya, Lorena** (2002), 90-6164-208-6, Urban Disaster Management: a case study of earthquake risk assessment in Carthago, Costa Rica
94. **Ahmad, Mobin-ud-Din** (2002), 90-5808-761-1, Estimation of Net Groundwater Use in Irrigated River Basins using Geo-information Techniques: A case study in Rechna Doab, Pakistan
95. **Said, Mohammed Yahya** (2003), 90-5808-794-8, Multiscale perspectives of species richness in East Africa
96. **Schmidt, Karin** (2003), 90-5808-830-8, Hyperspectral Remote Sensing of Vegetation Species Distribution in a Saltmarsh
97. **Lopez Binnquist, Citlalli** (2003), 90-3651-900-4, The Endurance of Mexican Amate Paper: Exploring Additional Dimensions to the Sustainable Development Concept
98. **Huang, Zhengdong** (2003), 90-6164-211-6, Data Integration for Urban Transport Planning
99. **Cheng, Jianquan** (2003), 90-6164-212-4, Modelling Spatial and Temporal Urban Growth
100. **Campos dos Santos, Jose Laurindo** (2003), 90-6164-214-0, A Biodiversity Information System in an Open Data/Metadatabase Architecture
101. **Hengl, Tomislav** (2003), 90-5808-896-0, PEDOMETRIC MAPPING, Bridging the gaps between conventional and pedometric approaches

102. **Barrera Bassols, Narciso (**2003), 90-6164-217-5, Symbolism, Knowledge and management of Soil and Land Resources in Indigenous Communities: Ethnopedology at Global, Regional and Local Scales
103. **Zhan, Qingming** (2003), 90-5808-917-7, A Hierarchical Object-Based Approach for Urban Land-Use Classification from Remote Sensing Data
104. **Daag, Arturo S.** (2003), 90-6164-218-3, Modelling the Erosion of Pyroclastic Flow Deposits and the Occurrences of Lahars at Mt. Pinatubo, Philippines
105. **Bacic, Ivan** (2003), 90-5808-902-9, Demand-driven Land Evaluation with case studies in Santa Catarina, Brazil
106. **Murwira, Amon** (2003), 90-5808-951-7, Scale matters! A new approach to quantify spatial heterogeneity for predicting the distribution of wildlife
107. **Mazvimavi, Dominic** (2003), 90-5808-950-9, Estimation of Flow Characteristics of Ungauged Catchments. A case study in Zimbabwe
108. **Tang, Xinming** (2004), 90-6164-220-5, Spatial Object Modelling in Fuzzy Topological Spaces with Applications to Land Cover Change
109. **Kariuki, Patrick** (2004), 90-6164-221-3, Spectroscopy and Swelling Soils; an integrated approach
110. **Morales, Javier** (2004), 90-6164-222-1, Model Driven Methodology for the Design of Geo-information Services
111. **Mutanga, Onisimo** (2004), 90-5808-981-9, Hyperspectral Remote Sensing of Tropical Grass Quality and Quantity
112. **Šliužas, Ričardas V.** (2004), 90-6164-223-X, Managing Informal Settlements: a study using geo-information in Dar es Salaam, Tanzania
113. **Lucieer, Arko** (2004), 90-6164-225-6, Uncertainties in Segmentation and their Visualisation
114. **Corsi, Fabio** (2004), 90-8504-090-6, Applications of existing biodiversity information: Capacity to support decision-making
115. **Tuladhar, Arbind** (2004), 90-6164-224-8, Parcel-based Geo-information System: Concepts and Guidelines
116. **Elzakker, Corné van** (2004), 90-6809-365-7, The use of maps in the exploration of geographic data
117. **Nidumolu, Uday Bhaskar** (2004), 90-8504-138-4, Integrating Geo-information models with participatory approaches: applications in land use analysis
118. **Koua, Etien L.** (2005), 90-6164-229-9, Computational and Visual Support for Exploratory Geovisualization and Knowledge Construction
119. **Blok, Connie A.** (2005), Dynamic visualization variables in animation to support monitoring of spatial phenomena
120. **Meratnia, Nirvana** (2005), 90-365-2152-1, Towards Database Support for Moving Object Data
121. **Yemefack, Martin** (2005), 90-6164-233-7, Modelling and monitoring Soil and Land Use Dynamics within Shifting Agricultural Landscape Mosaic Systems
122. **Kheirkhah, Masoud** (2005), 90-8504-256-9, Decision support system for floodwater spreading site selection in Iran
123. **Nangendo, Grace** (2005), 90-8504-200-3, Changing forest-woodland-savanna mosaics in Uganda: with implications for conservation
124. **Mohamed, Yasir Abbas** (2005), 04-15-38483-4, The Nile Hydroclimatology: impact of the Sudd wetland (Distinction)

125. **Duker, Alfred, A.** (2005), 90-8504-243-7, Spatial analysis of factors implicated in *mycobacterium ulcerans* infection in Ghana
126. **Ferwerda, Jelle, G.,** (2005), 90-8504-209-7, Charting the Quality of Forage: Measuring and mapping the variation of chemical components in foliage with hyperspectral remote sensing
127. **Martinez, Javier** (2005), 90-6164-235-3, Monitoring intra-urban inequalities with GIS-based indicators. With a case study in Rosario, Argentina
128. **Saavedra, Carlos** (2005), 90-8504-289-5, Estimating spatial patterns of soil erosion and deposition in the Andean region using Geo-information techniques. A case study in Cochabamba, Bolivia
129. **Vaiphasa, Chaichoke** (2006), 90-8504-353-0, Remote Sensing Techniques for Mangrove Mapping
130. **Porwal, Alok** (2006), 90-6164-240-X, Mineral Potential Mapping with Mathematical Geological Models
131. **Werff, Harald van der** (2006), 90-6164-238-8, Knowledge-based remote sensing of complex objects: recognition of spectral and spatial patterns resulting from natural hydrocarbon seepages
132. **Vlag, Daniël van de** (2006), 90-8504-384-0, Modeling and visualizing dynamic landscape objects and their qualities
133. **Joshi, Chudamani** (2006), 90-8504-470-7, Mapping cryptic invaders and invisibility of tropical forest ecosystems: *Chromolaena odorata* in Nepal
134. **Bandara, K.M.P.S.** (2006), 90-8504-406-5, Assessing irrigation performance by using remote sensing
135. **Dilo, Areti** (2006), 90-8504-461-8, Representation of and Reasoning with Vagueness in Spatial Information. A system for handling vague objects
136. **Debba, Pravesh** (2006), 90-8504-462-6, Sampling scheme optimization from hyperspectral data
137. **Huisman, Marco** (2006), 90-6164-246-9, Assessment of rock mass decay in artificial slopes
138. **Lemmens, Rob** (2006), 90-6164-250-7, Semantic interoperability of distributed geo-services
139. **Chacón Moreno, Eulogio** (2007), 90-8504-559-2, Ecological and spatial modeling: Mapping ecosystems, landscape changes, and plant species distribution in Llanos del Orinoco, Venezuela
140. **Amer, Sherif** (2007), 90-6164-253-1, Towards Spatial Justice in Urban Health Services Planning
141. **Obakeng, Obolokile Thothi** (2007), 90-6164-254-X, Soil moisture dynamics and evapotranspiration at the fringe of the Botswana Kalahari, with emphasis on deep rooting vegetation
142. **Cho, Moses Azong** (2007), 978-90-8504-622-6, Hyperspectral remote sensing of biochemical and biophysical parameters
143. **Farifteh, Jamshid** (2007), 978-90-6164-259-6, Imaging Spectroscopy of salt-affected soils: Model-based integrated method
144. **Minang, Peter Akong**, (2007), 978-90-6164-260-2, Implementing global environmental policy at local level: community carbon forestry perspectives in Cameroon

145. **Noomen, Marleen F.** (2007), 978-90-8504-671-4, Hyperspectral reflectance of vegetation affected by underground hydrocarbon gas seepage
146. **Trias Aditya Kurniawan Muhammad**, (2007), 978-90-6164-261-9, The National Atlas as a Metaphor for Improved Use of a Geospatial Data Infrastructure
147. **Alkema, Dinand** (2007), 978-90-6164-239, Simulating floods. On the application of 2D-hydraulic models for flood hazard and risk assessment
148. **Ruitenbeek, Frank van** (2007), 978-90-6164-262-6, Hydrothermal Processes in the Archean – New Insights from Imaging Spectroscopy
149. **Turdukulov, Ulanbek D.** (2007), 978-90-6164-264-0, Visualizing the evolution of image features in time-series: supporting the exploration of sensor data

PE&RC PhD Education Certificate

With the educational activities listed below the PhD candidate has complied with the educational requirements set by the C.T. de Wit Graduate School for Production Ecology and Resource Conservation (PE&RC) which comprises of a minimum total of 32 ECTS (= 22 weeks of activities)

Review of Literature (5 credits)
- Plant biodiversity assessment using hyperspectral imagery (2003)

Writing of Project Proposal (7 credits)
- Plant biodiversity assessment using hyperspectral imagery (2003)

Laboratory Training and Working Visits (0.7 credits)
- Chemical assay of foliar nutrients, Wageningen University (2004-2005)
- Cryo-scanning electron microscopy, Wageningen University (2006)

Post-Graduate Courses (5 credits)
- PhD course on spatial and temporal aspects of resource ecology; PE&RC (2005)
- Advance geo-statistical methods; ITC (2005)
- Consumer resource interactions: adaptive foraging adaptive defences and ecosystem engineering; FE, PE&RC and SENSE (2006)

Deficiency, Refresh, Brush-up and General Courses (1 credit)
- Spatial statistics analysis; ITC (2003)

Competence Strengthening / Skills Courses (3.5 credits)
- Scientific writing; ITC (2004)
- Scientific presentation; ITC (2004)
- IDL basic programming; ITC (2006)

Discussion Groups / Local Seminars and Other Scientific Meetings (8.2 credits)
- Campman day (2003)
- Forth-nighty PhD discussion,; ITC (2003-2007)
- PhD day (2004 & 2005)
- International workshop on physical based approaches in remote sensing: scaling from leaves to ecosystems (2006)

PE&RC Annual Meetings, Seminars and the PE&RC Weekend (3 credits)
- Five natural resources days organized by Department of Natural Resources; ITC (2004 & 2005)
- PE&RC day (2005 & 2006)
- Two PhD master class with president of ESRI and UNHABITAT general secretary (2005 & 2006)

International Symposia, Workshops and Conferences (5 credits)

- SPIE symposium on optics and photonics: remote sensing and modelling of ecosystem for sustainability (2006)
- ISPRS technical commission VII symposium: remote sensing from pixels to processes; thematic processing, modelling and analysis of remotely sensed data (2006)
- Spatial data quality 2007: 5th international symposium on spatial data quality:" modelling qualities in space and time" (2007)